THE
PHYSICAL REVIEW
A journal of experimental and theoretical physics established by E. L. Nichols in 1893

SECOND SERIES, VOL. 65, NOS. 11 AND 12 JUNE 1 AND 15, 1944

On the Problem of the Existence of Mesotrons in Auger Showers

ANATOLE ROGOZINSKI
Ryerson Physical Laboratory, University of Chicago, Chicago, Illinois
(Received March 13, 1944)

A discussion is given of the different possibilities which would lead to the assumption of the presence of mesotrons in extensive atmospheric showers, or the so-called Auger showers. The difficulties involved in the problem of the experimental evidence for the existence of these mesotrons are shown to be, in general, considerable. Three kinds of experiments are described in which mesotrons associated simultaneously with other particles are found. These particles are present even at large distances (~20 meters) from the observed mesotrons. However, they are much more infrequent than the particles which are found in the Auger showers, investigated under conditions similar to those of the present experiments. Qualitatively, the observed phenomena could be due, not to mesotrons associated with an Auger shower, but to single mesotrons accompanied by collision electrons which are projected by these mesotrons along their path in the air. There exists, however, a definite quantitative disagreement between the observed values and the theoretical values which are calculated for the considered collision processes. Therefore, at least part of the observed mesotrons could actually belong to an Auger shower. But, on the other hand, explanations are formulated which might, at least partly, account for the mentioned quantitative disagreement. Thus, only after these explanations are tested by experiment will it be possible to decide more definitely as to the presence of mesotrons in Auger showers.

PRELIMINARY CONSIDERATIONS

THE problem of the presence of mesotrons in extensive atmospheric cosmic-ray showers, or Auger showers (here referred to as *A* showers) has been investigated since the first experiments were carried out on these showers.[1] The particular interest of this problem arises from its possible relation to different phenomena, which are mainly: (a) the development of a cascade shower originating from a particle of very high energy, up to 10^{16} ev, and (b) the mechanism itself of the generation of mesotrons in cosmic rays.

We shall briefly examine here the different possibilities which would lead to the assumption of the presence of mesotrons in *A* showers, and then discuss the problem of their experimental evidence.

An analogous discussion can be applied, in part, for heavy penetrating particles, other than mesotrons, which might also be present in *A* showers.

A. Showers Originating from Primary Soft Particles

In case the primary soft particles (electron or photon) multiply only by processes described in the theory of cascade showers and if one admits that the cascade theory is valid for particles having energies up to 10^{16} ev, then one should not expect to find mesotrons in *A* showers since

[1] P. Auger, R. Maze, and T. Grivet-Meyer, Comptes rendus **206**, 1721 (1938); W. Kolhörster, J. Matthes, and E. Weber, Naturwiss. **26**, 576 (1938); P. Auger, P. Ehrenfest, R. Maze, J. Daudin, Robley, and A. Freon, Rev. Mod. Phys. **11**, 288 (1939); H. Euler and H. Wergeland, Naturwiss. **27**, 484 (1939); N. Hilberry, Phys. Rev. **60**, 1 (1941).

this theory does not predict at all any creation of mesotrons in the multiplication process leading to the building up of the shower.

B. Showers Originating Indirectly from High Energy Mesotrons

An *A* shower can originate from a mesotron by a close collision process with an electron,[2,3] by a bremsstrahlung process providing a high energy photon,[3] or possibly by a decay of a short life mesotron of very high energy. The main difference between cases A and B is that the high energy parent particle of the *A* shower is a secondary instead of being a primary. In the present case, however, the *A* shower starts at any altitude in the atmosphere wherever the high energy secondary particle is created, and not at the top of the atmosphere, as in the case of the primary parent particle. We will leave aside the question of how far the origin of the *A* showers could be attributed to such mechanisms since our intention is to limit the present discussion only to the problem of the presence of mesotrons in *A* showers.

It is expedient to remark here that in order to obtain a widespread shower, the energy transfer from the mesotron to the high energy soft particle should have taken place in the upper atmosphere, otherwise only a burst of particles of a small extension could be observed. In any case, the probability of detecting in the whole shower the only present mesotron—which is the source of that shower and is assumed to have lost only part of its energy in the above-described processes—will be very small. On the other hand, the probability of detection of this mesotron should decrease at least in proportion to the frequency of its occurrence in the differential energy spectrum of the mesotron radiation.

C. Secondary Production of Mesotrons

1. The problem of detecting mesotrons in the *A* showers would look less hopeless if there should be a creation of a larger number of mesotrons within these showers. In case the created mesotrons are of high energy, they must have originated in the core of the *A* shower. They will travel together with the high energy particles of the central part (core) of that shower and remain close to its axis.

In order to detect these mesotrons one will have to eliminate from the core of the *A* shower the soft high energy particles which are mixed together with the mesotrons.

2. From the experimental point of view, the identification of the high energy mesotrons in the core of the *A* shower will present great difficulties. Indeed, *in counter experiments*, the only reliable criterion for the identification of the mesotron is its small probability of creating a shower after having traversed a larger number of radiation units of any material. Generally, it is sufficient to place below this material a group of counters, the function of which is to distinguish between a single particle or a shower emerging below the material. If, however, there are present many mesotrons of high energy, they could discharge this group of counters and would act then in the same way as a cascade shower. The above criterion will fail in this case. It will therefore be necessary to increase still more the thickness of material in order to eliminate eventually the less energetic mesotrons until one single mesotron remains. Such a procedure could lead to the use of prohibitively large thicknesses of absorbing material. However, if one could rely on the strict validity of the cascade theory for extremely high energies (10^{13}–10^{16} ev) of the soft particles which are involved in the *A* showers, then all particles, whatever their number might be, emerging below, for example, a lead absorber of a thickness of, say, ½ meter, should consist of penetrating particles (mesotrons), or at any rate of particles originating from a penetrating particle. This follows from the fact that any soft particle of an *A* shower of energy up to 10^{16} ev should be stopped in the indicated lead absorber since the cascade theory shows that for high energy soft particles the average cross section for the pair production and the fractional energy loss by radiation processes are practically independent of the energy of these particles and are, for one radiation unit of length of any material (0.5 cm for Pb), equal to ~ 1. In any case, there will always be a possibility that the mesotrons finally identified were, originally, not present at all in the *A* shower, but were created in the

[2] H. J. Bhabha, Proc. Roy. Soc. **164**, 257 (1938).
[3] R. F. Christy and S. Kusaka, Phys. Rev. **405**, 411 (1941).

absorber—for example, a lead absorber—where the cross section for such a process might be very different from that in air. Therefore, it would be best to use, as absorbers, materials having about the same atomic number as air, e.g., water. Such experiments could be carried out by immersing the detecting apparatus in a lake.

3. In cases where one could demonstrate that the particles emerging below the thick absorber did not belong primarily to a dense part of an *A* shower, in other words, if one could prove that the density of particles which are then present *above* the absorber is relatively low, the particles below the absorber could be attributed to a mesotron with a considerably higher probability than in the previous case. Indeed, in the present case, the particles below the absorber could not have originated from a high energy electron or photon, since such particles would almost always be accompanied either by other particles of the core of the *A* shower, or by a cascade shower originated along their path in air, or even more frequently by both. It is evident that these cases in which the mesotrons are present in the low density region (wing) of the *A* shower are the most favorable ones for their detection. However, as will be seen more in detail in the experimental part of this paper, the question may then arise whether the observed mesotrons belong actually to an *A* shower or whether they can be considered as single mesotrons ejecting electrons along their path in air by collision processes.

4. Finally, it should be pointed out that in case the mesotrons created within the core of the *A* showers are of low energy, of the order of magnitude of their rest mass energy, the probability of their detection would again be small since they would very likely be stopped in an absorber of a thickness smaller than required to filter out all the high energy soft particles present in the core. They would naturally be stopped already in the air, in case they are created high in the atmosphere.

D. Delayed Particles in *A* Showers

As a direct consequence of the possible presence of low energy mesotrons in an *A* shower there should exist a certain number of electrons, resulting from the decay of the mesotrons, and occurring with delays—of the order of magnitude of the mean lifetime ($\sim 2\times10^{-6}$ sec.) of the mesotron—with respect to all other particles in the same parent *A* shower. Inversely, a demonstration of the existence of such delayed particles in an *A* shower would provide probably the best evidence of the presence of mesotrons in *A* showers. For that purpose, an apparatus was built which makes it possible to measure delays occurring between a group of counters selecting *A* showers and another counter placed in the neighborhood of this group of counters. This outfit records only those delays which occur within $\sim 10\times10^{-6}$ sec. A more detailed account of this method will be given at a later date.

EXPERIMENTS

Several types of counter-tube experiments were performed in order to obtain direct evidence of the possible presence of mesotrons in *A* showers. These investigations were carried out at sea level (Chicago, altitude 610 feet) and at a higher altitude[4] (Echo Lake, Colorado, altitude 10,618 feet). In all experiments here described the master group method was used. The general principle of this method was described in a previous paper,[5] to which we shall refer here as I. All counters used in the present experiments are filled with a mixture of argon and alcohol.[6] They have an effective area of $5\times50=250$ cm^2 and operate at 1200 volts. The resolving time of the coincidence circuits is about 2×10^{-6} sec. for a separation between counters less than 2 meters and about 4×10^{-6} sec. for a separation of 22 meters.

Throughout this paper, any counter which does not belong to the master group will be called an analyzing or distant counter. When speaking about discharges or counting rates in such a counter, it should be understood, unless specified otherwise, that the master group was simultaneously discharged.

The discharges of the analyzing counters were recorded on a photographic film by means of neon lamp flashes. The photographic recorder was of a type similar to that used by Schein,

[4] During the Mount Evans Expedition of the University of Chicago in August-September, 1943.
[5] A. Rogozinski, Phys. Rev. **65**, 207 (1944).
[6] These counter tubes were designed by Dr. V. H. Regener.

Jesse, and Wollan[7] in their stratosphere experiments.

Experiment I

In the first experiment,[8] which was carried out at sea level and was of a preliminary character,

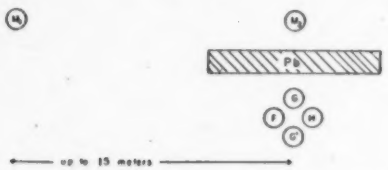

FIG. 1. Counter arrangement in Experiment I.

the master group consisted of two counters M_1 and M_2 connected in twofold coincidence and separated by a horizontal distance up to 15 meters. The role of this master group was to select A showers (Fig. 1). A set of 4 analyzing counters F, G, G', H, placed below M_2 could be separated from that counter by lead absorbers up to 12.5 cm of thickness. The counters M_2, F, G, G', and H were located inside a Celotex box which was placed in open air and could be heated. The counter M_1 was placed indoors below a thin tile roof.

It was found, for different thicknesses of the lead absorber, that a certain fraction of the fourfold coincidences M_1M_2GG' was not accompanied by a discharge in any of the counters F and H. Therefore, it is assumed that these events could be attributed to single non-shower producing particles present in that part of the A shower which strikes the lead absorber. These particles which emerge below a lead thickness of several radiation units without producing an abundant shower should be heavy particles of the penetrating type, such as mesotrons.

Experiment II

1. In order to determine the density of particles in the region of the shower in which the penetrating particle is located, experiments were performed (at Echo Lake) with the same counter arrangement as described in I. In this experiment the master group consisted of two counters M_1 and M_2 connected in twofold coincidence and placed one above the other. In order to increase the counting rate, two counters connected in parallel were used for M_1 and for M_2 (Fig. 2). At a horizontal distance of 22 meters from the master group there was placed the set of seven analyzing counters K_1, K_2, K_3, F, G, G', H, of which the upper set of counters, K_1, K_2, K_3, could be separated from the lower set, F, G, G', H, by variable thicknesses of a lead absorber. The four counters of the master group were put outdoors in a small wooden box which had a wall thickness of $\frac{1}{2}$ in. and which could be heated. The set of analyzing counters was located indoors under a thin wooden roof.

2. The results obtained in Experiment II dealing with those cases where a shower emerges below a lead absorber (coincidences $M_1M_2FGG'H$) were already described in I. Here we shall investigate in detail such events, which could be attributed to penetrating particles, like mesotrons, emerging below the lead absorber without being accompanied by a shower. These events are recorded as coincidences M_1M_2GG', which are not accompanied simultaneously by a discharge in any of the counters F and H. Such an "anticoincidence" will be represented by the symbol $M_1M_2GG'-FH$.

The results of these experiments are summarized in Table I. However, for comparison with those cases in which a shower emerges below the lead absorber, the corresponding data are also given in this table. The first column of Table I gives the total time of recording for a certain thickness of lead, which is indicated in column II. The columns from III to XI represent average counting rates, expressed in number of coincidences per 10 hours. Column III gives the frequencies of the anticoincidences

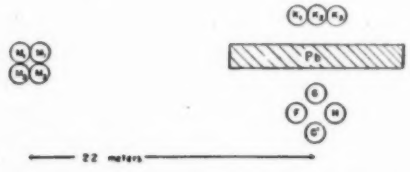

FIG. 2. Counter arrangement in Experiment II.

$M_1M_2GG'-FH$ or the coincidences $M_1M_2FGG'H$, regardless of discharges which might have occurred simultaneously in the upper set of counters K_1, K_2, K_3. Columns IV to X give the frequencies of those events $M_1M_2GG'-FH$ or

[7] M. Schein, W. P. Jesse, and E. O. Wollan, Phys. Rev. 59, 615 (1941).
[8] P. Auger and A. Rogozinski, Phys. Rev. 65, 64 (1944).

TABLE I. Experiment II. Coincidences, per 10 hours, occurring between the master group M_1M_2 and the different analyzing counters $F, G, G', H, K_1, K_2, K_3$.

I	II	III	IV	V	VI	VII	VIII	IX	X	XI
Hours of recording	cm Pb	$M_1M_2GG'-FH$ (1) or $M_1M_2FGG'H$ (2)	$M_1M_2GG'-FH$ or $M_1M_2FGG'H$ in coincidence with K_1	K_2	K_3	K_1K_2	K_1K_3	K_2K_3	$K_1K_2K_3$	Δ
7	2.5	(1) 75	12	10.5	7.5	6	3	0	3	33
		(2) 66	3	3	4.5	9	3	12	22.5	9
29.8	5.0	(1) 56	7.7	8.4	6.7	1.7	3	1.3	8.4	18.8
		(2) 64.8	1.7	3.7	3.4	6.4	3.7	6	33	6.8
20.5	10.0	(1) 27.8	4.4	3.4	4.4	1.5	1	1.5	1	10.6
		(2) 26	1	0.5	0.5	1	1	0.5	20	1.5

$M_1M_2FGG'H$ which are accompanied by simultaneous discharges in the 7 possible combinations of counters of the upper set K_1, K_2, K_3. The last column Δ represents the differences between the frequency of $M_1M_2GG'-FH$ or $M_1M_2FGG'H$ and the sum of all the frequencies of the corresponding 7 types of coincidences listed in columns IV to X. These Δ values represent the frequency of events $M_1M_2GG'-FH$ or $M_1M_2FGG'H$ which are *not* accompanied by a simultaneous discharge in any of the upper counters K_1, K_2, K_3. The average frequencies (counts per 10 hours) of coincidences between the master group and just one, or just two, or all three counters K_1, K_2, K_3, were, respectively, 320, 80, and 170, regardless of any discharge which might have occurred in the lower set of counters. It results from these figures that the average frequency of those A showers, which discharge at least one of the counters K_1, K_2, or K_3 in coincidence with the master group, is $320+2\times80+170=650$ in 10 hours.

3. As we have mentioned in I, the chance coincidences could be neglected for the higher order coincidences reported there. In the present case, however, this factor has to be considered, mainly for the single-particle events $M_1M_2GG'-FH$, where larger thicknesses of lead were used. Although such an event is essentially a fourfold coincidence, the computation of the chance coincidences in the actual case involves coincidence rates of different orders, the most important contribution of which comes from the twofold coincidence rates between (a) the proper twofold coincidence rate M_1M_2 of the master group and (b) the proper twofold coincidence rate of the telescope GG'. The frequencies of the chance coincidences (per 10 hours), thus calculated, for $M_1M_2GG'-FH$ are, respectively, 19.2, 18, and 16 for lead thicknesses of 2.5, 5.0, and 10.0 cm. This shows that the corresponding Δ values for 5.0 and for 10.0 cm of lead could be due entirely to chance coincidences. For 10.0 cm of lead, the Δ value of 10.6, which is appreciably lower than the value of 16 which represents the calculated chance coincidence frequency, could be due to a fluctuation in the average number of the chance coincidences; in addition, it could be caused by a small contribution of chance coincidences arising from the fivefold coincidences $M_1M_2GG'K_1$, $M_1M_2GG'K_2$, and $M_1M_2GG'K_3$.

Incidentally, the above-mentioned reasons—apart from the fact that the geometrical arrangement of the counter telescope GG' presents a certain "leak," regarding the solid angle of GG' which is not entirely covered by the upper set of counters—makes uncertain, on the basis of the present data, any attempt to correlate with a non-ionizing particle the passage of a single penetrating particle through the lead absorber.

4. In order to obtain a clearer picture of the meaning of the experimental data of Table I concerning the density of particles which strike the lead absorber in case of events $M_1M_2GG'-FH$, a comparison was made in Table II between these events and the shower events which are respectively coincident with a discharge occurring in one or more of the upper counters K_1, K_2, K_3. For this purpose, the counting rates for $M_1M_2GG'-FH$ and $M_1M_2FGG'H$ were each reduced to a value of 100, and the counting rates of the corresponding higher order coincidences

were calculated accordingly. The equivalent three counting rates for coincidences between $M_1M_2GG'-FH$ or $M_1M_2FGG'H$ on one hand, and K_1, K_2, or K_3 on the other hand, were replaced by their sum. The same was done for the three counting rates involving K_1K_2, K_1K_3, or K_2K_3, instead of K_1, K_2, or K_3. In computing the values of Table II, the calculated chance coincidence rates of 19.2 and 18 were taken into account for 2.5 and 5.0 cm of Pb, respectively; the chance coincidence rate for 10.0 cm of Pb was taken equal to 10.6 in order to make the Δ value which corresponds to this thickness of lead equal to zero.

Discussion of Experiment II

Let us consider, in Table II, the data referring to single or shower events which occur below the lead and are associated with simultaneous discharges in the upper set of counters K_1, K_2, K_3. One can notice immediately the apparent fact that for all lead thicknesses, the single-particle events $M_1M_2GG'-FH$ are much more frequently accompanied by discharges in a single upper counter than the shower events $M_1M_2FGG'H$. These, on the contrary, are more frequently accompanied by discharges in two and mainly in three upper counters than the single-particle events. In particular, for 10 cm of Pb, the ratio between the percentages of events $M_1M_2GG'-FH$ or $M_1M_2FGG'H$, each accompanied by

TABLE II. Experiment II. Relative values of counting rates for coincidences occurring between (1) $M_1M_2GG'-FH$, or (2) $M_1M_2FGG'H$, and the upper counters K_1, K_2, K_3.

cm Pb	$M_1M_2GG'-FH$ (1) or $M_1M_2FGG'H$ (2)	$M_1M_2GG'-FH$ or $M_1M_2FGG'H$ in coincidence with $(K_1+K_2+K_3)$	$(K_1K_2+K_1K_3+K_2K_3)$	$K_1K_2K_3$	Δ
2.5	(1) 100	54	16	5.5	24.5
	(2) 100	16	36.5	34	13.5
5.0	(1) 100	60	16	22	2
	(2) 100	13.5	25	51	10.5
10.0	(1) 100	71	23	6	0
	(2) 100	7.7	9.6	77	5.7

discharges in the upper set of counters, changes from $71:7.7\simeq 9$ when a discharge occurs in just one of the upper counters, to $6:77\simeq 1/13$ when a discharge occurs in all three upper counters K_1, K_2, K_3. This variation is of the order of magnitude of $9:1/13\simeq 100$. The obvious consequence which follows from these figures is that the mean density of particles which are associated, *above* the lead, with single-particle events $M_1M_2GG'-FH$ is very small in comparison with the corresponding density for the shower events $M_1M_2FGG'H$.

This fact that a single-particle event $M_1M_2GG'-FH$, which is presumably caused by a mesotron, is usually associated with a very small number of ionizing particles in its immediate neighborhood, could be interpreted in two different ways: Either the mesotron belongs to a low density region (wing) of an A shower and, hence, is present at a relatively large distance from the core of the A shower (A shower hypothesis), or the mesotron is located in a shower of low particle density, other than an A shower. Such a shower could arise, for example, from collisions of the mesotron with electrons along its path in the air (collision-electron hypothesis).

Thus, if the A shower hypothesis is correct, the mean density of particles which cover a certain relatively large area around the mesotron should be approximately constant all over this area. In other words, one should expect that the considered particle density at any point of this area would be approximately independent of the distance (a few meters) of this point from the mesotron trajectory since in the present case the mesotron would be located far from the high density region of its parent A shower.

In case the collision-electron hypothesis is correct, the just considered density of particles should be an essentially decreasing function of the distance from the mesotron trajectory. This follows from the fact that, on one hand, electrons arising from collision processes of mesotrons in air should have an increasing energy in order to reach points located at increasing distances from the parent mesotron, and, on the other hand, the probability of ejecting a collision electron of a certain energy decreases, in first approximation, as the square of that energy. A theoretical computation of this effect is given in the paper (III) which follows the present one.

Experiment III

As a consequence of these considerations further attempts were made to determine which one of the considered hypotheses is correct.

1. In the experiments I and II the master group could be discharged by both soft and penetrating particles of energies higher than the minimum energy of a few Mev which is necessary to penetrate the counter walls. In the experiments which are to be described, the master group selected only particles which are able to penetrate 10 cm of lead, and, in particular, those particles which emerge below the lead without being accompanied by a shower and are, therefore, classified as mesotrons. One can say that in the latter case the master group worked as a kind of a mesotron selector.

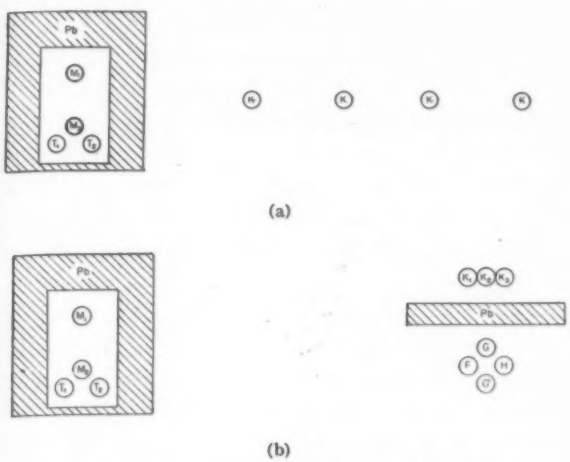

FIG. 3. Counter arrangement in Experiment III.

Thus, the master group consisted of a vertical telescope in twofold coincidence M_1M_2 and, in addition, of two side counters T_1 and T_2 which could be connected in anticoincidence to M_1M_2 (Fig. 3). T_1 and T_2 were in most cases connected in parallel. The whole master group was surrounded by a lead shield 10 cm thick. According to what was explained above, the anticoincidence events $M_1M_2-T_{1,2}$ were attributed to penetrating non-shower-producing particles, such as mesotrons. In some very rare cases, however, which will be discussed below, high energy soft particles might also produce such an anticoincidence event.

2. Two series of experiments were carried out. In the first, several analyzing counters were placed at different distances from the master group (Fig. 3a). In that way it was possible to obtain, from the same record of coincidences, the counting rate in an analyzing counter as a function of its distance from the mesotron selector. In the second series of experiments, a set of 7 analyzing counters, similar to the set described in experiment II, was used in order to investigate the penetrating power of the particles associated with those particles which discharge the master group (Fig. 3b). Since all the data obtained in these experiments, which were carried out in Chicago and at Echo Lake, are not yet analyzed and since similar experiments are still in progress, only part of the results will be reported here and summarized in Table III.

In Table III the first two columns I and II are self-evident; column III (1, 2) gives the proper counting rate (counts per 10 hours) of the master group for the two cases where only mesotrons ($M_1M_2-T_{1,2}$) or both mesotrons and high energy soft particles (M_1M_2) are registered; column IV gives the counting rate (also per 10 hours) of discharges in an analyzing counter for different distances D of that counter from the master group; column V represents the ratio ν between the counting rates which figure in columns IV and III for events $M_1M_2-T_{1,2}$. The last column VI gives the theoretical values for ν, which represent the ratio ν_{th} between (a) the frequency of discharges in a distant counter, arising from collision electrons ejected in air by those mesotrons which traverse the selector, and (b) the proper counting rate of the selector. The formula

TABLE III. Experiment III. Coincidences, per 10 hours, occurring between (1) the mesotron selector $M_1M_2-T_{1,2}$, or (2) the master group M_1M_2, and an analyzing counter K.

I Hours of recording	II D in meters	III $M_1M_2-T_{1,2}$ (1) or M_1M_2 (2)	IV $(M_1M_2-T_{1,2})K$ (1) or M_1M_2K (2)	V $\nu=\frac{(M_1M_2-T_{1,2})K}{M_1M_2-T_{1,2}}$	VI ν_{th}
		Chicago; Altitude: 610 ft.			
50	0.5	(1) 2.7×10^4	19.7	7.1×10^{-4}	8.6×10^{-4}
34		(2) 3.4×10^4	48.3		
50	1.0	(1) 2.7×10^4	8.6	3.2×10^{-4}	4.2×10^{-4}
34		(2) 3.4×10^4	22		
50	2.0	(1) 2.7×10^4	5.2	1.9×10^{-4}	2.0×10^{-4}
34		(2) 3.4×10^4	13.3		
		Echo Lake; Altitude: 10,618 ft.			
51	2.0	(1) 5.0×10^4	15.3	3.1×10^{-4}	1.4×10^{-4}
26.5		(2) 6.2×10^4	67.4		
76	5.0	(1) 5.0×10^4	6.7	1.3×10^{-4}	0.5×10^{-4}
42		(2) 6.2×10^4	43.8		

for this ratio is derived in paper III and is given by

$$\nu_{th} = (BS/\pi D)\theta_{max}(D, E_1).$$

Here, B is a constant factor which is equal to 10^{-2} for standard air if the effective area S of the counter, placed at a distance D from the selector, is expressed in m^2 and D in meters; $\theta_{max}(D, E_1)$ is a function of D and of the minimum energy E_1 which is necessary for an electron to traverse the wall of the counter. Some of the calculated values for $\theta_{max}(D, E_1)$ are given in Table IV.

In Table III the values of ν_{th} were computed for $S = 2.5 \times 10^{-2}$ m² and $E_1 = 2$ Mev. The altitude effect on ν_{th} was taken into account (see Altitude Effect, in III).

Discussion of Results of Experiment III

It was found that: (a) the frequency of discharges occurring in an analyzing counter in coincidence with a discharge in the mesotron selector is, at least for the first few meters, a strongly decreasing function of the distance D of this counter from the selector; (b) most of the discharges in any particular analyzing counter are only very occasionally accompanied by a discharge in other analyzing counters; and (c) the counting rates in these analyzing counters are considerably lower than those which are usually observed for A showers using unshielded counters separated by the same distance D.

A proof that the observed phenomena, in which only the passage of a mesotron through the selector $M_1M_2 - T_{1,2}$ is involved, are of a different nature from those which involve soft particles, is given by the experiments in which the side counters T_1 and T_2 are removed. In these experiments, the master group M_1M_2 could record, in addition to mesotrons, also the high energy soft particles which emerge with a large shower below a lead thickness of 10 cm. Although in this case the proper counting rate of the master group increased only by ~25 percent, the corresponding increase in the counting rate of the analyzing counters was of the order of ~300 percent. Moreover, the proportion of cases where multiple coincidences between the different analyzing counters occurred increased at the same time by an even more considerable factor.

Because of the strong dependence of the counting rate of an analyzing counter upon its distance from the selector, the observed phenomena seem so far to be in qualitative agreement with the collision-electron hypothesis. But, on the other hand, it is seen from Table III that there exists a considerable discrepancy between the experimental and theoretical values calculated on the basis of the collision-electron hypothesis. Therefore, it would be legitimate to conclude that at least part of the observed mesotrons belong actually to A showers. However, there is a possible explanation, which could account, at least partly, for the above-mentioned discrepancy.

As we have seen, the role of the mesotron selector is to register only those events in which the vertical telescope M_1M_2 is discharged, but not any of the side counters T_1 and T_2. It is well known that the great majority of these events can be attributed to single mesotrons

TABLE IV. Values of $\theta_{max}(D, E_1)$.

E_1 Mev \ D meters	1	2	5	10
2	0.53	0.50	0.41	0.30
4	0.42	0.40	0.34	0.27

emerging below the lead absorber which surrounds the selector. In two cases, however, the selector will fail in its function as mesotron selector.[9] First, the selector will miss all mesotrons which emerge below the absorber with a collision electron discharging one of the two side counters T_1 or T_2. This effect, however, reduces the counting rate of the distant counters by only a few percent. Second, a high energy soft particle emerging, for example, with a narrow shower accompanied by a few side particles, could discharge the telescope M_1M_2 and very occasionally miss both[10] side counters T_1 and T_2. Such an event will be recorded and considered naturally as being produced by a single mesotron. The influence of this effect on the counting rate of the distant counter will, on the average, be much more important than in the first case since a high energy soft particle has a much higher

[9] See also Section C2 of the preliminary considerations.

[10] Counter inefficiencies are too small to contribute appreciably to such a double missing. On the other hand, the anticoincidence *circuit* is practically 100 percent efficient.

probability than a mesotron to be accompanied by a shower; hence, the probability of discharging the distant counter will, in first approximation, also increase in proportion to this effect. It was emphasized before that in connecting the anticoincidence counters into the circuit of the master group, one reduces the proper counting rate of the master group by ~20 percent, while the corresponding reduction of the counting rate in the distant counter is then ~75 percent. Therefore, it is easy to understand that in case several percent, out of about 80 percent of the discharges of the master group which are attributed to mesotrons, were actually due to high energy soft particles, the corresponding reduction in the counting rate in the distant counter could be appreciably higher than the observed ~75 percent. Consequently, the frequency of discharges in the distant counter, occurring simultaneously with a passage of a mesotron through the master group, might be actually much smaller. It should be pointed out, however, that the hitherto admitted occurrence of that particular narrow shower below a lead thickness of 10 cm is probably a very infrequent event and, hence, could account only partly for the observed large discrepancy.

It would be possible to obtain a more precise idea of the importance of the just-described effect—and to reduce it eventually—in using, for example, counters of a smaller size for the telescope M_1M_2 and of a larger size for the side counters T_1 and T_2. Considerable difficulty would, however, arise then from a very strong reduction of the observed counting rates which are already very low in the present investigations.

This is the characteristic difficulty in counter experiments since it is not known whether a discharge in a counter was produced by a single particle or by several particles. Therefore, a few cloud-chamber photographs[11] of the particles which discharge the mesotron selector would be of great value in analyzing this effect.

The altitude effect, which should be different for each of the two hypotheses, could throw some light on the problem considered here. In case of the collision-electron hypothesis, the observed effect should increase parallel to the increase in the intensity of the mesotron component of the cosmic radiation. In the alternate case, this effect should follow the increase in the frequency of the A showers. We found that between Chicago and Echo Lake the increase in the intensity of the mesotron component is 1.9, whereas the increase of the frequency of A showers of an average extension is ~7. The observed increase in the counting rate of a distant counter is ~3 and lies between these two values. But before a significant comparison regarding the altitude effect can be made, it will be necessary to carry out further measurements in order to extend the common range of the distance D for the two altitudes and to prolong the time of observation.

[11] Valuable photographs of tracks in a cloud chamber controlled by distant counters were obtained, at an altitude of 3200 meters, by P. Auger and J. Daudin, Comptes rendus 209, 481 (1939).

CONCLUSIONS

By way of conclusion, we shall point out that: (a) Counter experiments are practically unable to give unambiguous information regarding the presence of mesotrons in the dense part of A showers. (b) Mesotrons were found to be associated with particles of very low density, which could be considered either as belonging to A showers or as collision electrons ejected by these mesotrons along their path in the air. (c) Although the hypothesis of mesotrons accompanied by collision electrons seems to agree qualitatively with the experimental results so far obtained, the experimental values, however, are considerably higher than those given by a theoretical calculation for this case. Therefore, it would be legitimate to conclude that at least part of the observed mesotrons actually belong to A showers. But on the other hand, explanations are indicated which might account, at least partly, for the above-mentioned qualitative disagreement. Thus, only after these explanations are tested by experiment will it be possible to decide more definitely as to the presence of mesotrons in A showers.

It is a great pleasure for me to express my gratitude to Dean A. H. Compton for placing at my disposal the facilities for this work, and to the Rockefeller Foundation for its generous support. I am also very thankful to Professor Pierre Auger and to Professor Marcel Schein for their continued interest in the present work.

PHYSICAL REVIEW VOLUME 65, NUMBERS 11 AND 12 JUNE 1 AND 15, 1944

Theory of Counter Experiments on Collision Electrons Ejected in Air by Mesotrons

ANATOLE ROGOZINSKI
Ryerson Physical Laboratory, University of Chicago, Chicago, Illinois

(Received March 13, 1944)

It was found in the preceding paper that mesotrons are associated with particles present at several meters distance from the mesotron trajectories. At least part of these particles are collision electrons ejected by these mesotrons along their path in the air. The theoretical results obtained in the present paper show that: (a) Only mesotrons of momenta $p > p_0 \sim 10^8$ ev/c can eject in air collision electrons sufficiently energetic to reach and to traverse a counter tube (C) placed at a distance D (a few meters) from the mesotron trajectory. (b) The number ν of collision electrons arising from a single mesotron and which are able to discharge (C) is practically independent of the mesotron momentum p if the influence of the spin of the mesotron is neglected and is given, in first approximation, by $\nu_0 = (BS/\pi D) \times \theta_{max}(D, E_1)$. In this formula, if the effective area of (C) is expressed in m² and D in meters, then $B = 10^{-2}$ for standard air. θ_{max} is a function of D and of the minimum energy E_1 necessary for an electron to penetrate the wall of the counter. For $E_1 = 2$ Mev, for example, θ_{max} decreases from 0.50 for $D = 2$ m, to 0.30 for $D = 10$ m. (c) When the mesotron spin (0 or ½) is taken into account, ν is about equal to ½ν_0 for the lowest mesotron momenta, but approaches asymptotically ν_0 as p increases. (d) A fraction of these collision electrons can give, by their subsequent cascade multiplication in air, a certain contribution to the counting rate in (C), in excess of ν. However, when averaged adequately over the mesotron spectrum, this shower effect appears as a small correction only.

THE preceding paper,[1] here referred to as II, describes experiments (III) which show that mesotrons are associated with particles present at several meters from the mesotron trajectories. At least a part of these particles are collision electrons ejected by these mesotrons along their path in the air.

The method used in these experiments consists of measuring the frequency of discharges occurring simultaneously (a) in a group of counter tubes, responding in principle only to mesotrons, and (b) in a counter tube located at a variable distance from that group. This group of counters, which will be called here mesotron selector or, in short, selector, is surrounded by a lead shield 10 cm thick; it consists of two counters in coincidence placed in a vertical plane, and of two side counters, connected in anticoincidence to the circuit of the two first counters. The principle of this selector is based on the assumption that any event in which the two counters in coincidence are discharged, but not any of the side counters, should be attributed to a penetrating particle, such as a mesotron, since a high energy soft particle would almost always emerge below the lead with a shower discharging at least one of the side counters.

The purpose of the present paper is to calculate the mean frequency of discharges in the distant counter, which arise from collision electrons ejected in air by those mesotrons which traverse simultaneously the selector.

A. NOTATIONS AND FORMULAS

1. The basic formulas for collision processes between mesotrons and electrons will be applied here in the form given by B. Rossi and K. Greisen.[2] The notations used below are similar to those of the authors quoted.

The velocity of light will be put $c = 1$; the velocity of a particle: $v = \beta c = \beta$; 1 Mev will be taken as a unit of energy and 1 meter as a unit of length. In that way, the rest mass of an electron μ_e or of a mesotron μ will be expressed by the same symbol as their respective rest energies. These energies are assumed to have the following values: $\mu_e = 0.5$ and $\mu = 100$. Instead of the mesotron momentum p, the ratio $r = p/\mu = \beta/(1-\beta^2)^{\frac{1}{2}}$ will mostly be used. This ratio r will be called the equivalent momentum of the mesotron.

2. As a result of a collision between a mesotron of momentum p and an electron, supposed to be free and initially at rest, the latter is projected at an angle θ with respect to the initial trajectory of the mesotron and acquires an energy E' given by

$$E' = 2\mu_e \frac{p^2 \cos^2\theta}{[\mu_e^2 + (p^2+\mu^2)^{\frac{1}{2}}] - p^2\cos^2\theta}. \quad (1)$$

[1] Anatole Rogozinski, Phys. Rev. **65**, 291 (1944).

[2] B. Rossi and K. Greisen, Rev. Mod. Phys. **13**, 240 (1941).

It will be seen later that the values of p to be taken into account for the present case will always be appreciably larger than μ. Therefore, neglecting μ_e^2 as well as μ^2 in comparison with p^2, and remembering that $2\mu_e=1$, (1) will be expressed by

$$E'=\frac{\cos^2\theta}{\sin^2\theta+1/r^2+1/p}. \tag{2}$$

3. It can be seen from (2) that, whatever the energy of the primary mesotron, one has always

$$E'<\cot^2\theta.$$

Thus, if, for example, $\theta=\pi/4$, the maximum energy which can be transferred to the collision electron by a mesotron of any energy is always less than 1 (Mev).

When $1/r^2\gg 1/p$, or $p\ll\mu^2=10^4$, that is, for momenta $p\ll 10^{10}$ ev/c, (2) can be written in the simpler form

$$E'=\frac{\cos^2\theta}{\sin^2\theta+1/r^2}. \tag{2'}$$

On the other hand, for $p\gg 10^{10}$ ev/c, (2) becomes

$$E'=\frac{\cos^2\theta}{\sin^2\theta+1/p}. \tag{2''}$$

For head-on collisions ($\theta=0$), E' reaches its maximum value E_m', given by

$$E_m'=1/(1/r^2+1/p)=\frac{p^2}{\mu^2+p}, \tag{3}$$

$$E_m'=r^2, \quad \text{for} \quad p\ll\mu^2, \tag{3'}$$

$$E_m'=p, \quad \text{for} \quad p\gg\mu^2. \tag{3''}$$

We shall use the expression (2') since it can be applied to the majority of the mesotrons present in the cosmic radiation. It should be understood, however, that for $p\gg\mu^2$, r^2 should eventually be replaced by p wherever it occurs in a formula which is derived originally from (2').

B. ASSUMPTIONS

The following assumptions are made: (a) The energy loss of the mesotron is neglected over a distance H_p which will be specified in the calculations; (b) the mesotron trajectory is a straight line, regardless of any collision processes which occur over the same distance H_p; (c) the scattering effects for both the mesotron and the collision electron are neglected; (d) the collision electrons lose energy only by ionization; the average ionization loss k per meter of standard air is taken as $k=0.25$ (Mev); the minimum energy E_1 necessary for the collision electron to penetrate the wall of a counter tube is of the order of a few Mev; (e) the atmosphere is homogeneous over the distance H_p considered in (a).

C. GEOMETRY; ENERGY FACTORS

Let us consider now a mesotron of momentum p, directed downwards along the axis Oz. At A, in a plane perpendicular to Oz at O, a counter tube (C) is placed whose effective dimensions are assumed to be small in comparison with $OA=D$ (see Fig. 1A).

This counter can be discharged by a collision electron of energy E' ejected at a point T, located at a distance $OT=H$ from the origin.

The total energy loss ($kD/\sin\theta+E_1$) suffered by the collision electron along the path $TA=D/\sin\theta$ in air, and by traversing the wall of the counter tube, should be such that

$$E'-(kD/\sin\theta+E_1)\geqslant 0, \tag{4}$$

or, replacing E' by the expression (2') and putting $\sin\theta=x$ one has

$$f(x)=x^3+ax^2+bx+c\leqslant 0, \tag{5}$$

with

$$a=kD/(E_1+1), \quad b=-(r^2-E_1)/r^2(E_1+1)$$

and

$$c=kD/r^2(E_1+1).$$

Collision electrons which satisfy (4) or (5) will be called "efficient" collision electrons.

It can be proved that the equation $f(x)=0$ has in general 3 roots: one negative, x_1, and two positive, x_2 and x_3, and that x should lie in between the positive roots in order to satisfy the physical conditions of the problem.

The general solution of (5) involves functions of the three parameters D, r, and E_1 requiring rather laborious calculations. It is more practical to proceed in the following way:

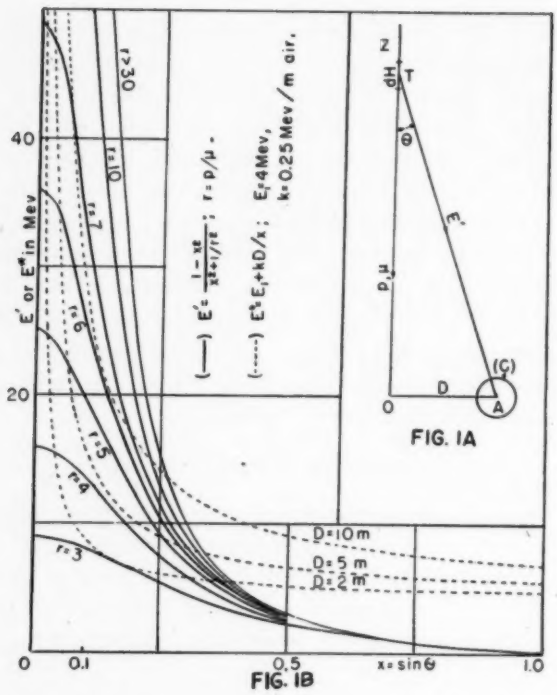

FIG. 1A

FIG. 1B

FIG. 1A. A mesotron of momentum p traveling along Oz ejects in T a collision electron of energy E' which discharges the counter tube (C) placed at a distance $OA=D$ from the mesotron trajectory.

FIG. 1B. Families of curves $E'=\cos^2\theta/(\sin^2\theta+1/r^2)$ and $E^*=E_1+kD/\sin\theta$ as a function of $x=\sin\theta$ for different values of the parameters $r=p/\mu$ and D [Eqs. (6) and (7)]. The minimum energy E_1 necessary for an electron to penetrate the wall of the counter (C) is taken $E_1=4$ Mev. In order to be able to discharge (C), a collision electron must be ejected at an angle θ such that $\sin\theta$ lies between the respective abscissae of the two points at which E' and E^* intersect.

Consider the two families of curves:

$$E'=(1-x^2)/(x^2+1/r^2) \tag{6}$$

and

$$E^*=E_1+kD/x \tag{7}$$

for different values of the parameters r, D, and E_1 as shown in Fig. 1B. The curves show that, in general, E' and E^* intersect at two points, the abscissae of which are identical with the two positive roots, x_2 and x_3, of the equation $f(x)=0$. One can also see that for any values of the parameters D and E_1 there exists a critical value $r_c(D, E_1)$ for which the corresponding curves E' and E^* are tangent to one another. The abscissa for the point of tangency gives directly the double root $x_d=x_2=x_3$, which $f(x)=0$ admits in this case.

For $r<r_c$ the roots are imaginary: This means, from the physical point of view, that mesotrons of momenta smaller than a certain critical momentum $p_c=\mu r_c$ will never project a collision electron which would be able to discharge the counter (C). On the other hand, it is easy to see that, for a given E_1, and for mesotrons of, say, $r=r_0$, collision electrons can discharge the counter only at distances D smaller than a certain critical distance $D_c(E_1, r_0)$. Beyond D_c, no collision electrons arising from mesotrons of $r<r_0$ are able to discharge the counter (C). The critical distance D_c can be determined best from the two families of curves E' and E^*, plotted as a function of $y=1/\sin\theta=1/x$,

$$E'=(y^2-1)/(y^2/r^2+1) \tag{6'}$$

and

$$E^*=E_1+kDy \tag{7'}$$

since then the family E^* is composed of straight lines (Fig. 2).

Table I gives approximate values of $r_c(D, E_1)$ for different distances D and for $E_1=4$ (Mev).

According to this table, if, for example, $D=5$ m, only mesotrons of momenta $p>4\times10^8$ ev/c will have to be considered at all.

It can be seen also from Figs. 1B and 2 that for $r>r_c$ the corresponding values of x_2 become small rapidly in comparison with x_3 and that x_3 can be considered as *independent of* r for values of r only

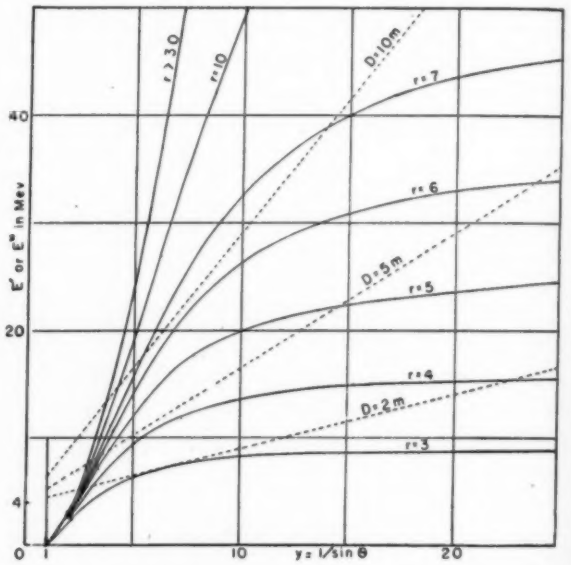

FIG. 2. Same families of curves E' and E^* as in Fig. 1B, but plotted as a function of $y=1/\sin\theta$ instead of $x=\sin\theta$ [Eqs. (6') and (7')].

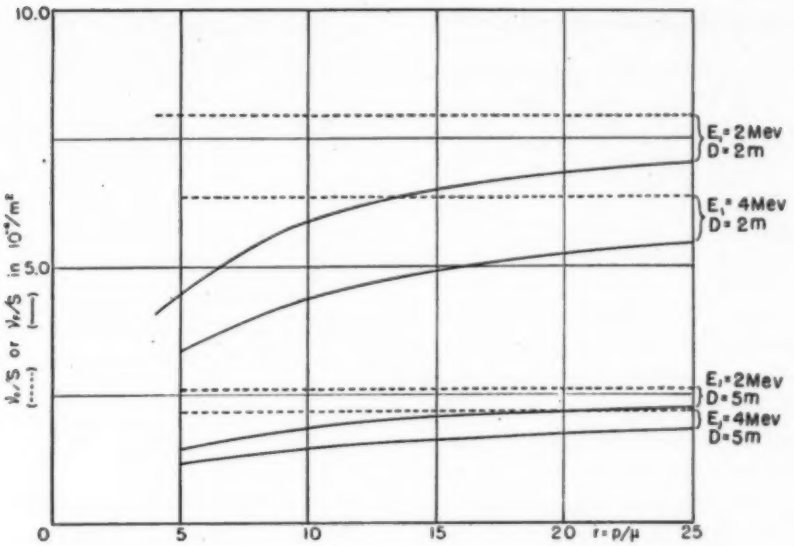

FIG. 3. Curves of ν/S expressed in m^{-2}, as a function of $r=p/\mu$ for different values of the parameters D and E_1. S is the effective area, in m^2, of the counter tube (C). In case of ν_F the mesotron spin (0 or $\frac{1}{2}$) is taken into account. When the spin term is neglected, and other less important approximations are made, ν reduces to ν_0, which is practically independent of the mesotron momentum.

slightly larger than r_c. In first approximation, this value of x_3 can be taken as equal to its asymptotic value $(x_3)_{\text{lim}}$ for $r\to\infty$. $(x_3)_{\text{lim}}$ can be calculated easily in this case from (5), which becomes then:

$$f(x)=x^2+\frac{kD}{E_1+1}x+\frac{1}{E_1+1}=0. \tag{8}$$

For $D<\sim 20$ meters, one obtains

$$(x_3)_{\text{lim}}\simeq\frac{1}{(E_1+1)^{\frac{1}{2}}}\left[1+\frac{k^2D^2}{8(E_1+1)}\right]-\frac{kD}{2(E_1+1)}. \tag{9}$$

If D is small, $(x_3)_{\text{lim}}\to(E_1+1)^{-\frac{1}{2}}$.

Table II gives certain values of $(x_3)_{\text{lim}}$, for different values of E_1 and D.

From the fact that x_2 becomes small rapidly in comparison with x_3, for $r>r_c$, one can show that, with a good approximation,

$$x_2=\frac{kD}{r^2-E_1}. \tag{10}$$

The values of x_2 and x_3 determine the "useful" portion $H_p=H_2-H_3$ of the mesotron trajectory which, through the collision electrons ejected along H_p, contributes to the discharges of the counter (C). The collision electrons ejected below $H_3=D\cot\theta_3$ and above $H_2=D\cot\theta_2=D/x_2-(1/k)(r^2-E_1)$, have insufficient energies to reach the counter and to penetrate its wall. Since $\cot\theta_3$ has a value comparable to unity and is practically independent of the mesotron momentum for $r>r_c$, H_3 is practically of the same order of magnitude as D, for all momenta of the mesotron considered. On the other hand, H_2 is a strongly increasing function of r, but it is practically independent of D. For example, for $r=10$, that is, for $p=10^9$ ev/c, $H_2=400$ meters. Hence, the useful portion H_p of the mesotron trajectory is approximately given by H_2.

TABLE I. Values of $r_c(D, E_1)$ for $E_1=4$ (Mev).

D meters	2	5	10
r_c	3	4	6

TABLE II. Values of $(x_3)_{\text{lim}}$.

E_1 (Mev)	D meters 2	5	10
2	0.50	0.41	0.30
4	0.40	0.34	0.27

D. COLLISION PROBABILITIES

The probability for a mesotron of momentum p and of velocity β to project, over a distance dH of its trajectory, collision electrons of energy between E' and $E'+dE'$ is given by

$$PdE'dH=\frac{B}{\beta^2}\frac{1}{E'^2}(1-F)dE'dH. \quad (11)$$

For standard air, if E' is expressed in Mev and H in meters, one obtains $B=0.98\times10^{-2}\simeq10^{-2}$.

The term F depends upon the mesotron spin which is not yet known. However, the results of experiments[3] on bursts occurring in an ionization chamber shielded by absorbers of different atomic number show a considerable disagreement with the hypothesis of mesotrons of spin 1; the agreement is much better for spin 0 or spin $\frac{1}{2}$. For these reasons, only the latter values of the mesotron spin will be considered here.

One has

$$F=\beta^2E'/E_m' \quad \text{for spin } 0 \quad (12)$$

and

$$F=\beta^2E'/E_m'-E'^2/2(p^2+\mu^2) \quad \text{for spin } \tfrac{1}{2}.$$

In case of spin $\frac{1}{2}$, the maximum value of the second term of F is equal to $p^4/2(p+\mu^2)^2(p^2+\mu^2)$ [see (3)]; for $p\ll\mu^2$, this term is always negligible; it is equal to $\frac{1}{8}$, for $p=\mu^2$, and approaches $\frac{1}{2}$, for $p\gg\mu^2$. When averaged over the mesotron spectrum, this term will constitute only a very small correction, and therefore, no distinction will be made in the present calculations between spin 0 and spin $\frac{1}{2}$.

For small values of E', one obtains in all cases practically $F=0$, and P then reduces to the Rutherford formula

$$P=B/\beta^2E'^2. \quad (13)$$

E. FREQUENCY OF THE EFFICIENT COLLISION ELECTRONS

(a) Approximate Formulas

1. Let N be the mean number of mesotrons per unit time following the axis Oz and $Ng(r)dr$ their fraction with equivalent momenta between r and $r+dr$. The function $g(r)$ represents the differential mesotron spectrum. The integral mesotron spectrum will be represented by the symbol $G(r)=\int_0^r g(r)dr$.

The differential spectrum $g(r)$ is normalized by

$$\int_0^\infty g(r)dr=1. \quad (14)$$

2. It will be assumed first $F=0$.

The mean number ν of collision electrons arising from a mesotron and able to discharge the counter tube (C) is given by

$$\nu=\int_{H_3}^{H_2}dH\int_{(\Delta E')}PdE'. \quad (15)$$

In (15), H_2 and H_3 determine the useful portion $H_p=H_2-H_3$ of the mesotron trajectory and are given, in first approximation, by (9) and (10), respectively. The energy difference $(\Delta E')$ is defined in the following way:

Let us consider first two cones forming angles θ and $\theta+d\theta$ with respect to their common axis Oz, and having T as their common vertex (Fig. 1A). The energy interval of the collision electrons ejected along dH into the solid angle $d\omega=2\pi\sin\theta d\theta$ which is comprised between the two cones is

$$dE'=\frac{1}{2\pi\sin\theta}\frac{dE'}{d\theta}d\omega. \quad (16)$$

Let d be the effective diameter of the counter tube (C), l, its effective length, and $S=d\times l$, its effective area. Since we have assumed that the two dimensions of the counter are small in comparison with D, the values of E', P, and $dE'/d\theta$ can be considered as constant all over the area S which defines a solid angle $\Delta\omega=S/(AT)^2=S\sin^2\theta/D^2$; thus,

$$\int_{(\Delta E')}PdE'=\int_{(\Delta\omega)}\frac{P}{2\pi\sin\theta}\frac{dE'}{d\theta}d\omega=\frac{S\sin\theta}{2\pi D^2}P\frac{dE'}{d\theta}. \quad (17)$$

On the other hand $dH=-(D/\sin^2\theta)d\theta$; hence,

$$\nu_{F=0}=\int_{H_3}^{H_2}dH\int_{(\Delta E')}PdE'=\frac{BS}{\pi D}\frac{1+r^2}{r^2}\int_{\theta_{\min}}^{\theta_{\max}}\frac{d\theta}{\cos^3\theta}, \quad (18)$$

[3] M. Schein and P. S. Gill, Rev. Mod. Phys. **11**, 267 (1939). R. F. Christy and S. Kusaka, Phys. Rev. **59**, 405, 414 (1941). S. Kusaka, Phys. Rev. **64**, 256 (1943). R. E. Lapp, Phys. Rev. **64**, 255 (1943).

where $\theta_{\min}=\arcsin x_2\simeq kD/(r^2-E_1)$ and $\theta_{\max}=\arcsin x_3$. The angle $\theta_{\max}$, as well as x_3, can be considered as independent of $r>r_c$.

Developing in (18) $\cos^3\theta$ in a series, one obtains

$$\nu_{F=0}=\frac{BS}{\pi D}\frac{1+r^2}{r^2}(\theta_{\max}+\tfrac{1}{2}\theta_{\max}{}^3-\theta_{\min}+\cdots), \quad (19)$$

where the terms neglected in the parenthesis are of power $\geqslant 5$ for $\theta_{\max}$, and of power $\geqslant 3$ for $\theta_{\min}$.

It has been seen that except for values of r very close to r_c, the value of x_2 or $\theta_{\min}$ is small in comparison with $\theta_{\max}$. Therefore, in first approximation, $\nu_{F=0}$ is equal to

$$\nu_0=\frac{BS}{\pi D}\theta_{\max}. \quad (20)$$

It should be emphasized that within the limits of the approximations assumed, the value of ν_0 which represents the contribution of a single mesotron to the number of discharges in the counter (C) is practically independent of the momentum of that mesotron; this is true in spite of the fact that the useful portion of the mesotron trajectory increases approximately proportional to r^2.

3. The mean frequency n of discharges in the counter (C) is given thus by:

$$n=\int_{r_c}^{\infty}Ng(r)dr\int_{H_3}^{H_2}dH\int_{(\Delta E')}PdE'$$

$$=N\int_{r_c}^{\infty}g(r)\nu_{F=0}dr. \quad (21)$$

In order to correlate n with those mesotrons which effectively discharge the selector, one should remark here that N is the frequency of the mesotrons which would be recorded by a hypothetical *unshielded* mesotron selector. In traversing the 10-cm thickness of the lead shield which, in fact, covers the selector (see II), all mesotrons of a range not larger than 10 cm of Pb are stopped. Let r_1 be the maximum equivalent momentum of these stopped mesotrons. The frequency of discharges in the mesotron selector N_{sel} will then be equal to

$$N_{sel}=N\int_{r_1}^{\infty}g(r)dr=N[1-G(r_1)]. \quad (22)$$

The exact shape of the differential mesotron spectrum, at least on the ground, is not yet known at its very low end. There are, however, experimental reasons to believe that the fraction of mesotrons with energies smaller than a few times 10^8 ev is rather small. Since for 10 cm of Pb one has $r_1\simeq 2.5$, corresponding to a mesotron energy of 1.7×10^8 ev, $G(r_1)$ can be considered as small and probably not larger than a few percent.

Taking into account (22), and using for ν its value from (20), one finds that n is given, in first approximation, by

$$n_0=N_{sel}\frac{1-G(r_c)}{1-G(r_1)}\frac{BS}{\pi D}\theta_{\max}. \quad (23)$$

According to Table I, the critical value r_c represents mesotron momenta of the order of a few times 10^8 ev/c. Therefore, $G(r_c)$ is, like $G(r_1)$, small and the ratio $[1-G(r_c)]/[1-G(r_1)]\simeq 1-G(r_c)+G(r_1)$ is approximately equal to 1. Hence,

$$n_0=N_{sel}\frac{BS}{\pi D}\theta_{\max}. \quad (24)$$

This (approximate) formula, which gives the frequency of discharges in a counter of effective area S placed at a distance D from the mesotron selector whose proper frequency of discharges is equal to N_{sel}, can be compared directly with the experimental data.

(b) Correction for the Mesotron Spin

In obtaining the above result the spin dependent factor F was neglected. It will now be taken into account (see Section D) in the case of spin 0, for which $F=\beta^2E'/E_m'$, and it will be assumed that $\beta=1$.

Only the final result of the evaluation of

$$\nu_F=\int_{H_3}^{H_2}dH\int_{(\Delta E')}P(1-F)dE' \quad (25)$$

will be given here. One finds:

$$\nu_F=\frac{BS}{\pi D}\left[\theta_{\max}+\frac{1+r^2}{2r^2}\theta_{\max}{}^3-\theta_{\min}-\frac{1}{r}h(r)\right],$$
$$h(r)=\arctan(r\sin\theta_{\max})-\arctan(r\sin\theta_{\min}). \quad (26)$$

For $r>30$, $h(r)$ can be considered as equal to its asymptotic value of $\pi/2$. On the other hand, the formula (26) shows immediately that ν_F approaches asymptotically ν_0 as r increases.

Table III gives $h(r)/r$ for different values of E_1 and D.

TABLE III. Values of $10^2\times h(r)/r$.

E_1 (Mev)	D meters	r 4	5	6	7	8	9	10	20	30
2	2	24.5	22	19.7	17.6	15.9	14.4	13.3	7.2	4.9
2	5	—	17.4	16.6	15.4	14.2	13.2	12.2	7.1	4.8
4	2	21	19	18	16	15	14	13	7.1	4.8
4	5	—	15.4	14.8	14	13	12.4	11.6	7.0	4.7

In Fig. 3 the values of ν_0/S and ν_F/S are plotted as a function of r.

When F is taken into account, a graphical integration of $\int g(r)\nu_F dr$ will give the final result for n since $g(r)$ is an empirical function.

F. INFLUENCE OF THE SHOWER PRODUCTION BY THE EFFICIENT COLLISION ELECTRONS

So far, we have considered single collision electrons losing energy only by ionization and discharging directly the counter tube (C). We know, however, that when the energy of such an electron is larger than its critical energy E_{cr}, which is equal to $\sim 10^8$ ev for air, it can undergo a multiplication by successive radiation and pair production processes. As a result of this multiplication, the average range of the produced shower is smaller than would be the range of its parent collision electron if it would not have multiplied. Therefore, in order to produce any effect on the counting rate in (C), *in excess of* ν, the energy of the shower particles arising from an efficient collision electron must be high enough to reach and to traverse the wall of the counter, otherwise the above effect could become even negative. On the other hand, to obtain an appreciable effect, the number of these shower particles should be, in addition, not too low; therefore, the energy E' of the collision electron and the distance $R=D/\sin\theta$, which separates the point of its ejection on the mesotron trajectory from the counter tube, would have to be appreciably larger than $E_{cr}(\sim 10^8$ ev) and λ_0, respectively, $\lambda_0(\sim 300$ meters) representing the radiation unit of length in air.

Let ν_s be the number of discharges in (C), *in excess of* ν, arising indirectly, by the shower particles, from a collision electron ejected in air by a mesotron of momentum p. Let, furthermore, $\sigma=\nu_s/\nu$ be the relative shower effect. One has $\sigma\equiv 0$ as long as $E'\ll E_{cr}$. On the other hand, it can be understood easily that provided $R>\sim\lambda_0$, the factor σ passes a negative minimum (a) when $E'>E_{cr}$ remains close to E_{cr} and (b) for E' remaining in the neighborhood of the highest energy [see Figs. 1B, 2 and Eq. (10)] which an efficient collision electron can possess and which is given by $1/(\theta_{\min}{}^2+1/r^2)\simeq E_m'$. Indeed, in both cases, if a multiplication of the collision electron takes place, the energy of any of the produced shower particles will be too small to reach and to discharge the counter.

An upper limit of σ can be obtained as follows: According to the theory of cascade showers the average maximum number ψ of shower particles of energy larger than E_{cr}, produced by an electron of energy $E'\gg E_{cr}$, is given by $\psi=E'/6E_{cr}$. If one considers only values of E' for which $\psi\gtrsim\psi_0$, one has evidently $E'\gtrsim E_{\psi 0}'=6\psi_0 E_{cr}$. The above maximum occurs for a thickness $t\simeq\lambda_0\log(E'/E_{cr})$ of material in which the shower develops. In the present case only small values of θ will have to be considered. At any rate, $\theta<\theta_s=D/\lambda_0$. For $D<10$ m, $\theta_s\simeq 10^{-2}$.

Thus [compare (17)], neglecting θ^2, θ^3, $\cdots$ in comparison with θ,

$$\sigma<\frac{1}{\nu}\int_{D\cot\theta_s}^{D\cot\theta_{\min}}dH\int_{(\Delta E')}P(1-F)\psi dE'$$
$$=\frac{1}{\nu}\frac{BS}{2\pi D\times 6E_{cr}}\int_{E_{\psi 0}'}^{E_m'}\theta dE'. \quad (27)$$

It can be shown that for $p\ll 1/\theta_s{}^2$, that is, $p\ll\sim 10^{10}$ ev/c, and consequently also for $E_m'\ll 1/\theta_s{}^2$, the integral

$$\int_{E_{\psi 0}'}^{E_m'}\theta dE'<\theta_s(E_m'-E_{\psi_0}')$$

and σ is smaller than a few percent. The factor σ increases with increasing p. For $p \gg 1/\theta_s^2$, the integral

$$\int_{E_{\psi_0}'}^{E_m'} \theta dE' \rightarrow \frac{\pi}{2} p^{\frac{1}{2}},$$

hence,

$$\sigma < \frac{1}{\nu} \frac{BS}{2\pi D} \frac{\pi}{12E_{cr}} p^{\frac{1}{2}}. \tag{28}$$

Since the mesotron momenta to be considered in this case are very high, ν can be replaced by ν_0. Now, $BS/\nu_0 2\pi D$ is approximately equal to 1. Therefore

$$\sigma < (\pi/12E_{cr}) p^{\frac{1}{2}}. \tag{29}$$

It can be seen from (29) that σ will still remain smaller than 1 even for $p = (12E_{cr}/\pi)^2$, that is, for mesotron momenta as high as 1.5×10^{11} ev/c.

It will be sufficient to remember that the frequency of the mesotron momentum in the differential mesotron spectrum decreases as $p^{-\gamma}(\gamma > 2)$ to make clear that the shower effect of the collision electrons, when averaged adequately over the mesotron spectrum, adds a very small contribution only to the frequency of discharges in the counter tube (C).

G. ALTITUDE EFFECT

Concerning ν, the only terms which in (20) or (26) depend upon the altitude, that is, upon the density of air, are B, $\theta_{\max}$, and $\theta_{\min}$. The variation of $\theta_{\min}$, which is anyway very small, can be neglected. The coefficient B is directly proportional to the density of air, and $\theta_{\max}$ depends upon this density only through the coefficient k. But, as can be seen from Figs. 1B or 2, $\theta_{\max}$ depends, at least for small distances D, very little upon k. For example, for $E_1 = 4$ Mev and $D = 2$ m, $\theta_{\max}$ would increase from ~ 0.40 at sea level ($k = 0.25$), to ~ 0.45 only at the top of the atmosphere ($k = 0$). Therefore, in first approximation, one can admit that ν is proportional to the density of air or to the atmospheric pressure. On the other hand, the effect of the altitude on the frequency n of discharges [see (21)] in the counter tube (C) follows, in the general case, the combined effects of: (a) the altitude increase of the intensity of the mesotron radiation, (b) the altitude dependence of the mesotron spectrum and, (c) the decrease of ν which, as has been seen above, is roughly proportional to the atmospheric pressure.

PHYSICAL REVIEW VOLUME 65, NUMBERS 11 AND 12 JUNE 1 AND 15, 1944

On the Perturbation of Boundary Conditions

HERMAN FESHBACH
George Eastman Research Laboratories, Massachusetts Institute of Technology, Cambridge, Massachusetts

(Received February 25, 1944)

The solution of both the scalar and vector wave equations in regions which are bounded by irregular surfaces which have non-uniform physical properties has been reduced to the solution of a secular equation. The secular determinant is Hermitian. The solution to the secular equation has been expressed in a form suitable for obtaining its value to any approximation. Similar results are given for the corresponding eigenfunctions. Extension of these results to the problem of scattering and to the situation where the bounding surfaces move is indicated. The description of a source located in such a region is also discussed.

I. INTRODUCTION

THE solution to many physical problems can be reduced to the solution of a system of partial differential equations with prescribed boundary conditions. In the past, exact solutions were limited to those cases in which the boundary conditions were "simple" and were satisfied on "simple" surfaces. "Simple" boundary conditions correspond to uniform physical properties of the surface involved. "Simple" surfaces are coordinate surfaces of coordinate systems in which the partial differential equations will separate. As a result, a great many physical problems of interest have not been treated theoretically.

This paper will discuss solutions of the scalar and vector wave equations satisfying non-simple

boundary conditions on non-simple surfaces. The scalar wave equation has been investigated previously by means of a perturbation technique in which results were sought for conditions in which the variation from simple boundaries and boundary conditions were small. First-order corrections to the unperturbed eigenvalue have been found by Froelich,[1] Brillouin,[2] and Cabrera.[3] First-order corrections to the wave functions, and second-order corrections to the eigenvalue in some cases, have been given in I.[4] Results have been given in the latter both for the case of discrete and continuous eigenvalues. Applications of I have been made to the acoustics of irregularly-shaped rooms yielding good agreement with experiment.[5]

The methods used here are not a continuation or extension of those used in I. Rather, a new method based on the use of Green's functions is employed. Formulae are given permitting the calculation not only of improved first-order results, but also of all the higher orders. The problem of discrete eigenvalues is reduced to the solution of a secular determinant.

The scalar and vector wave equations can be used to describe phenomena occurring in the fields of acoustics, elasticity, and electromagnetic theory. For example, our results can be used to treat the acoustics of irregularly-shaped rooms, scattering from irregularly-shaped objects, propagation down irregularly-shaped pipes. Moreover, simple boundary conditions need not be obeyed. For example, the walls of an irregularly-shaped room might be absorbing.

The same technique can be applied to the determination of source functions satisfying certain prescribed boundary conditions. These functions can be used in the solution of inhomogeneous wave equations. Application can be made, for example, to the calculation of the sound field due to a source placed in an irregularly-shaped room.

II. STATEMENT OF PROBLEM

The equations to be discussed can be grouped according to type of boundary condition. The methods used in their solution vary in the same way although the general basic idea remains the same. In all cases, the equation is to be satisfied in a region R bounded by a surface S. The boundary conditions are to be satisfied on S.

The scalar wave equation to be considered is:

$$\nabla^2\varphi+k^2\varphi=0. \tag{2.1}$$

The boundary conditions satisfied by φ can be stated generally as $\partial\varphi/\partial n=F\varphi$ where F is a function which may vary on surface S. In acoustics, F is related to the acoustic impedance. The outwardly drawn normal to the surface is designated by n. We distinguish two cases:

$$\begin{aligned} &\text{B.C.I} \quad \partial\varphi/\partial n=F\varphi \qquad\qquad F \text{ small},\\ &\text{B.C.II} \quad \varphi=(1/F)(\partial\varphi/\partial n) \quad F \text{ large}. \end{aligned} \tag{2.2}$$

Simple boundary conditions are limiting cases of (2.2). They are:

$$\begin{aligned} &\text{B.C.IA} \quad \partial\varphi/\partial n=0,\\ &\text{B.C.IIA} \quad \varphi=0. \end{aligned} \tag{2.3}$$

A general vector wave equation occurs in the theory of elasticity and may be written in the following form:

$$\alpha \text{ grad div } \mathbf{s}+\beta\nabla^2\mathbf{s}+\kappa^2\mathbf{s}=0, \tag{2.4}$$

where α and β are constants of the material. The vector $\mathbf{s}$ can always be split into two vectors $\mathbf{A}$ and $\mathbf{B}$ such that div $\mathbf{A}=0$, curl $\mathbf{B}=0$. In the latter case, a scalar potential can be defined and the vector equation reduced to a scalar one. In the first case, the vector equation can be written

$$\text{curl curl } \mathbf{A}-k^2\mathbf{A}=0 \tag{2.5}$$

where $k^2=\kappa^2/\beta$. This equation is also satisfied by the vector potential of the electromagnetic field. The boundary conditions satisfied by $\mathbf{A}$ can be stated generally as

$$(\mathbf{n}\times\mathbf{A})=(\mathbf{n}\times\text{curl } \mathbf{A})\cdot\mathfrak{Z} \tag{2.6}$$

where $\mathfrak{Z}$ is a dyadic. Two cases can again be distinguished

$$\begin{aligned} &\text{B.C.III} \quad (\mathbf{n}\times\mathbf{A})\\ &\qquad\qquad =(\mathbf{n}\times\text{curl } \mathbf{A})\cdot\mathfrak{Z} \quad \mathfrak{Z} \text{ small},\\ &\text{B.C.IV} \quad (\mathbf{n}\times\text{curl } \mathbf{A})\\ &\qquad\qquad =(\mathbf{n}\times\mathbf{A})\cdot\zeta \quad \zeta \text{ small}, \end{aligned} \tag{2.7}$$

[1] H. Froelich, Phys. Rev. **54**, 945 (1938).
[2] L. Brillouin, Comptes rendus **204**, 1863 (1937).
[3] N. Cabrera, Comptes rendus **207**, 1175 (1938).
[4] H. Feshbach and A. M. Clogston, Phys. Rev. **59**, 189 (1941). This paper will be referred to as I.
[5] Bolt, Feshbach, and Clogston, J. Acous. Soc. Am. **14**, 65 (1942).

where $\zeta=(\mathfrak{Z})^{-1}$ and we have assumed that the determinant of the dyadic $\mathfrak{Z}$ does not vanish. In electromagnetic theory $\mathfrak{Z}$ is related to the dyadic impedance. The simple boundary conditions are

$$\begin{aligned} &\text{B.C.IIIA} \qquad (\mathbf{n}\times\mathbf{A})=0, \\ &\text{B.C.IVA} \qquad (\mathbf{n}\times\operatorname{curl}\mathbf{A})=0. \end{aligned} \tag{2.8}$$

Case III can be reduced to case IV and vice versa. Since div $\mathbf{A}=0$, a vector $\mathbf{D}$ can be defined satisfying the relation $\mathbf{A}=\operatorname{curl}\mathbf{D}$. The wave equation obeyed by $\mathbf{D}$ is the same as that for $\mathbf{A}$. Boundary conditions III become $(\mathbf{n}\times\operatorname{curl}\mathbf{D})=k^2(\mathbf{n}\times\mathbf{D})\cdot\mathfrak{Z}$. This is in the form given by boundary condition IV.

All these cases will be considered separately for both the discrete and continuous eigenvalue problems. The general technique to be used consists of reducing equations (2.1) and (2.5) to their corresponding integral equations by means of a Green's function. This has the advantage of introducing the boundary condition directly into the equation to be solved rather than its usual use as an auxiliary condition imposed on the solution. From these integral equations approximate formulae can be immediately derived. Solutions of the equations will then be derived by the method of successive approximations, and by expansion of the solution in eigenfunctions. The latter method leads to a secular equation.

Boundary condition I will be discussed in detail. The procedure to be used in the other cases will be outlined. Only specific differences from the treatment for boundary condition I will be noted. General remarks, unless otherwise noted, will be valid throughout.

III. BOUNDARY CONDITION I $\partial\phi/\partial n=F\phi$

The reduction of Eq. (2.1) to its equivalent integral equation is made possible by the use of a Green's function satisfying the inhomogeneous equation

$$\nabla_\xi^2 G_k(x,\xi)+k^2G_k(x,\xi)=\delta(x-\xi), \tag{3.1}$$

where x represents the observation point, ξ the source point. $\delta(x-\xi)$ is the Dirac δ function. The subscript k is used to show that G_k is the Green's function corresponding to the wave number k.

G_k must satisfy Eq. (3.1) throughout a region R_0 which includes the region R. Moreover, it can satisfy any convenient boundary condition on the surface S_0 of R_0. Usually, S_0 is a simple surface and the boundary conditions simple ones.

Combining (2.1) and (3.1) we obtain:

$$\varphi(x)=\int\Big[\varphi(\xi)\frac{\partial G_k(x,\xi)}{\partial n_\xi}-G_k(x,\xi)\frac{\partial\varphi(\xi)}{\partial n_\xi}\Big]dS_\xi \tag{3.2}$$

where the integration is performed over surface S.

Introducing boundary condition I we have

$$\varphi(x)=\int\varphi(\xi)\Big[\frac{\partial G_k(x,\xi)}{\partial n_\xi}-F(\xi)G_k(x,\xi)\Big]dS_\xi. \tag{3.3}$$

The result for the simple boundary condition IA follows immediately.

An important special case occurs when S is a simple surface. Choosing a G_k satisfying boundary condition IA on S we obtain:

$$\varphi(x)=-\int\varphi(\xi)F(\xi)G_k(x,\xi)dS_\xi. \tag{3.4}$$

Equation (3.3) satisfies Eq. (3.1) as can be seen immediately by substitution of (3.3) in (2.1). Thus we can conclude that this integral equation is equivalent to the original differential equation and automatically includes the boundary condition.

Equation (3.3) states that it is possible to predict the required wave function in the interior of R by means of a proper distribution of sources on the surface S. This is essentially a statement of Huygens' principle differing from the usual formulation in the use of a general Green's function and the direct introduction of the boundary conditions. Huygens' principle has been previously used in discussing scattering and diffraction problems.[6]

Equations (3.3) and (3.4) can be reduced to a "true" integral equation involving only values of the unknown function on the surface S by noting that they can be used to predict the value

[6] See, for example: H. Lamb, *Hydrodynamics* (Cambridge University Press, 1932), p. 517; A. Sommerfeld, *Die Differential und Integralgluchungen der Mechanik und Physik* (Friedr. Vieweg. und Sohn, Braunschweig, 1935), Vol. 2, p. 853.

of φ on the surface. The resulting equation has a symmetric kernel and will involve one dimension less than the original integral equation. This procedure is used in discussions of potential theory.[7] It is particularly advantageous in those cases for which the boundary perturbation has a simple geometry, for then the equation may often be solved in closed form. It is also useful in two-dimensional problems since the resulting integral equation will be in one dimension and therefore susceptible to numerical techniques. Finally, if the perturbation is small compared to the wavelength, the kernel can be replaced by the simpler kernel of potential theory and the problem reduced to a potential problem. Once the value of φ on S is known, the value of φ in the interior can be immediately calculated from (3.3).

This method is complicated in the case of (3.3) by the fact that φ, being zero outside of R is discontinuous at the surface S. (Cf. Appendix I.) We shall, therefore, specify the value of φ at a point on the surface by approaching the point from the interior of R. In the case of (3.4), the solution φ has a discontinuity in slope at S. These discontinuities limit the rapidity of convergence of an expansion of φ in orthonormal functions.

It is very useful to separate the integral in Eq. (3.3) into two parts, one of which is known. This is particularly true if the known part is a good approximation to the unknown φ.

Suppose the known part ψ_n is a member of an orthonormal set of functions 0 satisfying (2.1) in a region R_0 including region R and satisfying convenient boundary conditions on S_0. G_k can then be expressed by means of an expansion in set 0. The term containing ψ_n can then be separated from the remaining terms of the expansion and its coefficient adjusted to one by means of a proper choice of normalization condition. Equation (3.3) becomes

$$\varphi(x)=\psi_n(x)+\int' \varphi(\xi) \times\left[\frac{\partial G_k(x,\xi)}{\partial n_\xi}-F(\xi)G_k(x,\xi)\right]dS_\xi, \quad (3.5)$$

where the prime on the integral sign indicates that the term involving ψ_n in the surface integral is to be omitted. The normalization condition is

$$\int_{R_0}\varphi\psi_n dV=1. \quad (3.6)$$

This is stated correctly only for the case of discrete eigenvalues. It can be extended to continuous eigenvalues by integrating the integral in (3.6) over a small volume element in wave number space corresponding to the wave numbers associated with ψ_n.

A second method employs the fact that (3.2) is satisfied by any solution of the wave equation and therefore by ψ_n. We must note, however, that (3.2) yields ψ_n only inside R and yields zero outside R. Let us call this discontinuous function Ψ_n. We now find that

$$\varphi(x)=\Psi_n(x)+\int\left\{[\varphi(\xi)-\psi_n(\xi)]\frac{\partial G_k(x,\xi)}{\partial n_\xi} -G_k(x,\xi)\left[F(\xi)\varphi(\xi)-\frac{\partial\psi_n}{\partial n_\xi}\right]\right\}dS_\xi. \quad (3.7)$$

Forms (3.5) and (3.7) yield exactly the same values for φ within region R. However, they behave differently outside of R leading to a different analytical behavior at S. Expansions of φ in orthonormal functions will have different rates of convergence depending on whether (3.5) or (3.7) is used.

Our attention, so far, has been focused on the wave function φ. However, the eigenvalue k^2 is of equal importance since it is needed for the specification of G_k. Suppose the eigenvalue associated with ψ_n is K_n^2. Using Green's theorem, it can be shown that

$$k^2=K_n^2+\int\left[\varphi\frac{\partial\psi_n}{\partial n}-\psi_n\frac{\partial\varphi}{\partial n}\right]dS\Big/\int_R\psi_n\varphi dV. \quad (3.8)$$

Introducing boundary condition I we find:

$$k^2=K_n^2+\int\varphi\left(\frac{\partial\psi_n}{\partial n}-F\psi_n\right)dS\Big/\int_R\psi_n\varphi dV. \quad (3.9)$$

A similar formula can be derived for the case of the continuous spectrum by performing a second integration in wave number space as described for formula (3.6).

[7] O. D. Kellogg, *Foundations of Potential Theory* (Frederick Unger Publishing Company, New York, 1929), p. 286.

Our problem has now been reduced to the solution of integral equation (3.3) which implicitly contains the boundary condition to be satisfied. Approximate formulae can be derived at once. If $\varphi \simeq \psi_n$, then from (3.5)

$$\varphi(x) \simeq \psi_n(x) + \int' \psi_n(\xi) \times \left[\frac{\partial G_k(x,\xi)}{\partial n_\xi} - F(\xi) G_k(x,\xi)\right] dS_\xi. \quad (3.10a)$$

From (3.7), one finds

$$\varphi(x) \simeq \Psi_n(x) - \int G_k(x,\xi) \times \left[F(\xi)\psi_n(\xi) - \frac{\partial \psi_n(\xi)}{\partial n_\xi}\right] dS_\xi. \quad (3.10b)$$

Formulae (3.10a) and (3.10b) are equivalent as has been pointed out above. The eigenvalue becomes:

$$k^2 \simeq K_n^2 + \int \psi_n \left(\frac{\partial \psi_n}{\partial n} - F\psi_n\right) dS. \quad (3.11)$$

This formula has been given previously. The eigenvalue can be found to a second approximation by using the first approximation results for the wave function.

The use of these results depends upon our knowledge of G_k. The latter is sometimes known in closed form, but then, the integrations are often unmanageable. In such case, it is useful to expand G_k in a series in set 0 as follows:

$$G_k(x,\xi) = \sum_t \frac{\psi_t(x)\psi_t(\xi)}{k^2 - K_t^2}. \quad (3.12)$$

This expansion will now be introduced into (3.10b) for this yields the more rapidly converging result.

$$\varphi(x) \simeq \Psi_n(x) + \sum_t' \frac{A_{tn}\psi_t(x)}{K_n^2 - K_t^2} \quad (3.13)$$

where the prime indicates omission of the $n=t$ term in the summation and

$$A_{tn} = \int \psi_t \left(\frac{\partial \psi_n}{\partial n} - F\psi_n\right) dS. \quad (3.14)$$

Expansion (3.13) can be introduced into (3.9) to yield a second approximation for the eigenvalue:

$$k^2 = K_n^2 + A_{nn}/N_{nn} + \sum_t' \frac{A_{tn}^2}{K_n^2 - K_t^2} \quad (3.15)$$

where

$$N_{tn} = \int_R \psi_t \psi_n dV. \quad (3.16)$$

Formulae equivalent to (3.13) and (3.15) have been given previously in I. They have been applied to the acoustics of trapezoidally shaped rooms and agree with experiment within the range of their validity.

The convergence of the series for φ given by (3.13) is fairly good, the tth term behaving asymptotically as $1/K_t^2$. This is sufficient to permit its introduction into (3.5) or (3.7) to yield a next approximation for the wave function. The resulting series will behave asymptotically as $1/K_t$ and could not be used to find either the next approximation to the eigenfunction φ or eigenvalue k^2.

One method of improving convergence would be to find a function which converges asymptotically as $1/K_t^2$ and subtract it from (3.13). The function χ satisfying

$$\chi(x) = -\int G_0(x,\xi) \times \left[F(\xi)\psi_n(\xi) - \frac{\partial \psi_n(\xi)}{\partial n_\xi}\right] dS_\xi \quad (3.17)$$

is of this type. On substitution of (3.12) into (3.17) one finds an expansion of the (3.13) type with k replaced by 0. χ is the solution of Laplace's equation for region R, with a source distribution $F\psi_n - (\partial\psi_n/\partial n)$. χ can often be calculated in closed form especially for two-dimensional problems. If this is so, the next approximation for φ can be found by introducing the amended (3.13) for Ψ_n in (3.7). Successive approximations could be found by continuing this procedure.

These difficulties do not appear when S is a simple surface. It is possible to find the solution

of the subsequent integral equation by means of the method of successive substitutions. This yields:

$$\varphi=\psi_n+\sum_t{}'\frac{F_{tn}}{k^2-K_t^2}\psi_t + \sum_{t,s}{}''\frac{F_{ts}F_{sn}}{(k^2-K_t^2)(k^2-K_s^2)}\psi_t + \sum_{s,t,n}{}'''\frac{F_{ts}F_{sr}F_{rn}}{(k^2-K_t^2)(k^2-K_s^2)(k^2-K_r^2)}\psi_t+\cdots, \quad (3.18)$$

$$k^2=K_n^2+F_{nn}+\sum{}'\frac{(F_{tn})^2}{k^2-K_t^2} + \sum{}''\frac{F_{ts}F_{sn}F_{tn}}{(k^2-K_s^2)(k^2-K_t^2)} + \sum{}'''\frac{F_{ts}F_{sr}F_{rn}F_{tn}}{(k^2-K_s^2)(k^2-K_r^2)(k^2-K_t^2)}+\cdots \quad (3.19)$$

where

$$F_{tn}=-\int\psi_t F\psi_n dS. \quad (3.20)$$

The primes indicate omission of the nth term in the summation over each index. It will be noted that the unknown k appears in these results so that (3.18) is really an equation which must be solved for k. It is, however, in a form which permits the evaluation of k^2 by means of successive approximations leading to a continued fraction solution for k^2 as compared to the usual power series. Its chief advantage over the latter lies in a considerably simplified formula.[8] Moreover, it is interesting to note that in acoustics F is a function of k, and so it would serve no useful purpose to eliminate the explicit appearance of k on the right-hand side of (3.18).

We shall now attempt a solution of the more general case of boundary condition I. It is possible to write down general solutions of (3.5) or (3.7) in terms of iterated kernels by means of the method of successive approximations. As a rule, the evaluation of the multiple integrals involved in closed form, i.e., not by expansion techniques, is possible only by numerical methods.

Another method which suggests itself would involve the substitution of a general expansion of φ in orthonormal functions ψ_n of set 0 on both sides of (3.3). The resulting linear equations for the unknown coefficients would yield a secular determinant. However, in this case this procedure is not valid since the $\varphi(x)$ occurring on the left-hand side of (3.3) is discontinuous at S. An expansion of φ in terms of set 0 would therefore have poor convergence. It could not be substituted in the right side of (3.3) since the expansion would not converge to the correct value at the surface S. This invalidates the above procedure for the general case.

However, this difficulty does not occur when S is a simple surface. This yields the secular equation:

$$|F_{tn}-\delta_{tn}(k^2-K_n^2)|=0. \quad (3.21)$$

A solution of this equation is given by formula (3.19) with associated wave function (3.18).

It is also possible to derive a secular equation for the more general case boundary condition I. Two general requirements should be noted. First, the secular determinant should be Hermitian. Secondly, its convergence should be sufficient to yield a well-converging expansion for φ, the tth term decreasing at least as strongly as $1/K_t^2$.

We shall expand φ in terms of the non-orthogonal set $\{\Psi_n\}$. Each member of this member of this set is discontinuous so that it is no longer necessary for the expansions to represent discontinuous functions. Note that this set is complete in region R.

Let $\varphi=\sum_t a_t\Psi_t$. Equation (3.3) yields

$$\sum_t a_t[A_{tn}-N_{tn}(k^2-K_n^2)]=0. \quad (3.22)$$

The resulting secular equation is:

$$|A_{tn}-N_{tn}(k^2-K_n^2)|=0. \quad (3.23)$$

From the equation:

$$N_{tn}=\frac{A_{nt}-A_{tn}}{K_n^2-K_t^2} \quad (3.24)$$

it follows that the secular determinant is Hermitian. Secondly, good convergence can be expected since the values of the non-diagonal elements decrease as their distance from a diagonal element increases.

[8] A short note giving similar results for secular perturbation theory is in preparation.

Equation (3.22) can be solved by the method of successive approximations for the coefficients a_t yielding:

$$\varphi=\Psi_n+\sum_{t\neq n} W_{nt}\Psi_t+\sum_{s\neq t\neq n} W_{ns}W_{st}\Psi_t + \sum_{r\neq s\neq t\neq n} W_{nr}W_{rs}W_{st}\Psi_t+\cdots \quad (3.25)$$

where

$$W_{nt}=-\frac{A_{nt}-N_{nt}(k^2-K_t^2)}{A_{tt}-N_{tt}(k^2-K_t^2)}. \quad (3.26)$$

The corresponding eigenvalue can be obtained from (3.9).

$$k^2=K_n^2 + \frac{A_{nn}+\sum_{t\neq n} W_{nt}A_{tn}+\sum_{s\neq t\neq n} W_{ns}W_{st}A_{tn}+\cdots}{N_{nn}+\sum_{t\neq n} W_{nt}N_{tn}+\sum_{s\neq t\neq n} W_{ns}W_{st}N_{tn}+\cdots}. \quad (3.27)$$

The rapid convergence previously demanded is exhibited by series (3.25). All the terms involved in these formulae involve only surface integrals except the normalization integrals N_{nn}. These formulae reduce in first approximation to those given by (3.13) and (3.15).

The results given above apply to those situations for which the eigenvalues are discrete. A great many problems, e.g., scattering, require the construction of a theory on which the eigenvalues have a continuous spectrum. The above theory can, with suitable modification, be applied to this case. Integral equation (3.3) applies to the continuous spectrum case as well as to the discrete spectrum. However, in view of the usual boundary condition of incident plus outgoing scattered waves, forms (3.5) and (3.7) are more convenient.

The first approximation (3.10) can be used directly. The usefulness of this approximation depends upon the proper choice of the Green's function and the closeness of ψ_n to the solution φ. No general rules can be made as to the latter since it depends mostly on physical intuition. However, as to the former, it can be said that G_k should be as close as possible to the Green's function for region R. This applies particularly over the region where the perturbation is most important. If the G_k chosen were actually the Green's function for region R, the first approximation would yield exact results.

In many cases, a second or higher approximation will be needed. The formulae developed above can be used if all the summations are replaced by integrations over the continuous spectrum. The function ψ_n will satisfy the normalization condition characteristic of continuous spectrum theory:

$$\int \psi_n\psi_{n'}dV=\delta(n-n').$$

The integrations over the continuous spectrum must be carried out in such a manner as to yield a solution satisfying the boundary conditions mentioned above. This usually requires the use of contour integrals in the complex plane for one of the wave numbers.

IV. BOUNDARY CONDITION II $\phi=1/F(\partial\phi/\partial n)$

As in the case of boundary condition I, this problem can be reduced to the integral equation:

$$\varphi(x)=\int \frac{\partial\varphi(\xi)}{\partial n_\xi} \times\left[\frac{1}{F(\xi)}\frac{\partial G_k(x,\xi)}{\partial n_\xi}-G_k(x,\xi)\right]dS_\xi. \quad (4.1)$$

The solution of this equation will be a function which has a discontinuous value at surface S. In the special case boundary condition IIA, the solution is discontinuous in slope at S.

Formulae corresponding to (3.5), (3.7), (3.9) can be derived for this case. They are

$$\varphi(x)=\psi_n(x)+\int' \frac{\partial\varphi(\xi)}{\partial n_\xi} \times\left[\frac{1}{F(\xi)}\frac{\partial G_k(x,\xi)}{\partial n_\xi}-G_k(x,\xi)\right]dS_\xi, \quad (4.2)$$

$$\varphi(x)=\Psi_n(x)+\int\left\{\frac{\partial G_k(x,\xi)}{\partial n_\xi} \times\left[\frac{1}{F(\xi)}\frac{\partial\varphi(\xi)}{\partial n_\xi}-\psi_n(\xi)\right] -G_k(x,\xi)\left[\frac{\partial\varphi(\xi)}{\partial n_\xi}-\frac{\partial\psi_n(\xi)}{\partial n_\xi}\right]\right\}dS_\xi, \quad (4.3)$$

$$k^2=K_n^2+\int\frac{\partial\psi}{\partial n}\times\left(\frac{1}{F}\frac{\partial\psi_n}{\partial n}-\psi_n\right)dS\Big/\int_R\psi_n\varphi dV. \quad (4.4)$$

If one assumes that $\varphi\simeq\psi_n$ within the surface integrals of (4.2), (4.3), (4.4) one can find approximate formulae analogous to (3.10) and (3.11).

Using expansion (3.12) we obtain the expression:

$$\varphi(x)\simeq\psi_n(x)+\sum_i{}'\frac{B_{ni}}{K_n^2-K_i^2}\psi_i \quad (4.5)$$

where

$$B_{ni}=\int\frac{\partial\psi_n}{\partial n}\left(\frac{1}{F}\frac{\partial\psi_i}{\partial n}-\psi_i\right)dS. \quad (4.6)$$

Convergence of this series is poor. Equation (4.5) can no longer be substituted in (4.4) to obtain the next approximation for the eigenvalue, nor can it be introduced with either (4.2) or (4.3) to obtain higher approximations for the eigenfunctions. Moreover, it is not possible to improve the convergence by means of an expansion in terms of the discontinuous set $\{\Psi_n\}$. For example, in the special case B.C.IIA, one needs an expansion in terms of functions which have discontinuous slope rather than value. Instead of considering such a set directly, it is more convenient to consider the vector $\mathbf{v}=-\nabla\varphi/k$. It satisfies the vector wave equation:

$$\nabla\nabla\cdot\mathbf{v}+k^2\mathbf{v}=0. \quad (4.7)$$

Its boundary conditions are:

$$\nabla\cdot\mathbf{v}=-k^2/F(\mathbf{n}\cdot\mathbf{v}). \quad (4.8)$$

In order to convert (4.7) into an integral equation, it is necessary to develop a vector Green's theorem and define the proper Green's function. The former is:

$$\int[\mathbf{u}\cdot\nabla(\nabla\cdot\mathbf{v})-\mathbf{v}\cdot\nabla(\nabla\cdot\mathbf{u})]dV=\int[(\mathbf{n}\cdot\mathbf{u})(\nabla\cdot\mathbf{v})-(\mathbf{n}\cdot\mathbf{v})(\nabla\cdot\mathbf{u})]dS. \quad (4.9)$$

The Green's function to be used with a vector wave equation is a dyadic satisfying

$$\nabla_\xi(\nabla_\xi\cdot\mathfrak{G}_k(x,\xi))+k^2G_k(x,\xi)=\delta(x-\xi)\mathfrak{I} \quad (4.10)$$

where $\mathfrak{I}$ is the idemfactor. In acoustics, $\mathbf{a}\cdot\mathfrak{G}$ gives the velocity due to an elementary source located at ξ, having the direction and magnitude of $\mathbf{a}$. $\mathfrak{G}_k(x,\xi)$ can be expanded in terms of the complete orthonormal set found by the vectors:

$$\mathbf{u}_i=-\nabla\psi_i/K_i \quad (4.11)$$

satisfying the orthogonality relation $\int_{R_0}\mathbf{u}_n\cdot\mathbf{u}_m dV=\delta_{nm}$. Then:

$$\mathfrak{G}_k(x,\xi)=\sum_i\frac{\mathbf{u}_i(x)\mathbf{u}_i(\xi)}{k^2-K_i^2}. \quad (4.12)$$

Combining (4.7), (4.9), and (4.10) we obtain

$$\mathbf{v}(x)=\int[\mathbf{n}_\xi\cdot\mathbf{v}(\xi)\nabla_\xi\cdot\mathfrak{G}_k(x,\xi)-\nabla_\xi\cdot\mathbf{v}(\xi)\mathbf{n}_\xi\cdot\mathfrak{G}_k(x,\xi)]dS_\xi. \quad (4.13)$$

Introducing boundary condition (4.8) we obtain the integral equation:

$$\mathbf{v}(x)=\int\mathbf{n}_\xi\cdot\mathbf{v}(\xi)\left[\frac{k^2}{F(\xi)}\mathbf{n}_\xi\cdot\mathfrak{G}_k(x,\xi)+\nabla_\xi\cdot\mathfrak{G}_k(x,\xi)\right]dS_\xi. \quad (4.14)$$

Comparison of (4.14) and (3.3) reveals their strong similarity enabling us to use procedures similar to those of Sec. III. The first approximation to $\mathbf{v}$ is

$$\mathbf{v}\simeq\mathbf{u}_n+\sum_i{}'\frac{C_{ni}}{K_n^2-K_i^2}\mathbf{u}_i \quad (4.15)$$

where

$$C_{ni}=\frac{K_i}{K_n}\int\frac{\partial\psi_n}{\partial n}\left(\frac{k^2}{K_i^2F}\frac{\partial\psi_i}{\partial n}-\psi_i\right)dS. \quad (4.16)$$

Convergence of (4.15) is sufficient to permit its introduction into (4.2) and (4.4) to yield higher approximation for both eigenvalue and eigenfunction. The eigenvalue result is of value:

$$k^2\simeq K_n^2+B_{nn}/N_{nn}+\sum{}'\frac{K_n}{K_i}\frac{C_{ni}B_{in}}{K_n^2-K_i^2}. \quad (4.17)$$

The particular case of S a simple surface permits the choice of $\mathfrak{G}_k$ so that $\nabla\cdot\mathfrak{G}_k=0$ (i.e.,

$\psi_n=0$ on S). The resulting integral equation can be solved exactly.

$$\mathbf{v}=\mathbf{u}_n+\sum_t{}'\frac{G_{nt}}{k^2-K_t^2}\mathbf{u}_t+\sum_{r,t}{}''\frac{G_{nr}G_{rt}}{(k^2-K_r^2)(k^2-K_t^2)}\mathbf{u}_t+\cdots \quad (4.18)$$

where

$$G_{nt}=\frac{k^2}{K_nK_t}\int\frac{\partial\psi_n}{\partial n}\frac{1}{F}\frac{\partial\psi_t}{\partial n}dS. \quad (4.19)$$

Introducing (4.18) into (4.2) one finds

$$\varphi=\psi_n+\sum_t{}'\frac{K_nK_t}{k^2}\frac{G_{nt}}{(k^2-K_t^2)}\psi_t+\sum_{r,t}{}''\frac{K_tK_nG_{nr}G_{rt}}{k^2(k^2-K_r^2)(k^2-K_t^2)}\psi_t+\cdots. \quad (4.20)$$

The value of k^2 is:

$$k^2=K_n^2+G_{nn}+\sum_t{}'\frac{G_{nt}G_{tn}}{k^2-K_t^2}+\sum_{r,t}{}''\frac{G_{nr}G_{rt}G_{tn}}{(k^2-K_t^2)(k^2-K_r^2)}+\cdots. \quad (4.21)$$

Result (4.21) can be derived from the secular equation satisfied by k^2:

$$|G_{tn}-(k^2-K_n^2)\delta_{tn}|=0. \quad (4.22)$$

A secular determinant can be developed for the more general case. $\mathbf{v}$ is expanded in terms of a complete but non-orthogonal set $\{\mathbf{U}_n\}$. $\mathbf{U}_n$ is a vector function equal to $\mathbf{u}_n$ inside R but zero outside. The resulting secular determinant is:

$$|C_{tn}-(k^2-K_n^2)M_{tn}|=0 \quad (4.23)$$

where

$$M_{tn}=\int_R\mathbf{u}_n\cdot\mathbf{u}_t dV=\frac{C_{nt}-C_{tn}}{K_n^2-K_t^2}. \quad (4.24)$$

This determinant is Hermitian. Solution of (4.23) can be given as before [cf. (3.25)],

$$\mathbf{v}=\mathbf{U}_n+\sum_{t\neq n}V_{nt}\mathbf{U}_t+\sum_{t\neq s\neq n}V_{ns}V_{st}\mathbf{U}_t+\cdots \quad (4.25)$$

where

$$V_{nt}=-\frac{C_{nt}-M_{nt}(k^2-K_t^2)}{C_{tt}-M_{tt}(k^2-K_t^2)}. \quad (4.26)$$

This permits the computation of φ from (4.2):

$$\varphi=\psi_n+\sum_{t\neq n}\frac{B_{nt}}{k^2-K_t^2}\psi_t+\sum_{s\neq t\neq n}\frac{K_n}{K_t}\frac{V_{nr}B_{rt}}{(k^2-K_t^2)}\psi_t+\cdots. \quad (4.27)$$

Finally, the result for the eigenvalue k^2 has the same form as (3.27), with A_{tn} replaced by C_{tn}, W_{nt} by V_{nt}, and N_{tn} by M_{tn}. Convergence of (4.25) and (4.26) is good.

Remarks given in the preceding section on extension of these results to the problem of scattering hold here.

V. BOUNDARY CONDITIONS III AND IV: $(\mathbf{n}\times\text{curl }\mathbf{A})=(\mathbf{n}\times\mathbf{A})\cdot\zeta$.

The reduction of wave equation (2.5) to an integral equation can be accomplished through the use of a dyadic Green's function satisfying the equation

$$\text{curl}_\xi\,\text{curl}_\xi\,\mathfrak{G}_k(x,\xi)-k^2\mathfrak{G}_k(x,\xi)=\delta(x-\xi)\mathfrak{I}. \quad (5.1)$$

We also need a vector Green's theorem:[9]

$$\int[\mathbf{A}\cdot\text{curl curl }\mathbf{B}-\mathbf{B}\cdot\text{curl curl }\mathbf{A}]dV=\int[\mathbf{A}\cdot(\mathbf{n}\times\text{curl }\mathbf{B})-\mathbf{B}\cdot(\mathbf{n}\times\text{curl }\mathbf{A})]dS. \quad (5.2)$$

It then follows that:

$$\mathbf{A}(x)=\int[\mathbf{A}(\xi)\cdot(\mathbf{n}_\xi\times\text{curl}_\xi\,\mathfrak{G}_k(x,\xi))-(\mathbf{n}_\xi\times\text{curl}_\xi\,\mathbf{A}(\xi))\cdot\mathfrak{G}_k(x,\xi)]dS_\xi. \quad (5.3)$$

Introducing B.C.IV we find the integral equation satisfied by $\mathbf{A}(x)$:

$$\mathbf{A}(x)=-\int(\mathbf{n}_\xi\times\mathbf{A}(\xi))\cdot[\text{curl}_\xi\,\mathfrak{G}_k(x,\xi)+\zeta(\xi)\cdot\mathfrak{G}_k(x,\xi)]dS_\xi. \quad (5.4)$$

This equation is very similar to (3.3) and permits the use of the techniques developed in Sec. III.

[9] J. A. Stratton, *Electromagnetic Theory* (McGraw-Hill Book Company, Inc., New York, 1941), p. 250.

Formulae corresponding to (3.5), (3.7), and (3.9) can be derived. They are:

$$\mathbf{A}(x)=\mathbf{D}_n(x)-\int'(\mathbf{n}_\xi\times\mathbf{A}(\xi))\cdot[\mathrm{curl}_\xi\,\mathfrak{G}_k(x,\xi)+\zeta(\xi)\cdot\mathfrak{G}_k(x,\xi)]dS_\xi, \quad (5.5)$$

$$\mathbf{A}(x)=\mathbf{\Delta}_n(x)-\int\{\mathrm{curl}_\xi\,\mathfrak{G}_k(x,\xi)\cdot[\mathbf{n}_\xi\times\mathbf{A}(\xi)-\mathbf{n}_\xi\times\mathbf{D}_n(\xi)]+[\mathbf{n}_\xi\times\mathbf{A}(\xi)\cdot\zeta(\xi)-(\mathbf{n}_\xi\times\mathrm{curl}_\xi\,\mathbf{D}_n)]\cdot\mathfrak{G}_k(x,\xi)\}dS_\xi, \quad (5.6)$$

where $\mathbf{D}_n$ is any solution of Eq. (2.5). $\mathbf{\Delta}_n$ is a vector equal to $\mathbf{D}_n$ within R and equal to 0 outside of R. If K_n^2 is the eigenvalue corresponding to $\mathbf{D}_n$, then,

$$k^2=K_n^2+\int(\mathbf{n}\times\mathbf{A})\cdot[\mathrm{curl}\,\mathbf{D}_n+\zeta\cdot\mathbf{D}_n]dS\Big/\int_R\mathbf{A}\cdot\mathbf{D}_n dV. \quad (5.7)$$

First-approximation results can be immediately obtained from (5.5), (5.6), (5.7) if $\mathbf{A}(x)\simeq\mathbf{D}_n(x)$ by replacing $\mathbf{A}(x)$ by $\mathbf{D}_n$ within the surface integrals.

Suppose $\mathbf{D}_n$ is normalized so that it is a member of an orthonormal set. The dyadic Green's function can then be expanded in terms of the set $\{\mathbf{D}_n\}$:

$$\mathfrak{G}_k(x,\xi)=-\sum_t\frac{\mathbf{D}_t(x)\mathbf{D}_t(\xi)}{k^2-K_t^2}. \quad (5.8)$$

Introducing this expansion into (5.6) and replacing $\mathbf{A}$ by $\mathbf{D}_n$ we obtain

$$\mathbf{A}(x)\simeq\mathbf{\Delta}_n(x)+\sum_t'\frac{D_{tn}}{K_n^2-K_t^2}\mathbf{D}_t(x) \quad (5.9)$$

where

$$D_{tn}=\int(\mathbf{n}\times\mathbf{D}_t)\cdot[\mathrm{curl}_\xi\,\mathbf{D}_n+\zeta(\xi)\cdot\mathbf{D}_n]dS_\xi. \quad (5.10)$$

A second approximation to the eigenvalue follows:

$$k^2\simeq K_n^2+\frac{D_{nn}}{P_{nn}}+\sum_t'\frac{(D_{tn})^2}{K_n^2-K_t^2} \quad (5.11)$$

where

$$P_{nt}=\int_R\mathbf{D}_n\cdot\mathbf{D}_t dV=\frac{D_{nt}-D_{tn}}{K_n^2-K_t^2}. \quad (5.12)$$

Poor convergence prevents calculation of further approximations from (5.9). However, in the special case where S is a simple surface choose $(\mathbf{n}\times\mathrm{curl}\,\mathfrak{G}_k)=0$ on S (i.e., $\mathbf{n}\times\mathrm{curl}\,\mathbf{D}_t=0$ on S). The resulting formulae have exactly the same form as (3.18). F_{tn} should be replaced by

$$\zeta_{tn}=\int(\mathbf{n}\times\mathbf{D}_n)\cdot\zeta\cdot\mathbf{D}_t dS. \quad (5.13)$$

The corresponding secular determinant is

$$|\zeta_{tn}-(k^2-K_n^2)\delta_{tn}|=0. \quad (5.14)$$

A secular determinant can be developed for the more general case. $\mathbf{A}$ is expanded in the complete set of discontinuous vectors $\{\mathbf{\Delta}_n\}$. The resulting secular determinant is

$$|D_{tn}-(k^2-K_n^2)P_{tn}|=0. \quad (5.15)$$

The determinant is Hermitian. Solution of (5.15) can be found as in Sec. III. Formulae (3.25) and (3.27) will apply to this case if Ψ_t is replaced by $\mathbf{\Delta}_t$, A_{nt} by D_{nt}, N_{tn} by P_{tn} throughout.

VI. GREEN'S FUNCTIONS

The formulae developed in the preceding sections apply only when there are no sources present in the region R being considered. This is usually not the case experimentally since sources must be present to excite the modes being investigated, or in the scattering situation the source is frequently not at infinity.

The description of the effect of a source is given by the Green's function which satisfies the boundary conditions imposed by the physical situation at the surface S of R. This Green's function can be constructed in those cases for which the boundary conditions are such that the solutions of the corresponding wave equation form an orthonormal set. The Green's function can then be expanded in terms of this orthonormal set according to Eqs. (3.11), (4.19), or (5.12). The various possible solutions of the wave equations yielding the desired set are given in the discussion above. It should be noted that these form an orthogonal set, but are not normalized as given.

However, for some boundary conditions the solutions are not orthogonal, or the expansion is unwieldy. It is then interesting to note that the Green's function also satisfies an integral equation from which approximate results for the new Green's function may be deduced. We shall give the details for the case of boundary condition I, giving only the results for the others.

Let the desired Green's function be $G_k(x, \xi)$. Let any other satisfying the wave equation for other boundary conditions be $L_k(x, \xi)$. Then

$$G_k(x, \xi) = L_k(x, \xi) + \int\int \left[G_k(x, \rho) \frac{\partial L_k(\rho, \xi)}{\partial n_\rho} - L_k(\rho, \xi) \frac{\partial G_k(x, \rho)}{\partial n_\rho} \right] dS_\rho. \quad (6.1)$$

The introduction of boundary conditions I on G_k yields

$$G_k(x, \xi) = L_k(x, \xi) + \int G_k(x, \rho) \times \left[\frac{\partial L_k(\rho, \xi)}{\partial n_\rho} - F(\rho) L_k(\rho, \xi) \right] dS_\rho. \quad (6.2)$$

For the other boundary conditions we get

B.C.II $$G_k(x, \xi) = L_k(x, \xi) + \int \frac{\partial G_k(x, \rho)}{\partial n_\rho} \times \left[\frac{1}{F(\rho)} \frac{\partial L_k(\rho, \xi)}{\partial n_\rho} - L_k(\rho, \xi) \right] dS_\rho, \quad (6.3)$$

B.C.IV $$\mathfrak{G}_k(x, \xi) = \mathfrak{L}_k(x, \xi) - \int \mathbf{n}_\rho \times \mathfrak{G}_k(x, \rho) \cdot [\operatorname{curl}_\rho \mathfrak{L}_k(\rho, \xi) + \zeta(\rho) \cdot \mathfrak{L}_k(\rho, \xi)] dS_\rho. \quad (6.4)$$

Any attempt to solve these integral equations by means of expansions leads again to the expansion in eigenfunctions mentioned above. It is possible, however, to find an approximate value of G_k if $G_k \simeq L_k$ by substituting the known L_k for the unknown G_k in the right side of Eqs. (6.2), (6.3), (6.4). This represents the chief use of these integral equations in practice since usually it is impossible to evaluate a second approximation by the reintroduction of the first approximation into these equations. A similar approximation used in a discussion of the Laplace equation has been given by Hadamard.[10]

VII. CONCLUSIONS

It has been found possible to reduce the scalar and vector wave equations to the solutions of a corresponding secular determinant by means of the following procedure.

1. Reduction to an integral equation through the use of a Green's function. This equation includes the boundary conditions.

2. For boundary conditions I and IV, expansion of the solution in terms of a discontinuous set of functions which vanish outside region R. This leads to a secular equation.

3. For boundary conditions II and III, the introduction of another auxiliary quantity whose boundary conditions and equations are similar to I and IV is necessary. The technique employed for these boundary conditions is then valid.

We note that the secular determinant is Hermitian. Its non-diagonal terms involve only surface integrals whereas the diagonal terms involve also volume integrals of the N_{nn} type.

Extension of these results to the scattering problem has been indicated at the end of Sec. III. Similar considerations as applied to source functions are given in Sec. VI. The solution of these equations in regions bounded by moving surfaces is found to the second approximation in Appendix II.

The procedure developed here appears to apply to any system of partial differential equations whose solutions form a complete orthonormal set or are orthogonal to another set. There is, however, a restriction for boundary conditions of type B.C.II. In this case, it is necessary for the solution of the auxiliary equation to satisfy some orthogonality relation. This condition has not been found in the case of the Schroedinger equation. However, for B.C.I, no such restriction applies. In this problem, the solutions found for the wave equation apply equally well to the Schroedinger equation. It is this boundary condition which occurs in the Wigner-Seitz theory of metals.

The author wishes to thank Professor P. M.

[10] P. Levy, *Leçons d'Analyse Fonctionelle* (Gauthier-Villars, Paris, 1922), p. 181.

Morse for his active interest and aid. He is also indebted to Professor J. C. Slater and Professor L. I. Schiff for some illuminating discussions and criticisms.

APPENDIX I

Here we shall show that the surface integral (3.2) represents any solution of the wave equation within R but is zero outside. Any function $f(x)$ which is zero outside R can be expanded in terms of the set 0 as follows:

$$f(x)=\sum_n\left(\int_R f\psi_n dV\right)\psi_n. \tag{I.1}$$

If, furthermore, f is a solution of the wave equation with eigenvalue k^2, it follows that

$$f(x)=\sum_n\frac{\int\left(f\frac{\partial\psi_n}{\partial n}-\psi_n\frac{\partial f}{\partial n}\right)dS}{k^2-K_n^2}\psi_n. \tag{I.2}$$

Using the expansion of the Green's function (3.12) we obtain Eq. (3.2).

APPENDIX II

In this appendix, we shall consider the problem of moving boundary surfaces. We shall restrict the discussion to the scalar equation and B.C.I since the extension to other cases involves the same calculations given in the main body of this paper. The function φ will now satisfy the time dependent equation

$$\nabla^2\varphi=(1/c^2)(\partial^2\varphi/\partial t^2). \tag{II.1}$$

The following discussion will be restricted to cases involving nearly simple harmonic time dependence. The extension to a more general type of time dependence can be easily carried out in terms of a Fourier integral superposing the various possible frequencies. We, therefore, consider the Green's function $G_k(x,\xi)e^{-i\omega t}=g_k$ which satisfies the equation

$$\nabla_\xi^2 g_k=1/c^2\frac{\partial^2 g_k}{\partial t^2}+\delta(x-\xi)e^{-i\omega t}. \tag{II.2}$$

Combining (II.1) and (II.2) we have

$$\varphi(x)e^{-i\omega t}=\int\left[\varphi(\xi)\frac{\partial g_k}{\partial n_\xi}-g_k\frac{\partial\varphi(\xi)}{\partial n_\xi}\right]dS_\xi +1/c^2\int\left[g_k\frac{\partial^2\varphi(\xi)}{\partial t^2}-\frac{\partial^2 g_k}{\partial t^2}\varphi(\xi)\right]dV_\xi. \tag{II.3}$$

Another result which can be derived in the same manner is

$$\frac{\partial^2\varphi(x)}{\partial t^2}e^{-i\omega t}=\int\left[\frac{\partial^2\varphi(\xi)}{\partial t^2}\frac{\partial g_k}{\partial n_\xi}-\frac{\partial^2 g_k}{\partial t^2}\frac{\partial\varphi(\xi)}{\partial n_\xi}\right]dS_\xi. \tag{II.4}$$

It will be noted that the time enters explicitly in these surface and volume integrals as a parameter. Equation (II.3) will be used in the present discussion since it yields a value of φ directly, whereas (II.4) would involve further integrations before value of φ is found. However, the latter equation has definite advantages because it involves only surface integration.

Introducing boundary conditions and time dependence of g_k we have

$$\varphi(x)=\int\left[\varphi(\xi)\frac{\partial G_k(x,\xi)}{\partial n_\xi}-F(\xi)G_k(x,\xi)\right]dS_\xi +1/c^2\int G_k(x,\xi)\left[\frac{\partial^2\varphi(\xi)}{\partial t^2}+\omega^2\varphi(\xi)\right]dV_\xi. \tag{II.5}$$

The surface integral term is identical to that which occurs in (3.3). As a first approximation let $\varphi\backsimeq\psi_n e^{-i\omega t}$. The volume integral drops out. The surface integral can be evaluated in two forms:

$$\varphi=e^{-i\omega t}\left[\psi_n+\sum_r{}'\frac{A_{nr}}{k^2-K_r^2}\psi_r\right] \tag{II.6}$$

or

$$\varphi=e^{-i\omega t}\left[\Psi_n-\sum_r{}'\frac{A_{nr}-N_{nr}(k^2-K_r^2)}{A_{rr}-N_{rr}(k^2-K_r^2)}\Psi_r\right]. \tag{II.7}$$

Formula (II.7) is taken from (3.25) and converges more rapidly than (II.6). Note that the matrix elements A_{nr}, N_{rr} are functions of time. It is most convenient to introduce (II.6) into the volume term since the ψ_r are independent of time whereas Ψ_r in (II.7) are not. The second approximation for the surface terms will just be the second term in (3.25). We finally find

$$\varphi=e^{-i\omega t}\left[\Psi_n+\sum_{r\neq n}W_{nr}\Psi_r+\sum_{r\neq s\neq n}W_{ns}W_{sr}\Psi_r +\frac{1}{c^2}\sum_{r\neq s\neq n}\frac{\ddot{A}_{ns}-2i\omega\dot{A}_{ns}}{(k^2-K_s^2)(k^2-K_n^2)}N_{sr}\psi_r\right]. \tag{II.8}$$

The dot notation has its usual significance of time derivative. These results are useful when the time dependence of φ is approximately simple harmonic. More general types of time dependence can be handled by means of a superposition of simple harmonic terms as suggested above. It would also be possible to make use of a more general formulation of Huygens' principle for the time dependent equation.

PHYSICAL REVIEW VOLUME 65, NUMBERS 11 AND 12 JUNE 1 AND 15, 1944

Theory of Cathode Sputtering in Low Voltage Gaseous Discharges

CHARLES HARD TOWNES
Bell Telephone Laboratories, Murray Hill, New Jersey

(Received March 25, 1944)

To determine the amount of sputtering in a glow discharge three functions must be known: the number of ions of a given energy striking the cathode, the amount of cathode material released from the cathode by each ion, and the fraction of material released from the cathode which diffuses away. Expressions derived for these allow determination of the dependence of total rate of sputtering on the geometry of the discharge, pressure, cathode fall, current, and constants of the gas and cathode surface. The result is most accurate for very low voltage, high pressure discharges. Comparison with experimental data shows quantitative agreement under these conditions.

CATHODE sputtering is the process which removes material from the surface of the cathode of a gaseous discharge and deposits this material as a film on the walls of the discharge tube or on other nearby surfaces. There is experimental evidence that sputtering is due to ionic bombardment of the cathode and that the material sputtered leaves the cathode in all directions and in an uncharged state.[1] By identifying the spectral lines of atomic material from the cathode in gaseous discharges and measuring their intensities, Von Hippel[2] showed that a large part, if not all, of the sputtered material present in the region of the discharge was in an atomic state. There have also been numerous attempts to deflect the sputtered particles by electric and magnetic fields with the resultant general conclusion that they are uncharged. Baum[3] succeeded in attaching charges to sputtered particles of silver and deflecting them after they had been extracted from the discharge region. He concluded that they were atoms which had velocities corresponding approximately to a temperature of 1000 degrees C. Seeliger and Sommermeyer[4] allowed a beam of ions to strike a silver surface in very low pressure gas and measured the amount of material sputtered in various directions, obtaining the result that the sputtered particles leave the cathode according to the cosine law.

If the mechanism for sputtering indicated by these results is accepted, i.e., that positive ions bombarding the cathode dislodge atomic material, the theoretical problem of calculating the amount of sputtering may be resolved into the calculation of three functions:

1. The fraction of atoms released from the cathode surface which find their way to other surfaces in the discharge.
2. The number of ions of given energy striking the cathode.
3. The number of atoms dislodged by an ion of given energy.

Most previous work on sputtering has dealt principally with the effect of function (3) and with some justification because sputtering under high voltage low pressure conditions has been principally discussed. It will be shown, however, that under certain conditions in low voltage discharges, function (2) giving the distribution of ionic energies plays a dominating role.

DIFFUSION OF SPUTTERED MATERIAL

If the mean free path of the sputtered particles is much larger than the distances between the cathode and the surrounding surfaces, then material which leaves the cathode may never return; but if the mean free path is much smaller than these distances, a large fraction of the atoms which leave the cathode diffuses back to the cathode surface. To obtain quantitatively the fraction of material diffusing away from the cathode, let

[1] In some cases chemical reactions take place between the gas and the cathode material, usually giving a large amount of cathode erosion. This type of sputtering will not be considered.

[2] A. Von Hippel, Ann. d. Physik **80**, 672 (1926).

[3] T. Baum, Zeits. f. Physik **40**, 686 (1926).

[4] R. Seeliger and K. Sommermeyer, Zeits. f. Physik **93**, 692 (1935).

$d\bar{s}_1$ = vector element of cathode surface S_1,
$d\bar{s}_2$ = vector element of surface S_2 surrounding cathode on which sputtered material is deposited,
J_0 = rate at which atoms leave cathode surface,
J = rate of deposition on S_2,
N = concentration of cathodic atoms between S_1 and S_2,
D, v, λ = diffusion coefficient, average velocity, and mean free path, respectively, of sputtered atoms in gas of discharge, and
C_1, C_2 = the fraction of the atoms which adhere on collision with S_1 and S_2, respectively.

Now

$$J = D\int \nabla N \cdot d\bar{s}_2$$

is the rate of deposition and

$$J_0 - J = C_1\frac{v}{4}\int N ds_1$$

gives the rate at which sputtered atoms are being returned to the cathode. If J_0 is constant so that a steady state is reached,

$$\nabla^2 N = 0$$

with the boundary conditions

$$C_2\frac{v}{4}\int_{S_2} N ds_2 = D\int_{S_2} \nabla N \cdot d\bar{s}_2$$

and

$$J_0 = \frac{C_1 v}{4}\int_{S_1} N ds_1 + D\int_{S_2} \nabla N \cdot d\bar{s}_2.$$

If $J_0 \gg J$ and if atoms are emitted uniformly over the cathode, the boundary conditions become

$$N_2 \approx 0$$

and

$$J_0 \approx \tfrac{1}{4} C_1 v N_1 S_1$$

where N_1 and N_2 are the values extant at S_1 and S_2, respectively. Then N may be written

$$N = f(x, y, z)N_1 = \frac{4J_0}{C_1 S_1 v} f(x, y, z)$$

and

$$J = \frac{4DJ_0}{C_1 S_1 v}\int_{S_2} \nabla f \cdot d\bar{s}_2,$$

where f is a solution of Laplace's equation which is zero on S_2 and unity on S_1. From kinetic theory, $D = \pi/8v\lambda$. Therefore,

$$J = \frac{\pi J_0 \lambda}{2C_1 S_1}\int_{S_2} \nabla f \cdot d\bar{s}_2. \qquad (1)$$

For the case where S_1 and S_2 are two parallel planes separated by a distance d, the number of atoms deposited per second per sq. cm becomes

$$j = \frac{\pi j_0 \lambda}{2C_1 d}$$

from which it is seen that the approximation $J_0 \gg J$ is justified when $\lambda \ll d$. For a spherical cathode of radius a surrounded by a concentric sphere of radius b, the total rate of deposition

$$J = \frac{\pi J_0 \lambda b}{a(a-b)}.$$

The inverse dependence of j on d for the plane case was found experimentally by Güntherschulze[5] and by Blechschmidt,[6] and derived theoretically by von Hippel.[7] It may be seen from these formulae that for a fixed rate of evaporation of atoms at the cathode, the actual rate of disappearance of material from the cathode is inversely proportional to the gas pressure and depends as well on the distance to the nearest surfaces where deposition may take place. A large part of the evaporated atoms returns to the cathode surface and perhaps forms the powder of small crystals which is often observed there. The evaporated atoms may, of course, condense in the discharge, form large aggregates, and thus materially change the rate of deposition, but in most cases the density of sputtered material in the discharge is too small to allow appreciable condensation.

ENERGIES OF IONS STRIKING THE CATHODE

To find the energy of a typical ion in an electric field E, let the ion start from rest and have a mean free path in the gas λ. It will move in the direction of the electric field an average distance

[5] A. Güntherschulze, Zeits. f. Physik **38**, 575 (1926).
[6] E. Blechschmidt, Ann. d. Physik **81**, 999 (1926).
[7] A. v. Hippel, Ann. d. Physik **81**, 1043 (1926).

λ, when it will have an energy $E\lambda$ electron volts, and collide with a molecule having a mass approximately equal to that of the ion. If the collision takes place as between hard spheres, the average ionic energy immediately after collision is $\frac{1}{2}E\lambda$. Since most of the velocity before the second collision is in the direction of E, the average energy just before the second collision will be approximately $E\lambda+\frac{1}{2}E\lambda$. Thus, if the field varies, we may write for the average total energy at a given collision the expression

$$\bar{\epsilon}\approx E_0\lambda+\tfrac{1}{2}E_1\lambda+\cdots(1/2)^nE_n\lambda+\cdots,$$

where E_n indicates the average value of the field between collisions n and $n+1$ before the given collision represented by the subscript 0. If E is constant over several mean free paths, then

$$\bar{\epsilon}\approx 2E\lambda.$$

This value is an upper limit for $\bar{\epsilon}$ since all of the ionic velocity is not in the direction of E.

To find the energy distribution function, consider variations in the energy contributions of only the last two free paths. This is justifiable because the average contribution of the next free path is only $\frac{1}{8}$ the total energy, and variations would be correspondingly small. The average energy contribution of all but the last two free paths is $\frac{1}{2}E\lambda$. During the last free path, there is a probability

$$\exp\left(\frac{-\epsilon_0}{E\lambda}\right)\frac{\Delta\epsilon_0}{E\lambda}$$

that an energy between ϵ_0 and $\epsilon_0+\Delta\epsilon_0$ will be contributed to the total energy. Variations in the energy contribution ϵ_1 of the next to the last free path occur both as a result of variations in the free path and of variations in the energy retained after collision. It may be shown that if f is the fraction of the precollision energy which an ion retains after collision, then all values of f from 0 to 1 are equally probable if the ion is considered a hard sphere. The number of ions having energy less than ϵ becomes, then

$$n(\epsilon)=\frac{n_0}{(E\lambda)^2}\int_0^{\epsilon-(E\lambda/2)}\int_0^1\int_0^{(\epsilon-\epsilon_0-E\lambda/2)/f}\times\exp\left(-\frac{\epsilon_0+\epsilon_1}{E\lambda}\right)d\epsilon_1\,df\,d\epsilon_0$$

for

$$\epsilon>E\lambda/2$$

where

$n_0=$ total number of ions,

$$\frac{dn(\epsilon)}{d\epsilon}=\frac{n_0}{E\lambda}\exp\left(-\epsilon/E\lambda+1/2\right)\times\left(\int_0^1\frac{1-\exp\left[\frac{1-f}{f}\left(\frac{-\epsilon}{E\lambda}+1/2\right)\right]}{1-f}df\right).$$

A tractable approximation for the above integral of form

$$\int_0^1 g(f)df \text{ is } \tfrac{1}{4}g(0)+\tfrac{1}{2}g(1/2)+\tfrac{1}{4}g(1)$$

which gives

$$\frac{dn(\epsilon)}{d\epsilon}=\frac{n_0}{E\lambda}\exp\left(-\epsilon/E\lambda+1/2\right)\times\left(\frac{9}{8}+\frac{\epsilon}{4E\lambda}-\exp\left(-\epsilon/E\lambda+1/2\right)\right). \quad (2)$$

In order to determine $E\lambda$, the gaseous discharge in which the sputtering takes place must be examined. If the discharge is at very low pressure so that the cathode dark space is large, E may actually be measured, or at least the cathode potential fall and length of cathode dark space may be measured. At higher pressures the cathode dark space may be too small to permit accurate measurement or may not even be seen. Considerations here will be confined to the common case when λ is a small fraction of D, the length of the dark space, and D is much less than the radius of curvature of the cathode surface. A number of experimental and theoretical investigations[8] have shown that the electric field in the cathode dark space of a glow discharge may be represented by a linear function which becomes zero at the edge of the negative glow,

$$E=\frac{E_c(D-x)}{D},$$

where Ec is the field strength of the cathode.

[8] M. J. Druyvesteyn and F. M. Penning, Rev. Mod. Phys. **12**, 87 (1940). L. B. Loeb, *Fundamental Processes of Electrical Discharge in Gases* (John Wiley & Sons, New York, 1939), p. 578.

On this assumption, it may be shown that

$$E_c = 2\left[\frac{\pi i V}{(1+\gamma)k}\right]^{\frac{1}{2}},$$

where i = current density at the cathode, V = cathode potential drop, γ = number of electrons released per ion impinging on the cathode, and k = ionic mobility. If

$$\lambda = \Lambda/p \quad \text{and} \quad k = K/p,$$

$$E_c\lambda = 2\Lambda\left[\frac{\pi}{K(1+\gamma)}\right]^{\frac{1}{2}}\left(\frac{Vi}{p^2}\right)^{\frac{1}{2}}.$$

The behavior of K with varying average energy $\bar{\epsilon}$ is in general complicated, but for the values of E/p usually encountered in the cathode dark space, K is thought to be inversely proportional to the mean ionic velocity, or

$$K = \frac{\kappa}{\sqrt{\bar{\epsilon}}}.$$

Thus,

$$E_c\lambda = 2\left[\frac{2\pi\Lambda^3}{(1+\gamma)\kappa}\right]^{2/5}[Vi/p^2]^{2/5} \qquad (3)$$

where the first bracket may be considered constant since $\gamma \ll 1$ and γ does not change rapidly. For many glow discharges the cathode fall V is very nearly equal to the total voltage across the discharge, so that the above formula gives the dependence of the energy with which ions strike the cathode on the voltage, current, and pressure. For known discharges $\bar{\epsilon} \approx 2E_c\lambda$ obtained from this expression varies from less than 1 ev to several hundred ev; for the higher voltage part of this range the approximations made in the derivation are poor.

When $E\lambda$ is only a few volts or less, it might be supposed that the work function of the cathode, or the energy acquired by the ion from its attraction to the cathode surface, is a very important part of the ionic energy. Thus if the force of attraction of an ion to the cathode surface is simply an image force and the ion approaches to 0.5A from the surface, the resulting energy is 7.2 ev. Massey[9] has shown, however, that an ion is usually neutralized before it strikes a metallic surface by capturing an electron from the surface. A rough calculation of the type made by Massey shows the probability that an electron has been captured in an nS level when a 1-volt proton approaches to within a distance b of the surface is

$$3\times 10^3 \frac{n}{(n!)^2} \exp\left(-2b/0.54n\times 10^{-8}\right).$$

Considering capture in a $2S$ state only, the proton would be neutralized when it reaches a distance of about 4A from the surface, having acquired an energy due to image forces of 0.9 ev. While the kinetic energy acquired by the ion due to image forces is not known exactly, it is probably small and not strongly dependent on ion velocities, so that it will be neglected.

The neutralized ion, to be sure, has considerable potential energy, but this energy will not be effective in releasing atoms from the surface. Massey[10] has computed the probability per second of the neutralized ion becoming deexcited and delivering its potential energy to one of the conduction electrons of the cathode. He obtained about 10^{16}/sec., so that this process is much more likely than the emission of radiation. Although the rate of transfer of excitation energy to a lattice point is unknown, it would be less than the rate of transfer of energy to the conduction electrons because of the larger momenta or shorter wave-lengths associated with the lattice points. It is assumed therefore that the excitation energy is delivered to one or more conduction electrons. Since the conduction electrons have a mean free path of the order of 10^{-6} cm, they are able to escape from the region of a few atomic radii about the center of disturbance without delivering energy to the lattice points.

Before attempting a calculation of the third function, the number of atoms released per ion of given energy (dJ_0/dn), it is helpful to consider the expected general behavior of dJ_0/dn and its influence on the desired total rate of sputtering. For ionic energy ϵ less than ϵ_0, the energy re-

[9] H. S. W. Massey, Proc. Camb. Phil. Soc. **26**, 386 (1930); **27**, 460 (1931).

[10] H. S. W. Massey, Proc. Camb. Phil. Soc. **26**, 386 (1930).

quired to release one atom from the cathode surface, dJ_0/dn, will be zero. From this point dJ_0/dn may be expected to rise rapidly at first and then continue to increase more slowly with increasing ϵ. If $\bar{\epsilon} \ll \epsilon_0$, then the exact shape of dJ_0/dn has little influence on J_0, and this function may be idealized as in Fig. 1(b). This is the case for very low voltage discharges and is the condition for which the present theory is most accurate. If $\bar{\epsilon} \sim \epsilon_0$, as in Fig. 2, both $dn/d\epsilon$ and dJ_0/dn must be known with some accuracy, and a quantitative treatment is difficult. For $\bar{\epsilon} \gg \epsilon_0$, the idealization of Fig. 3(b) may be made. This is the condition under which most observations on sputtering have been made, i.e., in high voltage, low pressure discharges.

An expression for dJ_0/dn may be calculated with the assumptions of von Hippel's[11] evaporation mechanism. Suppose that an ion delivers its energy ϵ almost instantaneously to a small hemispherical region of radius r_0 and that this energy is propagated just as is heat. An approximate solution for the temperature at any distance r from the center of disturbance and at time t is[12]

$$T=\frac{1.7\times10^{-21}\epsilon}{\rho s\left(\frac{ct}{\rho s}\right)^{\frac{1}{2}}}\exp\left(-r^2\rho s/4ct\right)+T_0 \quad \text{if} \quad \frac{ct}{\rho s}>r_0^2,$$

where T_0 = temperature of surface before collision, ρ, s, c = density, specific heat, and conductivity of cathodic material. This formula may be used when $t \geq t_0$ where t_0 corresponds to the

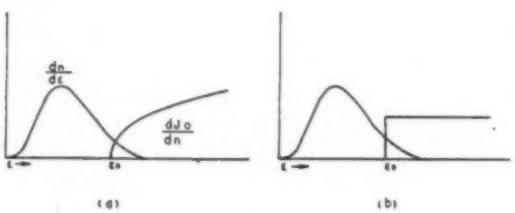

FIG. 1. $\bar{\epsilon} \ll \epsilon_0$.

time of collision and its magnitude in seconds is to be chosen about equal to r_0^2 in cm^2, to give

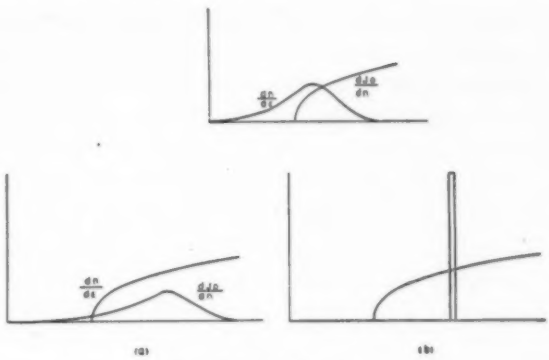

FIG. 2 (*Above*). $\bar{\epsilon} \sim \epsilon_0$.
FIG. 3 (*Below*). $\bar{\epsilon} \gg \epsilon_0$.

the correct initial distribution of energy. If

$$t_0=4\times10^{-16},$$

$$\epsilon=4 \text{ ev},$$

$$\rho s=0.5,$$

$$c=0.5,$$

then

$$T=1700\exp\left[-r^2/(1.6\times10^{-15})\right]+T_0.$$

There is over a region of a few atomic radii and for a time of the order of 10^{-16} a very high temperature. It may be easily shown that heat radiation during this time is negligible and that no other ion is likely to strike within this area and time.

The rate of evaporation of the cathode material may be found if the vapor pressure is assumed to be

$$p=\exp\left(b-a/kT\right),$$

where a and b are constants characteristic of the cathode material, a being the heat of vaporization of one molecule. The number of molecules leaving unit surface area per second is

$$\nu=C_2p/mv,$$

where m is the molecular mass, v the average velocity of molecules in the vapor state, and C_2 the fraction of molecules which stick to the surface on striking it. Hence

$$\nu=\frac{C_2\exp\left(b-a/kT\right)}{2\left(\frac{2}{\pi}mkT\right)^{\frac{1}{2}}}.$$

[11] A. v. Hippel, Ann. d. Physik **81**, 1043 (1926). E. Blechschmidt and A. v. Hippel, Ann. d. Physik **86**, 1006 (1928).

[12] H. S. Carslaw, *Mathematical Theory of the Conduction of Heat in Solids* (Macmillan Company, London, 1921), p. 149.

To find the total number of molecules evaporated by collision of a single ion with the surface, the maximum rate of evaporation per unit area will be multiplied by the length of time Δt required for the temperature to fall to such a value that the rate of evaporation is one-half its maximum, and by the area ΔS over which the rate of evaporation is not less than one-half maximum. This yields, on neglecting T_0,

$$\frac{dJ_0}{dn}=\frac{1.5\times10^{-55}C_2\epsilon^{\frac{1}{2}}}{a^2c^{5/4}(\rho s t_0)^{\frac{1}{4}}m^{\frac{1}{4}}}\times\exp\left[b-\frac{a(ct_0)^{\frac{1}{2}}}{2.3\times10^{-37}\epsilon(\rho s)^{\frac{1}{2}}}\right]. \quad (4)$$

The usefulness of this expression is limited by an inexact knowledge of several quantities involved in addition to the assumptions under which it is derived. The thermal constants s and c may have values considerably different from those measured under ordinary conditions. The proper value of t_0 determines the radius over which the kinetic energy of the impinging ion is assumed to be distributed by the collision. Substituting reasonable values

$\rho s=1.0$ cal./degree; $c=0.5$ cal./sec. cm^2 degree; $t_0=3\times10^{-16}$ sec.; $a=6\times10^{-12}$ erg ($\epsilon_0=3.8$ ev); $b=43$; $m=10^{-22}$ g; $C_2=1$.

The above formula gives

ϵ	dJ_0/dn
4 ev	2×10^{-3} atom/ion
6	0.2
8	2

This shows that the above calculation gives a correct order of magnitude and demonstrates the rapid variation of dJ_0/dn near the energy required to remove one atom from the surface.

The total rate at which atoms leave the cathode surface may be found by integrating

$$J_0=\int_{\epsilon_0}^{\infty}\frac{dJ_0}{dn}\frac{dn}{d\epsilon}d\epsilon$$

$$=\frac{IG(E\lambda)^{\frac{1}{2}}}{1+\gamma}\int_{\epsilon_0/E\lambda}^{\infty}\left(\frac{9}{8}+\frac{x}{4}-\exp(-x+1/2)\right)x^{\frac{1}{2}}\times\exp\left(-x-\frac{H}{E\lambda x}+1/2\right)dx$$

where

$$G=\frac{1.5\times10^{-55}C_2e^b}{a^2c^{5/4}(\rho s t_0)^{\frac{1}{4}}m^{\frac{1}{4}}},$$

$$H=\frac{a(ct_0)^{\frac{1}{2}}}{2.3\times10^{-37}(\rho s)^{\frac{1}{2}}},$$

$$\frac{I}{1+\gamma}=\text{ionic current in ions/sec.}$$

This integral can be expressed in terms of error functions, but the result is complicated, and sufficient accuracy may be obtained without the complete expression. For the low pressure high voltage case where $E\lambda\gg\epsilon_0$,

$$J_0\approx\frac{21(\pi e)^{\frac{1}{2}}G}{16}\frac{I}{1+\gamma}(E\lambda)^{\frac{1}{2}}. \quad (5)$$

For the opposite case, where $E\lambda\ll\epsilon_0$,

$$J_0\approx\frac{GI\epsilon_0^{\frac{1}{2}}}{1+\gamma}\exp\left(-\frac{\epsilon_0}{E\lambda}-\frac{H}{\epsilon_0}+1/2\right)\left(\frac{\epsilon_0}{4E\lambda}+\frac{7}{4}\right). \quad (6)$$

As was expected, the expression for $E\lambda\gg\epsilon_0$ depends entirely on the function giving the number of atoms knocked off the cathode per impinging ion, and not on the distribution of ionic energies, whereas the rapidly varying exponential part of the expression for $E\lambda\ll\epsilon_0$ depends entirely on the energy distribution function. Since $dn(\epsilon)/d\epsilon$ is much better known than dJ_0/dn, the second expression should be correspondingly more accurate than the first.

Using (1), (3), (5), and (6), we have

if $E\lambda\gg\epsilon_0$

$$J=\frac{AI}{p}\left(\frac{Vi}{p^2}\right)^{3/5}; \quad (7)$$

if $E\lambda\ll\epsilon_0$

$$J=\frac{BI}{p}\exp(-c\epsilon_0)\left[\frac{p^2}{Vi}\right]^{2/5}\left(\frac{c\epsilon_0}{4}\left[\frac{p^2}{Vi}\right]^{2/5}+\frac{7}{4}\right), \quad (8)$$

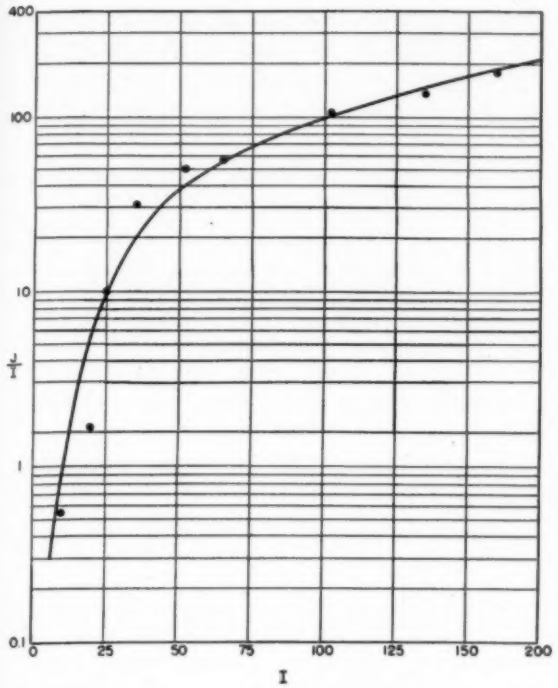

FIG. 4. Neon argon discharge. Ne, 99 percent; A, 1 percent. Rate of sputtering per unit current curve: $J/I=\text{const.}\,[7+(20.5/I^{2/5})]\exp[-(20.5/I^{2/5})]$, I = total current in milliamp., J = rate of sputtering measured as 1000/tube life in hours.

where A and B may be roughly determined from geometry of the discharge and from constants of the gas and cathode material,

$$c=1/2\left[\frac{(1+\gamma)K}{2\pi\Lambda^3}\right]^{2/5},$$

and I is the total discharge current. Although formula (7) agrees qualitatively with experimental results, it is formula (8) which is of particular interest here and will be compared in detail with experiment.

Sputtering measurements in the region $E\lambda\ll\epsilon_0$ have been very meager because the rate of sputtering in this case is extremely slow. Recently, however, Rockwood[13] has measured these slow rates of sputtering by measuring the rate of disappearance of the thin layer of active material on the cathodes of commercial cold cathode gas tubes. He showed that the aging of cold cathode tubes is due to sputtering of active material from the cathode, and by measuring the life of a number of tubes obtained the points in Fig. 4 for sputtering rate *vs.* current. A continuous fixed current was passed through each tube until it showed a characteristic increase in voltage drop. This increase in voltage marked the end of useful tube life and the disappearance of a large part of the cathode coating. Each point on Fig. 4 represents the mean of three tubes. These tubes contain neon gas at 60 mm Hg with a small admixture of argon and operate at 60 volts with constant cathode area (2.7 cm²) over a range of current from about 5 to 200 milliamperes, making good the approximations involved in deriving (8). Agreement between theory and experiment is obtained as shown in Fig. 4 by properly choosing two constants to fit an expression of the form

$$J=aI^{-b/I^{2/5}}(7+b/I^{2/5})$$

to the experimental points.

Using the experimentally determined value of b and comparing its theoretical expression

$$c\epsilon_0\left[\frac{p^2}{Vi}\right]^{2/5},$$

we may evaluate ϵ_0. Since it is thought that most of the ions striking the cathode are argon,[14] moving in a gas which is essentially neon, we estimate from Table I, the values

TABLE I. Value of constants Λ and K where $\Lambda=\lambda p$ (λ = mean free path in cm), p = pressure in mm Hg, and $K=kp\sqrt{\epsilon}$ (k = mobility of potassium ion in electrostatic units, ϵ = ionic energy in electron stat-volts).

	Λ*	K**
H_2		1.8×10^5
He	1.42×10^{-2}	
Ne	1.01×10^{-2}	
N_2	4.77×10^{-3}	
A	5.07×10^{-3}	3.1×10^4

* E. H. Kennard, *Kinetic Theory of Gases* (McGraw-Hill Book Company, Inc., New York, 1938).
** A. V. Hershey, Phys. Rev. **56**, 908 (1939).

$$\Lambda=7.0\times10^{-3},$$

and

$$K=7.0\times10^4,$$

so that

$$c=8.3\times10^3$$

if p is measured in mm of Hg, V and i in static units. This gives $\epsilon_0=0.013$ electron stat-volts or

[13] G. H. Rockwood, A.I.E.E. Technical Paper (May, 1941), pp. 4–117.

[14] M. J. Druyvesteyn and F. M. Penning, Rev. Mod. Phys. **12**, 87 (1940).

TABLE II. Sputtering data.

Discharge pressure p mm Hg	Discharge current I milliamperes	Rate of sputtering J arbitrary units	I/p^2	J/p
5	2.6	<4.0	0.104	<0.8
10	11.5	5.8	0.115	0.58
15	27	14.2	0.120	0.95
20	47	20	0.118	1.0

3.9 electron volts which is in agreement with the observed values of ϵ_0 for metals varying from about 1 to 10 ev, and in particular with 2.1 ev given for pure Ba or Sr.[15] The cathode material is a mixture of Ba, Sr, and their oxides.

The second constant which is determined by the experimental data may be expressed in terms of the average number of atoms released by each ion of energy greater than ϵ_0. A tube operating at 25 milliamperes has a lifetime of 400 hours, during which time 1.8×10^{23} ions will have struck the cathode, and of these ions 3.6×10^{21} will have energy greater than 3.9 ev [Eq. (2)]. The cathode coating consists of about 1.0 mg of material of average atomic weight 100, and if we suppose that $\frac{1}{4}$ of this must be sputtered off to end the useful life of the tube, the number of sputtered atoms is found to be 1.5×10^{18}. The shape of the cathode and tube walls allows no simple evaluation of the fraction of atoms released from the cathode which are deposited on the tube walls, but a rough calculation from formula (1) gives 10^{-3}, so that about 1.5×10^{21} atoms are evaporated by the cathode or 0.4 atom per ion of energy greater than 3.9 ev. The fraction 0.4 seems physically reasonable and also agrees with the values found above from expression (4) for dJ_0/dn.

Rockwood also made measurements on a series of tubes containing pure argon at different pressures and operating at currents which were nearly proportional to the square of the pressure, so that the expression (p^2/Vi) would remain constant.[16] In this case, it is easily seen that according to Eq. (8), the rate of sputtering will be simply proportional to pressure. Table II shows that this is true within experimental error. This fact is not a test of the specific form of Eq. (8), for by making p^2/Vi constant, equivalent discharge conditions are obtained with the same ionic energies, so that it is only a test of fundamental assumptions and of Eq. (1) for the fraction of evaporated material which escapes from the cathode.

The rate of sputtering in a pure gas is complicated by the fact that ions exchange their charges rapidly in the neutral atoms of their own kind. This phenomenon probably does not occur in the mixture of gases cited above because the argon ions carry a large part of the discharge current, and argon is present in such small quantities that exchange of charge between an argon ion and an argon atom may be shown to be quite improbable. The effect of such an exchange would be to decrease the ionic mean free path and to make it strongly dependent on ionic velocity. Kallman and Rosen[17] show that the mean free path is decreased by a factor of two by the exchange of charge in He. The results quoted above for pure argon with varying pressures would not be affected because (p^2/Vi) and hence the ionic energies and free paths were kept constant. However, since the free path probably changes rapidly with change in ionic

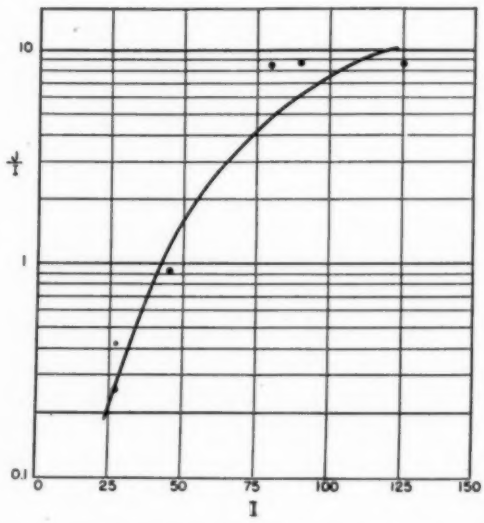

FIG. 5. Pure argon discharge. 100 percent A. Rate of sputtering per unit current curve: $J/I=$const. $[7+(30.6/I^{2/5})]\times\exp[-(30.6/I^{2/5})]$, $I=$total current in milliamp., $J=$rate of sputtering measured as 1000/tube life in hours.

[15] F. R. Bichowsky and F. D. Rossini, *The Thermochemistry of the Chemical Substances* (Reinhold Publishing Corporation, New York, 1936).
[16] Private communication.
[17] H. Kallman and B. Rosen, Zeits. f. Physik **64**, 806 (1930).

energy, formula (8) will not be accurate under more general conditions.

With this reservation, it is interesting to compare measurements made by Rockwood[18] on variation of sputtering with current for argon-filled tubes. His points are fitted to Eq. (8) in Fig. 5. Treating the experimentally determined constants as before, and assuming that the ionic mean free path is just half the atomic mean free path because of electron exchange and that consequently the mobility of an argon ion in argon gas is half that of a potassium ion in argon we obtain $\epsilon_0=3.1$ ev and $dJ_0/dn=0.27$. These quantities agree as well as can be expected with their more accurate determination from the neon-argon discharge.

[18] Private communication.

PHYSICAL REVIEW VOLUME 65, NUMBERS 11 AND 12 JUNE 1 AND 15, 1944

On the Extraction of Electrons from a Metal Surface by Ions and Metastable Atoms*

A. COBAS,** *Columbia University, New York, New York, and University of Puerto Rico, Rio Piedras, Puerto Rico*

AND

W. E. LAMB, JR., *Columbia University, New York, New York*

(Received March 31, 1944)

An elementary theory is developed for the process by which a helium ion or a 2^3S metastable helium atom may extract an electron from a metal surface. The helium ion after collision may become a neutral atom although sometimes an excited or even a metastable atom. In the case of the metastable atom the collision involves an exchange of electrons between the metal and the atom, the excess energy being carried away by the ejected L shell electron. The average distance of transition δ for He^+ and for the 2^3S metastable helium atom is calculated for different velocities. For $v=10^8$ cm/sec., $\delta_{met}=2a_0$ and $\delta_{ion}=11.5a_0$ where $a_0=0.528\times10^{-8}$ cm. For $v=3\times10^7$ cm/sec., δ_{met} comes out less than $0.1a_0$ and $\delta_{ion}=6.0a_0$. These values are different from the values obtained by Massey in a similar computation. The theory accounts for some but not all of the experimental evidence. The probable shape of the potential that the metal surface offers to a metastable atom is found.

I. INTRODUCTION

A POSITIVE ion or a metastable atom colliding with a metal surface may undergo a collision of the second kind with the aid of one of the metallic electrons. In the case of a metastable atom whose radiative transition to the ground state is forbidden by the spin conservation selection rule $\Delta S=0$, the collision can involve an exchange of electrons between the metal and the atom which leaves the atom in a state of different multiplicity—let us say, the ground state. The positive ion simply captures the metallic electron, thereby becoming a neutral atom, although sometimes an excited or even a metastable atom. In the latter case, the metastable atom may decay with secondary electron emission.

The electron emission due to impact of mercury metastable atoms on a nickel surface was first definitely proved by Webb.[1] This was followed up by the work of Messenger[2] and Coulliette.[3] Sonkin[4] studied this electron emission using a tungsten surface under various conditions. Oliphant[5] also studied the emission of electrons from metal surfaces as a result of impact by helium metastable atoms. Besides the above-

* Submitted by Amador Cobas in partial fulfillment of the requirements for the degree of Doctor of Philosophy, in the Faculty of Pure Science, Columbia University, New York, New York. Publication assisted by the Ernest Kempton Adams Fund for Physical Research of Columbia Universiy.

** On leave from the University of Puerto Rico. Guggenheim Fellow 1943–44.

[1] H. W. Webb, Phys. Rev. **24**, 113 (1924).
[2] H. A. Messenger, Phys. Rev. **28**, 962 (1926).
[3] H. J. Coulliette, Phys. Rev. **32**, 636 (1928).
[4] S. Sonkin, Phys. Rev. **43**, 788 (1933).
[5] M. L. E. Oliphant, Proc. Roy. Soc. **A124**, 228 (1929).

mentioned direct studies, the extraction of electrons from metal surfaces by metastable atoms has been suggested as a mechanism to account for various phenomena. Uyterhoeven and Harrington[6] made use of the action of metastable atoms on metal surfaces to explain the emission of electrons from cold electrodes in discharges of neon, argon, and helium. In a similar manner Found and Langmuir[7] tried to explain the secondary emission from a negative probe in a neon discharge. Other authors[8–10] considered the action of metastable atoms on metal surfaces in their discussion of electrical and resonance radiation phenomena in gases, making use of some of the before-mentioned investigations. Penning[11] investigated the electron emission produced by positive neon ions which pass down a fine metal canal. Oliphant[5] pointed out that Penning's results probably include a contribution from metastable atoms produced as in his work.

The extraction of electrons by positive ion bombardment has been studied by many more people than the case of the metastable atoms. We shall mention only those where the energy of the bombarding ions is of the order of a few hundred volts. The reason for this limitation is that at higher energies the positive ion is able to eject secondaries from the metal by virtue of its motion besides merely capturing electrons due to its electric field. Oliphant[12] studied the electron emission from a metal surface due to He^+ bombardment. Chaudhri[13] investigated the secondary emission from a nickel surface by Hg^+ bombardment. He admitted the possibility that metastable mercury atoms could be responsible for part of the emission. Ramsauer and Kollath[14] studied the reflection of protons from solid bodies. Brasefield[15] measured the efficiency of argon ions and argon metastables in extracting electrons from a metal surface. Healea and Chaffee[16] studied the electron emission from a hot nickel target bombarded with molecular hydrogen ions. Veith[17] measured the ion reflection and the electron emission while bombarding metals with K^+. Guntherschulze and Bar[18] studied the emission of electrons from a MgO cathode in the glow discharge using He, Ne, A, H_2, N_2, and O_2. Healea and Houtermans[19] measured the electron emission and the ion reflection from a degassed nickel target bombarded by He, Ne, and A ions. Korff and Present[20] made use of the transition of ions into metastable atoms near a metal surface in their discussion of the discharge mechanism of Geiger counters. The energy involved in this process is thermal energy.

Oliphant and Moon[21] explained the neutralization of positive ions during a collision with a metal surface by the auto-electronic emission into a state of equal energy in the atom under the influence of the electrostatic field of the approaching ion. This theory was admittedly not made very precise. Massey[22] made a quantum mechanical calculation of the neutralization of a positive hydrogen ion when colliding with a metal surface and found the average distance at which this transition takes place. He assumed that for the case of a He^+ this distance is larger by a factor of two or more. He also made a similar calculation for the emission of electrons during the impact of metastable helium atoms and a metal surface. When the helium ion is neutralized, it may assume the triplet 2^3S state. He used perturbation theory to find the probability of a transition as a function of the distance from the metal surface and obtained the result that the probability of transition for the positive ions approached unity at a smaller distance from the

[6] W. Uyterhoeven and M. C. Harrington, Phys. Rev. **35**, 438 (1930); **36**, 709 (1930).
[7] C. Found, Phys. Rev. **34**, 1625 (1929); I. Langmuir and C. Found, Phys. Rev. **36**, 604 (1930); C. Found and I. Langmuir, Phys. Rev. **39**, 237 (1930).
[8] K. K. Darrow, *Electrical Phenomena in Gases* (Williams and Wilkins, 1932).
[9] L. B. Loeb, *Fundamental Processes of Electrical Discharge in Gases* (John Wiley & Sons, Inc., New York, 1939).
[10] A. C. G. Mitchell and M. W. Zemansky, *Resonance Radiation and Excited Atoms* (The Macmillan Company, New York, 1934).
[11] F. M. Penning, Vers. K. Ak. Amst. **36** (1927); Physics **8**, 13 (1928).
[12] M. L. E. Oliphant, Proc. Roy. Soc. **A127**, 373 (1930).
[13] R. M. Chaudhri, Proc. Camb. Phil. Soc. **28**, 349 (1932).
[14] C. Ramsauer and Kollath, Ann. d. Physik **16**, 560 (1933).
[15] C. J. Brasefield, Phys. Rev. **44**, 1002 (1933).
[16] M. Healea and E. L. Chaffee, Phys. Rev. **49**, 925 (1936).
[17] W. Veith, Ann. d. Physik **29**, 189 (1937).
[18] A. Guntherschulze and W. Bar, Zeits. f. Physik **107**, 11–12, 730 (1937); Zeits. f. Physik **108**, 11–12, 780 (1938).
[19] M. Healea and C. Houtermans, Phys. Rev. **58**, 608 (1940).
[20] S. A. Korff and R. D. Present, Phys. Rev. **65**, 253 (1944).
[21] M. L. E. Oliphant and P. B. Moon, Proc. Roy. Soc. **A127**, 388 (1930).
[22] H. S. W. Massey, Proc. Camb. Phil. Soc. **26**, 386 (1930); **27**, 460 (1931).

metal surface than for the case of the metastable atoms. This means that if helium ions and metastable 2^3S helium atoms are approaching a metal surface, the average distance at which the metastable atoms will decay is larger than the average distance at which the ions will be neutralized.

II. METASTABLE CASE

In this paper we shall show that in Massey's analysis of the metastable case the wrong matrix element was taken for the calculation of the decay constant. Taking the correct matrix element, one obtains the more reasonable result that the average distance for transition is larger in the case of the ion than in the case of the metastable atom. We proceed to develop our theory for the case of the triplet 2^3S metastable helium atom colliding with a metal surface.

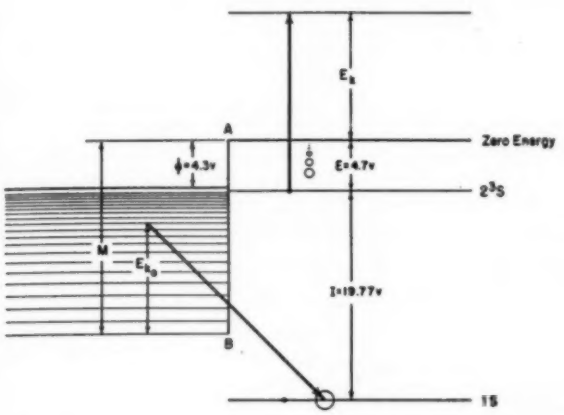

FIG. 1. Energy balance diagram for the extraction of electrons by metastable helium atoms from molybdenum. The region to the left of AB represents the potential well equivalent to the metal surface; the lines represent the continuous energy levels of the metallic electrons, the spacing of the lines roughly representing the density of the levels. The region to the right of AB represents the levels of the atomic electrons. The thick arrows indicate the transition which involves an exchange of electrons. An empty circle represents a vacancy in one of the atomic energy levels. A black dot represents an occupied level.

a. Energy Balance

Figure 1 shows the energy levels of the helium electrons, the metallic electrons, and the final free electron for the case of a Mo surface. The thick arrows indicate the transition which involves an exchange of electrons. The lines to the left of AB represent the continuous energy levels of the metallic electrons, the spacing of the lines roughly representing the density of levels. An empty circle represents a vacancy in one of the energy levels of the helium atom. A black dot represents an occupied level. Equating initial and final energies, we get for the transition shown

$$-M+E_{k_0}-\epsilon=-(I+\epsilon)+E_k,$$

$$E_k=I-M+E_{k_0},$$

where

I = energy difference between the 2^3S and the $1S$ states,
ϵ = energy of the 2^3S state,
E_{k_0} = kinetic energy of the metallic electron,
E_k = energy of the free electron after the transition,
M = energy of the potential well which represents the metal.

From this equation and the values shown in Fig. 1 it is clear that any metallic electron is capable of making the transition in the case of a Mo surface.

b. Decay Rate

From the quantum mechanical theory of collision, one finds that the rate at which metastable atoms decay as a function of the distance s from the metal surface is

$$\lambda(s)=[nmk\Omega^2/\pi\hbar^3]|H|^2,$$

where

m = mass of the electron,
$\hbar=h/2\pi$ = Bohr unit of angular momentum,
$k=(2mE)^{\frac{1}{2}}/\hbar$, where E is the kinetic energy of the emitted electron,
n = density of free electrons,
Ω = volume used for normalizing the wave functions,

and H is the matrix element of the Hamiltonian for the transition where the initial state is a triplet 2^3S metastable helium atom and a free electron of momentum $\hbar k_0$ inside the metal and the final state is a helium atom in the ground state and a free electron of positive total energy and momentum $\hbar k$.

c. Matrix Element

The matrix element is the following:

$$H=\int\int\int u_{1s}^*(r_3)u_{1s}^*(r_2)[\exp(-i\mathbf{k}\cdot\mathbf{r}_1)]/\sqrt{\Omega}\times\left[\frac{2e^2}{r_3}-\frac{e^2}{r_{13}}\right]u_{1s}(r_2)u_{2s}(r_1)\times[\exp(i\mathbf{k}_0\cdot\mathbf{r}_3)]/\sqrt{\Omega}\,d\tau_1 d\tau_2 d\tau_3, \quad (1)$$

where the u's represent hydrogenic wave functions and the subscripts 1, 2, and 3 attached to the r's refer to the three electrons involved in the transition. e is the electronic charge.

$$u_{1s}(r_3)u_{1s}(r_2)=(1/\sqrt{\pi})(Z'/a_0)^{\frac{3}{2}}\exp(-Z'r_3/a_0)\times(1/\sqrt{\pi})(Z'/a_0)^{\frac{3}{2}}\exp(-Z'r_2/a_0)=[a^3\exp a(-r_2-r_3)]/\pi,$$

$$u_{1s}(r_2)u_{2s}(r_1)=(1/\sqrt{\pi})(Z_1/a_0)^{\frac{3}{2}}\exp(-Z_1r_2/a_0)\times(1/4\sqrt{2\pi})(Z_2/a_0)^{\frac{3}{2}}(2-Z_2r_1/a_0)\times\exp(-Z_2r_1/2a_0)=[(bc)^{\frac{3}{2}}/\pi]\times(1-br_1)\exp(-br_1-cr_2),$$

where

a_0 = one Bohr radius $= 0.528\times10^{-8}$ cm,

$a=Z'/a_0=1.69/a_0$,

$b=Z_2/a_0=1.19/a_0$,

$c=Z_1/a_0=2.04/a_0$.

The numerical values assigned to Z', Z_1, and Z_2 are those used by Bethe.[23]

This matrix element has the physical interpretation that in the initial state electron 3 is a metal electron, and electrons 1 and 2 are the atomic electrons; and that in the final state, electron 1 is a free electron, and electrons 2 and 3 are the atomic electrons.

Massey[22] starts with an expression which is identical to Eq. (1), but in his subsequent calculations he actually uses the following matrix element:

$$H=\int\int\int u_{1s}^*(r_1)u_{1s}^*(r_2)[\exp(-i\mathbf{k}\cdot\mathbf{r}_1)]/\sqrt{\Omega}\times\left[\frac{2e^2}{r_3}-\frac{e^2}{r_{13}}\right]u_{1s}(r_2)u_{2s}(r_3)\times[\exp i\mathbf{k}_0\cdot\mathbf{r}_3]/\sqrt{\Omega}d\tau_1 d\tau_2 d\tau_3. \quad (2)$$

This matrix element implies that electron 3 has initially both the wave function $\exp i\mathbf{k}_0\cdot\mathbf{r}_3/\sqrt{\Omega}$ and the wave function $u_{2s}(r_3)$ and that similarly electron 1 has finally the wave function $[\exp(-i\mathbf{k}\cdot\mathbf{r}_1)]/\sqrt{\Omega}$ and the wave function $u_{1s}(r_1)$.

The contribution from $2e^2/r_3$ in Eq. (1) is not very small because $u_{2s}(r_1)$ is not orthogonal to $[\exp(-i\mathbf{k}\cdot\mathbf{r}_1)]/(\Omega)^{\frac{1}{2}}$. If we were to use a more exact wave function for the free electron, the orthogonality would be better, and for this reason we neglect this contribution.

If we substitute for the u's the hydrogenic wave functions they represent, Eq. (1) becomes:

$$H=A\int_{\text{all space}}\int\int[\exp a(-r_2-r_3)-i\mathbf{k}\cdot\mathbf{r}_1]\times[1/r_{13}](1-br_1)\times\exp(-br_1-cr_2+i\mathbf{k}_0\cdot\mathbf{r}_3)d\tau_1 d\tau_2 d\tau_3. \quad (3)$$

$$A=[e^2a^3(bc)^{\frac{3}{2}}]/\pi^2\Omega.$$

Now we undertake the evaluation of H. The integration with respect to $d\tau_2$ can be carried out immediately. This gives a factor $8\pi/(a+c)^3$. The remaining integral

$$\int_{\text{all space}}\int[\exp(-ar_3-i\mathbf{k}\cdot\mathbf{r}_1)]\times[1/|\mathbf{r}_1-\mathbf{r}_3|](1-br_1)\times\exp(-br_1+i\mathbf{k}_0\cdot\mathbf{r}_3)d\tau_1 d\tau_3 \quad (3')$$

is rather complicated, but one can get a fairly good approximation, valid for large distances s of the atom from the metal surface; s being large compared to an atomic radius. Then $\exp(-ar_3)$ falls off much quicker than $1/|\mathbf{r}_1-\mathbf{r}_3|$, and one can substitute $1/|\mathbf{r}_1-\mathbf{s}|$ for the expression $1/|\mathbf{r}_1-\mathbf{r}_3|$.

The integral with respect to $d\tau_3$ is the following:

$$\int_0^{2\pi}\int_0^{\pi/2}\int_{s\sec\theta_3}^{\infty}[\exp ik_0r_3(\cos\theta_3\cos\theta_{k_0}+\sin\theta_3\sin\theta_{k_0}\cos\phi_3)-ar_3]r_3^2dr_3\sin\theta_3 d\theta_3 d\phi_3,$$

where we have taken $\mathbf{s}$ as the polar axis and where the integration over θ_3 is taken from 0 to $\pi/2$ to take care of the fact that the wave function of the metallic electron is zero outside the metal. The integration with respect to ϕ_3 gives $2\pi J_0(k_0r_3\sin\theta_3\sin\theta_{k_0})$. Because of the overlapping of the wave functions, the integrand

[22] H. Bethe, *Handbuch der Physik*, Vol. 24/1, p. 365.

will have non-vanishing values only for θ_3 small. Therefore we can replace the Bessel function by unity and do the rest of the integration immediately obtaining

$$2\pi[\exp(ik_0\cos\theta_{k_0}-a)s]/as \times[-s^2/(ik_0\cos\theta_{k_0}-a) +2s/(ik_0\cos\theta_{k_0}-a)^2-2/(ik_0\cos\theta_{k_0}-a)^3].$$

The square of the absolute value of this expression is a factor in $|H|^2$, and we are interested in knowing how it depends on θ_{k_0}. For $s=3a_0$ and $\theta_{k_0}=\pi/2$ this absolute value squared is bigger by a factor of 1.44 than for the same s, but $\theta_{k_0}=0$. For $s=4a_0$ the ratio is 1.40. If we assume k_0 to be zero, i.e., if we take the initial metallic electron to be at rest inside the metal, the integral becomes just

$$\int \exp(-ar_3)d\tau_3 =[2\pi/a_3](as+2)\exp(-as). \quad (4)$$

The square of this integral for $s=3a_0$ gives a value 1.32 times the value obtained when we assume k_0 to be perpendicular to the metal surface. Thus it is reasonable to believe that it does not matter very much whether the initial electron is at rest or moving in any direction whatsoever. The case of the electron moving perpendicularly to the metal surface but away from the surface gives a result identical to the case where the electron is moving towards the metal surface.

We now consider the integration with respect to $d\tau_1$. The integral we have to do is the following:

$$\int_0^{2\pi}\int_0^{\pi}\int_0^{\infty}[1/|\mathbf{r}_1-\mathbf{s}|](1-br_1) \times[\exp(-br_1-i\mathbf{k}\cdot\mathbf{r}_1)]r_1^2dr_1\sin\theta_1\,d\theta_1\,d\phi_1.$$

We can expand $1/|\mathbf{r}_1-\mathbf{s}|$ in terms of spherical harmonics and $\exp(-i\mathbf{k}\cdot\mathbf{r}_1)$ in terms of spherical harmonics and Bessel functions. The integration over θ_1 and ϕ_1 can be done immediately.

The integration over r_1 reduces to

$$\int_0^s \sum_l (-i)^l P_l(\cos\theta_k)[r_1^{l+2}/s^{l+1}] \times\exp(-br_1)[1-br_1](\pi/2kr_1)^{\frac{1}{2}}J_{l+\frac{1}{2}}(kr_1)dr_1 +\int_s^{\infty}\sum_l (-i)^l P_l(\cos\theta_k)[s^l/r_1^{l-1}] \times\exp(-br_1)[1-br_1](\pi/2kr_1)^{\frac{1}{2}}J_{l+\frac{1}{2}}(kr_1)dr_1.$$

The integration with respect to dr_1 can be evaluated numerically for arbitrary values of s. For large s, one can obtain a good approximation by considering only the first integral and taking the limits of integration over r_1 from 0 to ∞ instead of from 0 to s.

We assume $\mathbf{k}$ to make an angle θ_k with the perpendicular to the metal surface and estimate its numerical value by letting $E_k=(19.77-4.3)$ ev, where 19.77 ev[24] is the difference in energy between the ground state and the 2^3S metastable state of helium, and 4.3 ev[25] is the approximate value of the work function of Mo, which is one of the metals Oliphant used. Neglecting all terms for which $l>2$, we get the following result:

$$(1.077\times10^{-24})/s-i(8.519\times10^{-23}\cos\theta_k)/s^2 +(6.520\times10^{-42}-1.955\times10^{-41}\cos^2\theta_k)/s^3.$$

Multiplying this expression by its conjugate, integrating over all space, and putting together our previous calculations, we find that the rate at which metastable helium atoms will decay is:

$$\lambda(s)=8nmk\Omega^2A^2\pi^2/\hbar^3a^4[8\pi/(a+c)^3]^2 \times\exp(-2as)[(3.956\times10^{-9}+0.796s)^2 +(3.268\times10^{-9}+0.404s)^2] \times[(2.320\times10^{-48})/s^2 +(5.033\times10^{-65})/s^4 +(7.649\times10^{-83})/s^6]. \quad (5)$$

This expression is a good approximation when s is of the order of $3a_0$ or greater.

One can find a reasonable value for $\lambda(0)$ by solving the problem anew for this special value of s. In this case one can no longer substitute $1/|\mathbf{r}_1-\mathbf{s}|$ for $1/|\mathbf{r}_1-\mathbf{r}_3|$ in the integral over $d\tau_1$ and $d\tau_3$. If we assume k_0 to be zero, the integral is as follows:

$$\int\int \exp(-ar_3-i\mathbf{k}\cdot\mathbf{r}_1)[1/|\mathbf{r}_1-\mathbf{r}_3|] \times(1-br_1)\exp(-br_1)f(r_3)d\tau_1d\tau_3,$$

where $f(r_3)$ is equal to unity inside the metal and is equal to zero outside the metal. We assume that half of the atom is inside the metal and the other half is outside, and take the polar axis per-

[24] *Handbuch der Physik*, Vol. 24, p. 348.
[25] *Handbuch der Physik*, Vol. 14, p. 69.

pendicular to the surface. We expand $1/|\mathbf{r}_1-\mathbf{r}_3|$ in terms of spherical harmonics and $\exp(-i\mathbf{k}\cdot\mathbf{r}_1)$ in terms of spherical harmonics and Bessel functions. The limits of integration for θ_3 are from 0 to $\pi/2$; this takes care of the discontinuity of $f(r_3)$. The integration over θ_1, θ_3, ϕ_1, and ϕ_3 can be done immediately. Part of the integration over r_1 and r_3 was done analytically, and part was done numerically. When the values of the constants as already defined are used, the integral reduces to the following expression:

$$1.589\times10^{-41}+i[5.707\times10^{-42}P_1(\cos\theta_k)+9.077\times10^{-43}P_3(\cos\theta_k)]+\text{higher order terms.} \quad (6)$$

Squaring this expression, integrating over all space, and substituting in the expression for $\lambda(0)$, one finds $\lambda(0)=1.97\times10^{15}$ sec.$^{-1}$. We thus have found a value for $\lambda(0)$ and an analytic expression for $\lambda(s)$ which is a good approximation when s is of the order of $3a_0$ or greater. Figure 2 shows $\log_{10}\lambda(s)$ plotted against s. The heavy line was obtained from the expression for $\lambda(s)$ and therefore was extended into $s=3a_0$. Point A corresponds to $\log_{10}\lambda(0)$, and point C corresponds to $\log_{10}\lambda(3a_0)$; these two points are known fairly well. We have drawn a dotted line to show the probable value of $\log_{10}\lambda(s)$ for $s<3a_0$. For $s=2a_0$ we took k_0 perpendicular to the metal surface and performed the integration over $d\tau_3$ exactly and the integration over $d\tau_1$ numerically for this particular distance. In this integration we again substitute s for r_3 in the denominator of Eq. (3'), which is not too bad an approximation for $s=2a_0$. Using our results we can get a fairly good value for $\log_{10}\lambda(2a_0)$. Point B corresponds to this value and falls on the extrapolated curve as shown.

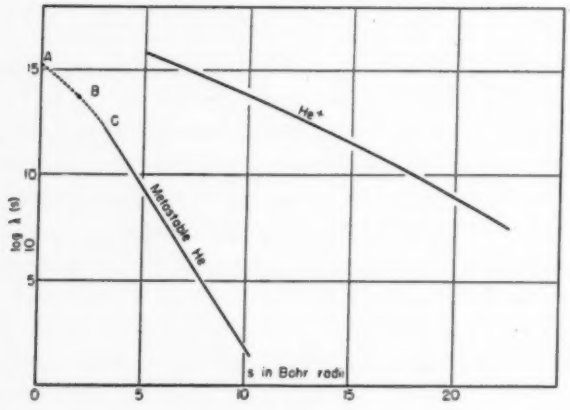

FIG. 2. Graph of $\log_{10}\lambda(s)$ as a function of s for He^+ and for 2^3S metastable He.

d. Probability of Transition

Actually the motion of the atom would make it necessary to derive a more complicated expression involving the time-variation of the perturbing potential. For velocities of collision such that the time-Fourier analysis of the perturbation does not contain appreciable amplitudes for frequencies of the order of an atomic frequency, one may regard the collision as adiabatic and use the time-independent perturbation at each distance. However, it is necessary to allow for the possible decay of the atom at some larger distance. Let $P(s)ds$ be the probability that the atom decays at position s in a distance ds. The probability that the atom reaches position s without decaying is

$$1-\int_s^\infty P(s)ds,$$

$$\therefore\quad P(s)=[\lambda(s)/v_0]\left[1-\int_s^\infty P(s)ds\right]ds,$$

where v_0 is the velocity of the helium atom, which we shall assume constant. The solution of this integral equation is

$$P(s)=B\exp\int\{1-d/ds[v_0/\lambda(s)]\}\lambda(s)/v_0ds,$$

where B is a constant of integration.

Approximating $\lambda(s)$ by the simple exponential form $\lambda(s)=A\exp(-\alpha s)$, where $A=9.626\times10^{16}$ and $\alpha=7.303\times10^8$ we find the expression for $P(s)$ becomes

$$P(s)=F\exp[-(A/v_0\alpha)\exp(-\alpha s)-\alpha s],$$

where F is a constant.

From the integral equation it is easy to see that for large s

$$P(s)=\lambda(s)/v_0=[A/v_0]\exp(-\alpha s)$$

and from the solution for $P(s)$ it is obvious that

for large s

$$P(s) = F \exp(-\alpha s),$$

$$\therefore \quad F = A/v_0$$

and

$$P(s) = [A/v_0] \exp[-(A/v_0) \exp(-\alpha s) - \alpha s].$$

Figure 3 shows a graph of $P(s)$ against s for $v_0 = 10^5$ cm/sec. It should be noted that the exponential form taken for $\lambda(s)$ keeps on increasing for values of $s < 2a_0$ while the graph of $\log_{10} \lambda(s)$ indicates that $\lambda(s)$ probably levels off. For this reason the graph of $P(s)$ may probably be less steep on the side of small s than is shown on Fig. 3. To get $\bar{s}$ the average distance for transition, one has to do the integral

$$\int_0^\infty sP(s)ds,$$

which can be done graphically or analytically. For $v_0 = 10^5$ cm/sec., $\bar{s} = 2a_0$ which is very near s_m, the value of s for which $P(s)$ is a maximum. For $v_0 = 3 \times 10^7$ cm/sec. s comes out less than $0.1a_0$. This last value of $\bar{s}$ does not have very much meaning because of the breakdown of the perturbation theory and the crudeness of the model used for the metal. For this velocity Massey[22] obtained a value of $\bar{s}$ of the order of $3a_0$, which according to our calculations is certainly too high. A very good approximation to $\bar{s}$ can be obtained by finding the s for which

$$\int_s^\infty \lambda(s)/v_0 ds = 1.$$

For $v_0 = 10^5$ cm/sec. one gets $1.9a_0$ for $\bar{s}$.

TABLE I. Relation between the velocity component perpendicular to the metal surface and the percentage of metastable atoms reflected.

Vel. perpendicular to surface in 10^6 cm/sec.	Percentage of ref. met. (Oliphant's results)	Average percentage
2.6	60 to 90	75
4.5	40 to 60	50
7.0	40 to 70	55
7.8	>50	
9.9	40	40
12.0	15 to 40	28
14.0	40 to 50	45
17.0	10 to 30	20
20.0	10 to 20	15
32.0	5	

From Oliphant's[12] results (shown in Table I) of the percentage of reflected metastable atoms at different velocities and different angles of incidence, it can be seen that the percentage of reflected metastable atoms varies fairly linearly with the component of velocity perpendicular to the surface. This might indicate that the percentage of reflected metastable atoms depends mainly on how close the atoms get to the metal surface.

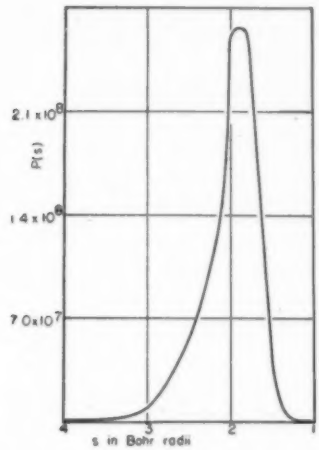

FIG. 3. Graph of $P(s)$ as a function of s for metastable helium atoms of velocity 10^5 cm/sec.

From these data one could calculate the distance from the metal surface at which most atoms turn back. Let us call this distance s_R. An approximate value of s_R can be obtained by solving for s_R in the equation

$$R = 1 - 2\int_{s_R}^\infty \lambda(s)/v_0 ds,$$

where R is the fraction of reflected metastable atoms. Knowing the initial energy of the metastable atoms and knowing where they turn back, one can get the shape of the repulsive potential that the surface offers to the metastable atoms. Figure 4 shows this potential as a function of s. In this analysis we have neglected the fact that we should use $P(s)$ instead of $\lambda(s)$ and v instead of v_0, where v is the instantaneous velocity. When we found $P(s)$ previously, we assumed that the atom decayed on its ingoing trip, but if we now consider the reflection coefficient R, we must solve the problem more rigorously. Let us call $P_i(s)$ the $P(s)$ we already calculated, meaning

that it is the probability that the atom decays on its ingoing trip. To get an expression for $P_0(s)$, the probability that the atom decays on its outgoing trip, one must solve the integral equation

$$P_0(s)=\left[1-\int_{s_R}^{\infty}P_i(s)ds-\int_{s_R}^{s}P_0(s)ds\right]\lambda(s)/v_0.$$

The solution of this equation is

$$P_0(s)=[A/v_0]\exp[-\alpha s+(A/\alpha v_0)\times\exp(-\alpha s)-(2A/\alpha v_0)\exp(-\alpha s_R)].$$

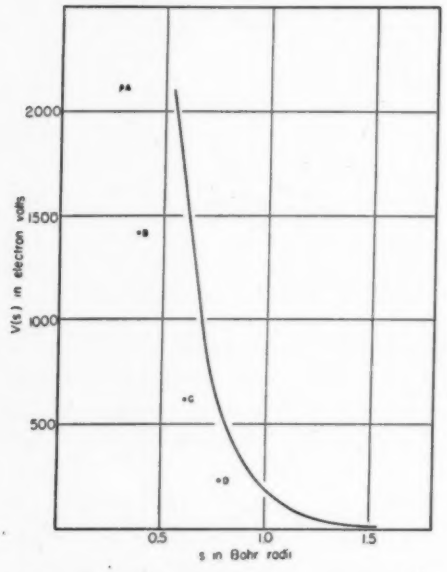

FIG. 4. Potential offered by a metal surface to a 2^3S helium atom.

Now s_R can be obtained by solving the equation

$$R=1-\int_{s_R}^{\infty}P_i(s)ds-\int_{s_R}^{\infty}P_0(s)ds=\exp[-(2A/\alpha v_0)\exp(-\alpha s_R)].$$

Calculating s_R from this formula, one finds that the curve representing the potential that the surface offers to the metastable atom is closer to the surface than what was previously obtained as shown by points A, B, C, and D on Fig. 4. We now correct for the fact that the velocity of the metastable atoms is not a constant v_0 but a function $v(s)$ which can be obtained from v_0 and the potential curve already found. By a process of iteration, the potential curve can be improved. Plotting $v(s)$ against s, one can find an analytic expression that fits the curve obtained. One can now find $P_i(s)$ and $P_0(s)$ by again solving the integral equations

$$\left[1-\int_{s}^{\infty}P_i(s)ds\right]\lambda(s)/v(s)=P_i(s),$$

$$\left[1-\int_{s_R}^{\infty}P_i(s)ds-\int_{s_R}^{s}P_0(s)ds\right]\lambda(s)/v(s)=P_0(s).$$

Again s_R was obtained from the equation

$$R=1-\int_{s_R}^{\infty}P_i(s)ds-\int_{s_R}^{\infty}P_0(s)ds.$$

This second correction brought the potential curve almost to coincide with the curve obtained by using

$$R=1-2\int_{s_R}^{\infty}\lambda(s)/v_0ds.$$

This means that apparently the two errors involved in using this approximation cancel each other. It is unfortunate that both Oliphant's results and our theory are rather crude and that therefore the curve we obtained is only a rough approximation. It does, however, indicate a method to obtain information about the repulsion of atoms by metals. The theory can probably be improved considerably when there is need for it, so that more precise data on the reflection of metastables from metal surfaces are to be desired highly.

e. Angular Dependence

Equations (5) and (6) show that if the transition takes place at the metal surface or at large distances from the surface, there is practically no angular dependence. No detailed experiments have been carried out to test this angular dependence, but Oliphant informed Massey[22] that he found no electrons ejected at an angle less than 15° with the surface. Our theory does not predict such angular distribution, and for this feature a more refined theory or experimental procedure is needed. For the special value $s=2a_0$ the integral over $d\tau$ gives

$$4\pi\times10^{-18}\{5.246P_0(\cos\theta_k)+2.916P_2(\cos\theta_k)-0.407P_4(\cos\theta_k)+0.017P_6(\cos\theta_k)+i[2.370P_1(\cos\theta_k)-1.350P_3(\cos\theta_k)+0.093P_5(\cos\theta_k)-0.003P_7(\cos\theta_k)]\}+\text{higher order terms.}$$

An expression whose absolute value squared has an angular dependence is shown in Fig. 5.[26] For thermal velocities this is the average distance of transition, and hence from our theory we should expect some angular dependence for these velocities. Oliphant's velocities were of the order of 10^7 cm/sec., and thus the atoms penetrated closer than $2a_0$ before decaying, making the angular distribution even less than that shown in Fig. 5.

Massey[22] explains the angular distribution found by Oliphant by assuming that "the portion of the wave function which gives rise to the ejection of electrons is that which falls within the boundary of the metal." Hence when a transition occurs, he regards the atomic electron as overlapping the metal, and when this electron is replaced by the metallic electron, it must therefore pass through the metal surface. Massey further states that the electron will be refracted similarly to a ray of light going from one medium to an optically denser one. There seems to be no basis for the assumption that the atomic electron must always be inside the metal for the transition to take place, as an inspection of Eq. (1) clearly shows. Again, we would expect that when the electron is refracted as it passes out through the metal surface, it is refracted away from the normal because its initial velocity parallel to the surface is unaltered after going through the surface but its normal velocity is diminished because of the work function. Hence if we were to include this effect in our theory, it would decrease the preference for electron emission perpendicular to the metal surface.

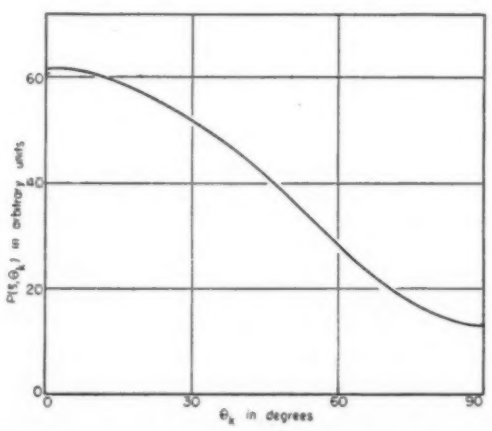

FIG. 5. Graph of $P(\delta, \theta_k)$ as a function of θ_k for 2^3S helium atoms of velocity 10^8 cm/sec.

[26] For this computation and for most of the other computations the WPA tables of exponential function and the WPA table of spherical Bessel functions were used.

III. HELIUM ION CASE

a. Energy Balance

The case of the helium ion colliding with a metal surface can be solved in a way analogous to the case of the helium metastable atom. Figure 6 shows the energy balance diagram for a Mo surface. This diagram shows that inside the metal there are electrons whose energy level is identical or very nearly identical to the 2^3S orbit. When the ion gets near the metal surface the potential field to which the metallic electrons are

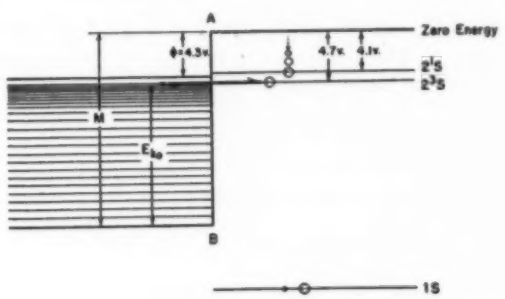

FIG. 6. Energy balance diagram for the extraction of electrons by helium ions from molybdenum. This diagram should be interpreted as explained under Fig. 1.

exposed is altered, and one of the above-mentioned electrons may pass through the metal surface and occupy the 2^3S orbit. In the case of Mo there are no electrons whose energy level is identical to the 2^1S or $1S$, and for this reason the only probable transition is the one to the 2^3S state. In the case of Pt, the work function is 5.01, 5.1, or 6.0 v[27] as obtained by different investigators, and our diagram would show that then the transition to the 2^3S would be impossible. This is not exactly correct because as the temperature of the surface increases, some of the higher electronic cells will be occupied. As shown by Sonkin[4] the behavior of a metallic surface is very easily affected by the conditions of the surface.

[27] *Handbuch der Physik*, Vol. 14, p. 69.

b. Matrix Element

In this case the matrix element is

$$H=\int\int\int[u^*_{2s}(r_1)u^*_{1s}(r_2)-u^*_{2s}(r_2)u^*_{1s}(r_1)]\times[-Ze^2/r_2+e^2/r_{12}]u_{1s}(r_1)\times[\exp i\mathbf{k}_0\cdot\mathbf{r}_2]/\sqrt{\Omega}d\tau_1 d\tau_2$$

where the variable r_2 must remain inside the metal. A good approximation for H can be obtained for large s by replacing r_{12} by r_2. If we make this assumption, H reduces to

$$H=\int\int(1-br_2)\exp(-br_2-cr_1)[1/r_2]\times\exp[-ar_1+ik_0(\cos\theta_{k_0}\cos\theta_2+\sin\theta_{k_0}\sin\theta_2\cos\phi_2)]d\tau_1 d\tau_2.$$

The integration over $d\tau_1$ can be done immediately. The integration over $d\tau_2$ can be done without much difficulty if we expand the Bessel function obtained from the integration over ϕ_2 and take only the first term of the expansion. The final result is

$$H=16\pi^2/(a+c)^3[\exp(ik_0\cos\theta_{k_0}s-bs)]/bs\times[(bs^2-s)/ik_0\cos\theta_{k_0}-b+(1-2bs)/(ik_0\cos\theta_{k_0}-b)^2+2b/(ik_0\cos\theta_{k_0}-b)^3].$$

The value of $|H|^2$ can be found for any large distance s and any direction of $\mathbf{k}_0$. For s of the order of $10a_0$ we found that the value when $\mathbf{k}_0$ was parallel to the metal surface was about four times the value when $\mathbf{k}_0$ was perpendicular to the metal surface. We took an average of these two values.

c. Decay Rate

The rate at which ions decay as a function of the distance from the metal is now given by $\lambda(s)=[mk_0\Omega/\pi\hbar^3]|H|^2$. This expression unlike the corresponding one for the case of the metastable atom does not have a factor $n\Omega$, the number of free electrons. This extra factor arose because in the averaging over k_0 all free metallic electrons were available. Any excess energy could be carried away as kinetic energy by the ejected L shell electron. In the case of the ion there is no final outgoing electron, so the energy of the metallic electron capable of performing the transition is uniquely defined by energy conservation within the limits of the uncertainty principle. When the numerical values of the constants are substituted,

$$\lambda(s)=2.390\times10^{49}\exp(-2.254\times10^8 s)\times[s/b+1/b^2+1/b^3s]^2.$$

Figure 2 shows a graph of $\log_{10}\lambda(s)$ as a function of s.

One can find $\bar{s}$ the average distance of transition from the integral

$$\bar{s}=\int_s^\infty sP(s)ds.$$

As previously shown, a good approximation is obtained by finding the s at which

$$\int_s^\infty\lambda(s)/v_0 ds=1.$$

For $v_0=10^5$ cm/sec., $\bar{s}=11.5a_0$ and, for $v_0=3\times10^7$ cm/sec., $\bar{s}=6.0a_0$.

Massey solved the case of a hydrogen ion which collides with a metal surface and performs the transition to the 2^3S state. He found that for $v_0=3\times10^7$ cm/sec. $\bar{s}_{H^+}$ is of the order of $1a_0$, and then assumed that $\bar{s}_{He^+}$ might be bigger by a factor of two or more. We calculated $\bar{s}_{H^+}$ for $v_0=3\times10^7$ cm/sec. and obtained an $\bar{s}$ of the order of $5a_0$. For the case of the hydrogen ion Massey used the correct matrix element but did not evaluate the integrals correctly.

IV. DISCUSSION

The extraction of electrons by He^+ colliding with a metal surface may be explained as the result of two separate processes. First the ion is neutralized, becoming a 2^3S metastable atom, and then if the metastable atom can get closer to the metal surface than $\bar{s}_{met}$, it will have a very high probability of assuming the ground state, the resulting energy being used in extracting an electron from the metal. Figure 7 shows that our values $\bar{s}_{He^+}$ and $\bar{s}_{met}$ for thermal velocities permit such a double process. For $v_0=3\times10^7$ cm/sec. $\bar{s}_{met}$ might seem too small to permit ions to be reflected as neutrals, but one must remember that

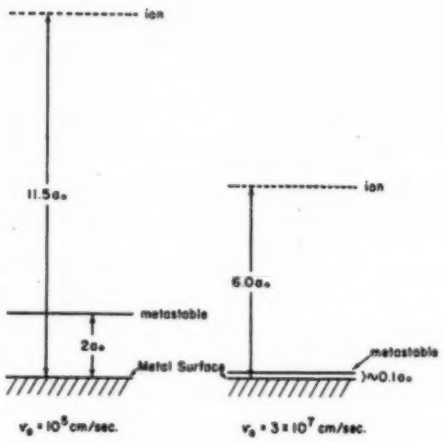

FIG. 7. δ for 2^3S helium atoms and for He^+ for two different velocities.

this is an average distance, which means that some ions after being changed into metastables will decay at a distance greater than $0.1a_0$. Besides, at these very small distances our theory can give only very approximate results.

Oliphant and Moon[21] in their discussion of the helium ion proposed the theory that the inverse transition metastable→ion was highly improbable because once the transition ion→metastable takes place the remaining metallic electrons would fill the cell previously occupied by the electron which is extracted from the metal. This would be true if the relaxation time were of the order of 10^{-15} sec. or less. A rigorous calculation of the relaxation time[28] is too involved, and we shall not attempt it. Nevertheless, our value of δ_{He^+} ($6.0a_0$ for $v_0 = 3 \times 10^7$ cm/sec.) indicates that a beam of He^+ ions colliding with a metal surface will be almost completely transformed into metastable and neutral atoms unless the metastable→ion transition is also highly probable. When Oliphant[12] produced a beam of metastable atoms by sending a beam of helium ions at a small angle with the metal surface, he also obtained many reflected ions which he removed from the beam by means of an electric field. This experimental evidence indicates that the relaxation time is too long to prevent the metastable →ion transition to take place.

We will therefore assume that the metallic electron will oscillate between the metal and the ion (Schüttelwirkung) once the ion gets closer to the metal surface than δ_{He^+}. Thus if a beam of ions is sent against a metal surface, once they are closer to the metal surface than the δ_{He^+}, they can no longer be identified as ions or metastable atoms.[29] The probability that an ion finally may achieve the ground state depends on how close the particle can get to the metal surface and on the number of ion⇄metastable jumps that can occur. These two factors depend on the energy of the ion, but the problem of finding this functional dependence is too involved.

ACKNOWLEDGMENT

One of the authors (A. C.) wishes to express his gratitude to the John Simon Guggenheim Memorial Foundation for the financial support given to this project in the form of a Latin American Fellowship. We are indebted to Dr. Joseph M. Keller for numerous stimulating discussions and suggestions.

[28] From dimensional considerations one may guess the following expression for τ.

$$\tau = A/[vn^{\frac{1}{3}}(e^2n^{\frac{1}{3}}/mv^2)^2],$$

where v is the velocity of the metallic electrons, n their density, m the electronic mass, and e the electronic charge. A is an undetermined constant. The numerical computation shows that $\tau \sim A10^{-14}$ sec.

[29] Most metals have a work function less than 5.0 volts and for this reason if 2^3S helium atoms are sent against these metals at absolute zero, all the electronic cells are filled up and the metastable atoms would remain as metastables until they perform the transition to the ground state and extract an electron.

New Absorption Band of Alkalis in the Presence of Foreign Gases*

CH'EN SHANG-YI
Physics Department, Yenching University in Chengtu, China
(Received April 6, 1944)

In the presence of foreign gases, a narrow and structureless absorption maximum was observed on the short wave-length side of certain members of the principal series of alkali metals. A résumé of the results obtained so far is given. It is suggested that the band is due to the increase in the energy of the optical electron through the process of collision with a foreign gas atom when the electron is at that energy level whose orbital radius is close to the distance of optical collision.

INTRODUCTION

THE influence of surrounding atoms on the frequency of the absorbing or emitting atoms as exhibited by broadening, asymmetry, and shift is well known and gives a new way to study the perturbations of energy levels; but during the study of the intensity distribution of the line due to pressure broadening, the narrow diffuse band[1,2] appearing very close to certain members of the principal series is very easily overlooked, yet it appears to be of considerable importance. Ny and the author first observed the band on the short wave-length side of the second member of the rubidium principal series in absorption.[1] Later on the corresponding band was also observed for caesium.[2] It was found that the width of the band and its position with respect to the corresponding series member depend on the nature of both the colliding and the absorbing atoms. The lighter the colliding or the absorbing atoms the greater the width and the separation between the series line and the band. In the investigation of the pressure effects of foreign gases on spectral lines the concentration of the foreign gas is always sufficiently high for the band to appear, even when the temperature of the absorption tube is rather low. The corresponding phenomenon was also studied for sodium.[3] It is very interesting to note that, for sodium, this sort of absorption band appears only in the neighborhood of the third member of the principal series. Very recently the phenomenon was also observed by the author and his collaborators for potassium. The narrow and structureless absorption maximum was observed on the short wave-length side of the second member of potassium principal series, and no bands of this kind were observed in the vicinity of the other members of the series. It is the purpose of this paper to present the results newly obtained for sodium and potassium and to give a résumé of the results obtained so far with a theory to account for the phenomenon.

EXPERIMENT

The experimental arrangement was essentially the same as that previously described.[4] Nitrogen and hydrogen were used as foreign gases in the presence of sodium and potassium. Pure nitrogen was prepared by decomposing ammonium nitrite. Hydrogen was prepared by the electrolysis of water whose contained air was first removed by repeated boiling and cooling in "vacuum." Several stages were also used to remove various kinds of possible impurities. Before the admission of hydrogen or nitrogen to the absorption tube, the gas was allowed to pass through a vapor trap of the same alkali as that whose absorption spectrum was to be studied, so that the residue of impurities (especially water vapor and oxygen) present in the gas were removed. A high intensity tungsten filament lamp and a hydrogen discharge tube were employed as light sources for the visible and the ultraviolet parts of the spectrum. A Hilger E-316 and a 10-foot grating spectrograph were used to register the entire absorption series of the alkali. The appearance of the band was studied by means of an automatic recording microphotometer.

Spectra were taken when the absorption tube

* In memory of the author's mother.

[1] Ny Tsi-Zé and Ch'en Shang-Yi, Nature **138**, 1055 (1936).

[2] Ny Tsi-Zé and Ch'en Shang-Yi, J. de phys. et rad. **9**, 169 (1938).

[3] Ke T'ing-Sui and Ch'en Shang-Yi, Chinese J. Phys. **5**, publication delayed by the war.

[4] Ny Tsi-Zé and Ch'en Shang-Yi, Phys. Rev. **51**, 567 (1937).

was heated to various temperatures. Great care was taken, so that the possibility that weak lines were overlooked owing merely to improper exposures is very small.

RESULTS AND DISCUSSION

Table I gives a résumé of the data obtained so far on the absorption bands of alkalis in the presence of foreign gases. It has been found that the pressure of the foreign gas does not appreciably affect the appearance of the band as long as the pressure is much higher than that of the alkali vapor. The pressure of the foreign gas is not so important and, therefore, is not listed in the table. In fact, for potassium the pressure in the absorption tube was 34 and 45.5 cm Hg for nitrogen and hydrogen, respectively. The corresponding values for sodium were 48 and 30 cm Hg, and for all the rest of the data the pressures were about one atmosphere.

TABLE I. New absorption bands of alkali metals in the presence of foreign gases.

Foreign gas	Alkali	Wavelength of band	Width of band	Separation between the band and the series member	Temperature of absorption tube
		A	A	A	°C
H_2	Na	2811.2	83	41.7 (3rd member)	544
	K	4007.2	42	38.5 (2nd member)	450
	Rb	4178.7	38	23.1 (2nd member)	300
	Cs	4541	30	14 (2nd member)	280
He	Rb	4182.5	35	19.3 (2nd member)	220
	Cs	4543	27	12 (2nd member)	200
N_2	Na	2818	70	34.8 (3rd member)	522
	K	4018.7	39	27.0 (2nd member)	484
	Rb	4183	24	18.8 (2nd member)	240
	Cs	4544	21	11 (2nd member)	210
Ne	Rb	4194.5	16	7.3 (2nd member)	220
	Cs	4549	12	6 (2nd member)	190
A	Rb	no band			
	Cs	no band			

The last column of Table I gives the most favorable temperatures of the absorption tube for observation of these bands. Certainly the lowest temperatures to render the band perceptible are much lower than those listed. For potassium, the lowest temperatures at which the band became visible were 410°C for hydrogen and 380°C for nitrogen. In all cases the temperatures were rather low, so that no molecular bands of alkalis or of alkali-foreign-gas compounds appeared.

The readings in the fifth column of Table I show in each case the distance between the maximum of the band and the $^2P_{3/2}$ component of the member of the series. The readings for the width (i.e., the half-width) of the band are only approximate.

Oldenberg, Kuhn, and others[5] have studied some bands which may conceivably be a similar phenomenon in emission spectra. They used various other metals and observed one or more bands appearing near all spectral lines. Obviously owing to the many complicating factors, such as the non-uniformity of the temperature of the discharge and of the vapor pressure of the metal, the pressure of ions, dipoles, etc., the condition for the production of these bands in emission is not so simple as that in absorption. The bands were interpreted by Oldenberg, Kuhn, and others as due to loosely bound molecules resulting from close collisions. According to their theory, bands of this type would occur with all metal lines, in agreement with their results.

Their theory is evidently not confirmed in the present work, in that this type of band appears only in the neighborhood of certain spectral lines. Nor is there any obvious rule for selecting these lines, as illustrated by the fact that in the series of sodium the absorption maximum appears by neither of the first and second members nor by its weaker members, except the third, $3^2S_{1/2}-5^2P_{3/2}$. Again for K, Rb, and Cs, the band appears only beside the second member of the principal series. Another fact also unexpected is that argon produces no band for Rb and Cs. Whether the bands observed by Oldenberg and Kuhn are of the same nature as those observed here is quite doubtful.

In the light of a systematic observation of this phenomenon as shown in Table I, it is easy to single out five points:

(1) The lighter the absorbing or perturbing atoms, the greater the separation between the band and the series line. Hence for a certain foreign gas the separation corresponding to Cs has the lowest value while that corresponding to Na possesses the highest value. For a certain absorbing alkali the separation corresponding to the lightest gas has the highest value and that corresponding to the heaviest gas has the lowest value. Consequently the separation correspond-

[5] Oldenberg, Zeits. f. Physik **47**, 184 (1928); **55**, 1 (1929). Kuhn and Oldenberg, Phys. Rev. **41**, 72 (1932). Krefft and Rompe, Zeits. f. Physik **73**, 681 (1932). Preston, Phys. Rev. **51**, 298 (1937).

ing to H_2-Na has the highest value of all and that corresponding to $Ne-Cs$ has the lowest value of all; as to the extreme case of argon and Rb or Cs, no band can be resolved.

(2) The lighter the absorbing or perturbing atoms, the greater the width of the band. Examples given in (1) can be similarly applied here.

(3) The wider the band, the higher the temperature of the absorption tube or the concentration of absorbing atoms that is needed to render the band perceptible.

(4) For heavier alkalis, *viz.*, K, Rb, and Cs, the band appears on the short wave-length side of the second member of the principal series, while for a lighter alkali, Na, the band appears on the short wave-length side of the third member of the series. It can be predicted without hesitation that the corresponding band for lithium will appear on the short wave-length side of the third or still higher member of the principal series.

(5) The band observed is narrow, structureless, and much fainter than the intensity of the series lines.

One more point should also be mentioned here.[6]

(6) When the pressure of the perturbing gas is very large in comparison with that of the absorbing vapor, the intensity of the band depends only upon the concentration of the absorbing vapor. If the pressure of the perturbing gas is reduced so that the concentration of the absorbing vapor becomes comparable with that of the perturbing gas, the intensity of the band will decrease with the decrease of concentration of either the absorbing or the perturbing atoms.

The production of the band may be suggested as due to the increase in the energy of the optical electron through the process of collision with the foreign gas atoms when the electron reaches that energy level whose orbital radius is close to the distance of optical collision. Foreign gas atoms can be regarded as evenly distributed in the surroundings of the absorbing atom. It is the effect, say the polarization effect, of the introduction of the foreign atoms within the space of the possible orbits of the optical electron of the alkali that contributes certain features of the well-known "pressure effects." As the spacing between foreign atoms is quite large, and the foreign atoms are moving with an enormous speed, the chance of collision between the excited electron and the foreign gas atom is rather small. But the chance of collision becomes considerable when the foreign gas atom reaches the location where collision between the foreign gas atom and the absorbing atom takes place because the colliding atom will spend the major part of its time around the district of closest collision. If that distance of closest collision happens to be near a certain energy level of the alkali atom, only the electron at that state will have appreciable chance to change energy. With this picture in mind the above six points can be accounted for without difficulty.

The magnitude of the separation between the band and the series line is a measure of the energy change of the optical electron at the instant of collision with the foreign gas atom. The lighter the colliding particle, the higher the relative speed of collision; consequently more energy will be given to the electron when it is excited to the energy level whose orbital radius is close to the distance of collision. For heavier alkalis, Rb and Cs, and a heavier gas, say argon, the separation might be so small that no band is perceptible. This is illustrated in point (1). The distribution of velocities has a wider range for lighter absorbing or perturbing particles, so the structureless band is wider for lighter atoms. This explains point (2). Point (3) is simply a matter of photometry because the amount of absorption depends only upon the concentration of the absorbing atom. For a broader band the energy is distributed over a wider range, thus a higher concentration of the alkali vapor is required to obtain the perceptible intensity.

Point (4) tells the approximate distance of optical collision. By applying the quantum mechanics expression for the average value of the electron nuclear distances at various energy levels, it is possible to tell the approximate value of the distance of collision between the nuclear and the colliding atom. The value for the third member of Na principal series, $3s-5p$, is 19A. For the second members of $K(4s-5p)$, $Rb(5s-6p)$, and $Cs(6s-7p)$ series the values are 19A, 28A, and 38A, respectively. Points (5) and (6) are simply a reflection of the probability of this kind of transition.

[6] Cf. references 1 and 2.

Cosmic-Ray Meson Spectra

D. M. Bose, Bibha Choudhuri, and M. Sinha*
Bose Institute, Calcutta, India
(Received April 22, 1944)

In a recent paper[1] (denoted hereafter as I), Hamilton, Heitler, and Peng have proposed a comprehensive theory of the origin of cosmic-ray mesons, which appears to provide at least a qualitative interpretation of a large number of observations on cosmic-ray penetrating particles. These authors aim at giving a connected account of cosmic-ray and nuclear phenomena, and have selected that form of the meson theory which gives the best account of nuclear forces, *viz.*, that proposed by Møller and Rosenfeld.[2] According to Heitler *et al.*,[3] the meson field of a fast proton of energy $E \gg \mu c^2$ when scattered in the field of a stationary nucleon, radiates an amount of meson energy $\epsilon \lesssim E$. We take the meson mass energy μc^2 to be 10^8 ev. The released energy ϵ may (1) result in a single meson of energy ϵ which in the process of being scattered in the field of the stationary nucleon gives rise to a single or a multiple of n mesons. The cross section γ_n for each multiplicity n has a maximum at some energy ϵ_n which increases with n. After the maximum, γ_n decreases rapidly, and the asymptotic expressions are

$$\gamma_1 \sim \epsilon^{-2}; \quad \gamma_n \sim \epsilon^{-2n-4} \quad \text{for} \quad n \neq 1. \qquad (1)$$

Alternately (2) it may also happen that only a part ϵ' of the radiated energy is used up in meson production, and the balance is taken up by the recoiling nucleon; the latter can then produce fresh mesons by nuclear collisions. This process is analogous to cascade production of electrons.

On the assumption of a suitable primary proton energy spectrum incident on the top of the atmosphere, an expression is deduced for the energy distribution in the single-meson spectra $f(\epsilon, x)$, where x is the depth from the top of the atmosphere. It is shown that the function $f(\epsilon, x)$ for a given value of x has a maximum value for $\epsilon \sim 3\mu c^2$ below which it falls rapidly to zero. These critical values of $\epsilon \sim 1/f$ where $f = f' \sim \frac{1}{3}$ are the coupling constants between a nucleon and the vector and pseudoscalar components of its meson field. The decay constants of the corresponding mesons are taken to be 10^{-8} and 10^{-6} sec., respectively.

Given below are some of the results we obtained which are in agreement with the predictions of the theory.

MESON SPECTRA

Several investigators have used Wilson chamber photographs of penetrating particles in magnetic fields to measure the meson energy spectra. The most reliable measurements for the low energy spectra appear to be those of D. J. Hughes.[4] His energy distribution curve shows a maximum near $\epsilon \sim 8 \times 10^8$ ev, and the number of penetrating particles of lower energy diminish rapidly. This is not in agreement with the distribution $f(\epsilon, x)$ in which the maximum occurs for $\epsilon \sim 3 \times 10^8$ ev.

Photographic plates exposed to cosmic rays at high altitudes are found to contain single and multiple star-like tracks. A detailed account of the results will be published by one of us (B.C.) elsewhere. In Table I are given our findings on the total frequency of multiple track distribution observed in photographic plates, kept at altitudes varying from 7000 ft. to 14,500 ft., under (1) air, (2) absorbers like water, paraffin, and wood, and (3) under lead. In every case the frequency distribution has a principal maximum at $n=1$, a second maximum at $n=3$; and in no plate was any multiple track with $n>7$ observed. The first

Table I. Frequency of multiple tracks.

Absorber	Frequency of tracks						
$n=$	1	2	3	4	5	6	7
Air	192	30	87	63	38	5	3
Hydrogeneous substances	86	14	22	20	20	0	0
Lead 0.5 cm to 5 cm	69	19.6	42.3	34.2	12.9	2.2	0

* At present at the Indian Institute of Science, Bangalore, India.
[1] Hamilton, Heitler, and Peng, Phys. Rev. **64**, 78 (1943).
[2] Møller and Rosenfeld, Kgl. Danske Vid. Sels. Math.-Fys. Medd. **17** (1940).
[3] Heitler and Peng, Proc. Camb. Phil. Soc. **38**, 296 (1942).
[4] D. J. Hughes, Phys. Rev. **57**, 592 (1940).

maximum is not significant, as it contains mainly tracks of ionizing particles originating outside the photographic emulsion. In a paper[5] on meson spectra, reasons were given for the conclusions that (1) the star-like tracks on photographic plates are mainly due to multiple meson production, the energy associated with each multiple n is $\epsilon_n = n \cdot \mu c^2 + k$, where $k \sim 10^7$ ev represents the kinetic energy of the particles; (2) protons (neutrons) are primarily responsible for such multiple production, (3) a transition effect is observed in lead, with a maximum under 1.5 cm Pb; in this case photons directly or indirectly are responsible for the additional multiples produced. The occurrence of a maximum at $n=3$ was noticed, but no satisfactory explanation for it could be suggested.

According to I, the frequency distribution curve for the occurrence of multiples of n mesons is approximately given by

$$f(\epsilon, x) \cdot (\gamma_n/\gamma_1). \qquad (2)$$

The asymptotic expression for γ_n/γ_1 is ϵ^{-2n-2}, which shows that within the energy interval for which the values of γ have been calculated, the ratio diminishes exponentially, i.e., the expectation of occurrence of high multiplicity becomes vanishingly small with increasing n. According to our findings (2) has a maximum for $n=3$ corresponding to $\epsilon \sim 3\mu c^2$, and this may be taken as a qualitative verification of the occurrence of the maximum predicted according to I. Further it appears to us to be more than a mere coincidence that the region of maximum occurrence of single mesons, $\epsilon \sim 8 \times 10^8$ ev, should also coincide with the region where the production of multiple mesons cease (i.e., $> 7\mu c^2$).

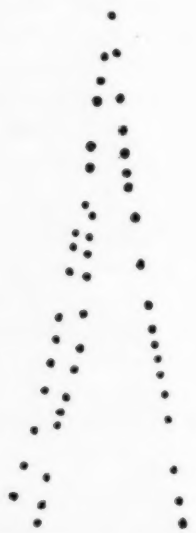

FIG. 1. Track in photographic emulsion traced by use of a camera lucida. Magnification ×760.

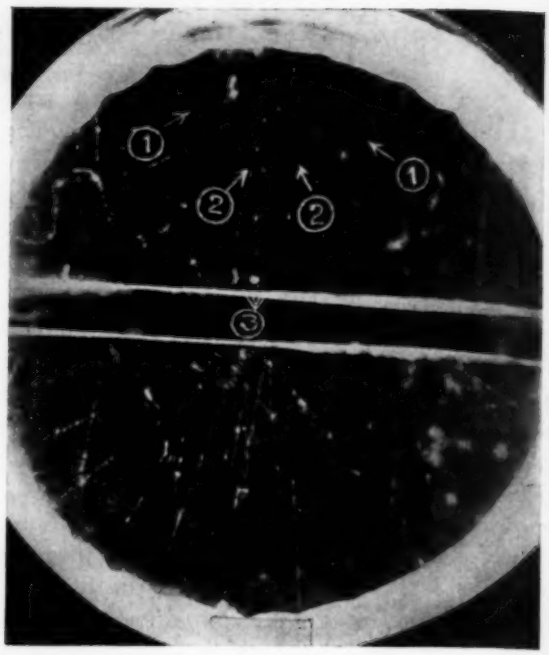

FIG. 2. Wilson cloud-chamber photograph showing production of mesons by a cascade process.

CASCADE PRODUCTION OF MESONS

According to I a cascade production of mesons can also be expected. Hazen[6] finds no evidence of their occurrence in his high altitude Wilson chamber photographs. On the photographic plates referred to in the previous paragraph, records of at least six such events have been found. A camera lucida tracing of one of them is given in Fig. 1. Since photographic plates are exposed to cosmic rays for at least six months, it is difficult to adduce conclusive evidence that all the tracks on a plate which are considered to be due to cascade meson production have been traversed by the mesons at the same instant of time. A Wilson chamber photograph obtained by one of us (M.S.) is given in Fig. 2. It shows the

[5] D. M. Bose, Trans. Bose Research Inst. **15**, 55 (1942).

[6] W. E. Hazen, Phys. Rev. **64**, 257 (1943).

production of mesons by a cascade process. All the tracks appear to be of the same age. The tracks in Group 1 have originated outside the chamber; the other two groups have originated within the chamber. The left-hand track of group 2 is absorbed in the lead plate (2.2 cm), and its energy is $<4\times10^7$ ev. The four tracks in group 3 appear to start as a pair which is doubled again. These tracks are not appreciably scattered during their traversal through the lead plate, but they have produced knock-on electrons.

BURST PRODUCTION

One of us (M.S.)[7] has recently published a photograph of a burst originating in the gaseous volume of a Wilson chamber. It appears to start as a number of ionization strands, diverging from a small region, which subsequently broaden and merge into a dense volume of ionization. A possible interpretation of the burst according to I is as follows: A high energy proton has by a process of nuclear collision given rise to a cascade production of fast vector mesons. The latter have within a short length disintegrated into high energy electrons, from which several cascade showers have started.

The above theory enables us to correlate and interpret many findings on penetrating particles obtained from Wilson chamber photographs and from tracks on photographic plates. A detailed comparison between the predictions of the theory and our findings will be given elsewhere.

[7] M. Sinha, Phys. Rev. **64**, 248 (1943).

PHYSICAL REVIEW VOLUME 65, NUMBERS 11 AND 12 JUNE 1 AND 15, 1944

Letter to the Editor

PROMPT publication of brief reports of important discoveries in physics may be secured by addressing them to this department. The closing date for this department is the third of the month. Because of the late closing date for the section no proof can be shown to authors. The Board of Editors does not hold itself responsible for the opinions expressed by the correspondents. Communications should not in general exceed 600 words in length.

On the Maximal Energy Attainable in a Betatron

D. IWANENKO AND I. POMERANCHUK
Physical Institute of the Moscow State University, Moscow, and Physico-Technical Institute of the Academy of Sciences of the U. S. S. R., Leningrad, U. S. S. R.

May 18, 1944

BY means of a recently constructed induction accelerator-betatron, Kerst succeeded in obtaining electrons up to 20 Mev.[1] The principle of operation of the betatron is the acceleration of electrons by a tangential electric field produced by a changing magnetic flux, which is connected with the magnetic field keeping electrons on the orbit by a simple relation. In contrast to a cyclotron, whose applicability is essentially limited to the non-relativistic region on the ground of defocusing of orbits due to the change of mass at high energies, there is no such limitation for the betatron.

We may point out, however, that quite another circumstance would lead as well to the existence of a limitation for maximal energy attainable in a betatron. This is the radiation of electrons in the magnetic field. Indeed, electrons moving in a magnetic field will be accelerated and must radiate in accordance with the classical electrodynamics. One can easily see that quantum effects do not play here any important role as the dimension of the orbit is very great. As was shown by one of us[2] an electron moving in a magnetic field $\mathbf{H}$ radiates per unit of path the energy

$$-(dE/dX)=2/3(e^2/mc^2)^2(E/mc^2)^2[(\mathbf{V}/c)\mathbf{H}]^2 \qquad (1)$$

where e is the charge, m the mass, $\mathbf{V}$ the velocity, and E the energy of the electron; E is assumed much greater than mc^2.

In the betatron $\mathbf{V}$ is normal to H and practically for the whole path equal to c. Then we have

$$-(dE/dX)=2/3(e^2/mc^2)^2(EH/mc^2)^2. \qquad (2)$$

The limiting value of energy E_0 is to be determined from the condition that the radiated energy (2) will be equal to energy gained by the electron in the electric field produced by magnetic flux per unit of path:[3]

$$\frac{2}{3}r_0^2\left(\frac{E_0H}{mc^2}\right)^2=\frac{e|d\phi/dt|}{2\pi R_0c}=\frac{e}{c}R_0|\dot{H}| \qquad (3)$$

$$\dot{H}=dH/dt \qquad r_0=e^2/mc^2.$$

Here R_0 is the radius of the orbit, ϕ is the induction flux.[1]

Hence:

$$\frac{E_0}{mc^2}=\left(\frac{3eR_0}{2r_0^2c}\frac{\dot{H}}{H^2}\right)^{\frac{1}{2}}. \qquad (4)$$

Taking for H and E the values now being in use we get $E_0\approx5\times10^8$ ev, which is only five times as great as the energy which one expects to obtain in the betatron now under construction. From (4) one sees that E_0 is inversely proportional to the magnetic field applied and proportional to the square root of energy gained in the rotation electric field per unit of path. All this requires the using of smaller H or of higher frequencies with the purpose of getting higher limiting values of E_0.

The radiative dissipation of energy of electrons moving in a magnetic field must be also of importance for the discussion of the focusing of the electronic beam, as the energy of particles being accelerated will grow more slowly with the growth of H if the radiation is taken into account. This latter question may deserve a separate discussion.

[1] D. W. Kerst, Phys. Rev. **61**, 93 (1942).
[2] I. Pomeranchuk, J. Phys. **2**, 65 (1940).
[3] D. W. Kerst and R. Serber, Phys. Rev. **60**, 53 (1941).

Proceedings of the American Physical Society

MEETING AT PITTSBURGH, PENNSYLVANIA, APRIL 28 AND 29, 1944

THE 260th meeting of the American Physical Society was held in the building of the Mellon Institute at Pittsburgh, Pennsylvania, on Friday and Saturday, the 28th and 29th of April, 1944. This proved to be one of our strongest meetings since Pearl Harbor; for instance, there were forty-four contributed papers, though the authors of some of these were not able to be present. A good share of the credit belongs to the officers of our new Division of Electron and Ion Optics, who assembled a programme of seven invited papers and induced the presentation of several of the contributed papers. This was the debut of the Division, and augurs well for the prosperity of its future. The titles of the invited papers are as follows.

Address of Welcome by the Chairman or the Vice Chairman of the Division.

Historical Background of Electron Optics. C. J. CALBICK, *Bell Telephone Laboratories.*

The Electron Microscope in Metallurgical Research. C. S. BARRETT, *Carnegie Institute of Technology.*

Extending Microscopic Examination of Metals. F. KELLER AND A. H. GEISLER, *Aluminum Company of America.*

The Magnetically Focused Radial Beam Vacuum Tube. A. M. SKELLETT, *Bell Telephone Laboratories.*

Kinematics of Reflection Oscillators. A. E. HARRISON, *Sperry Gyroscope Company.*

The Thickness of Electron Microscopic Objects. ROBLEY C. WILLIAMS AND RALPH W. G. WYCKOFF, *University of Michigan.*

Another good share of the credit belongs to the Physical Society of Pittsburgh, whose officers arranged for four invited addresses as follows.

Address of Welcome. SIGMUND HAMMER, *Gulf Research and Development Company.*

The Mechanism of Crystal Growth and Its Consequences. WHEELER P. DAVEY, *The Pennsylvania State College.*

Modern Theories of Plasticity in Solids. FREDERICK SEITZ, *Carnegie Institute of Technology.*

Hipersil, the New Transformer Iron. T. D. YENSEN, *Westinghouse Research Laboratories.*

Another feature of the meeting was a symposium on cosmic rays with five participants as follows.

The Nature of Cosmic-Ray Phenomena. MARCEL SCHEIN, *University of Chicago.*

The Role of the Primary Cosmic Radiation. W. F. G. SWANN, *Bartol Research Foundation.*

On the Lateral Spread of Cosmic-Ray Showers. L. W. NORDHEIM, *Duke University.*

Nuclear Disintegrations Produced by Cosmic Radiation. M. GOLDHABER, *University of Illinois.*

Production of Neutrons by Cosmic Radiation. S. A. KORFF, *New York University.*

Five additional papers on a diversity of subjects, listed below, were also presented.

Potential Barriers to Internal Rotation in Organic Compounds. J. G. ASTON, *The Pennsylvania State College.*

Photoelectric Measurement of Weak Emission Spectra. D. H. RANK, *The Pennsylvania State College.*

The Philosophical Foundations of Quantum Mechanics. HANS REICHENBACH, *University of California.*

Physics and Phenomenology. HENRY MARGENAU, *Yale University.*

Physics Bulletins for High School Bulletin Boards (The Pennsylvania Conference of College Physics Teachers).

No local committee has ever handled one of our meetings better than the one headed by Mr. A. G. Worthing and comprising several others of the physicists of Pittsburgh. About four hundred people registered for the meetings, and over two hundred were present at the dinner, which was held at the Hotel Schenley on Friday evening with President A. J. Dempster presiding over the after-dinner programme.

At the meetings of the Council, one hundred and twenty-six candidates were elected to membership and four Members were advanced to Fellowship; the list is appended.

The Council approved a text of by-laws for the Division of Electron and Ion Optics, excerpts from which are being distributed to the members of the Division. The Council also approved a text of by-laws for the Division of High Polymer Physics, contingent on certain modifications

which are now being made and are being submitted to the Organizing Committee for this Division. A petition for a Division of Applied Spectroscopy having been received, the Council acted upon it by passing a motion of which a part is here quoted: "The Council approves in principal the formation of a Division of Spectroscopy: it authorizes the President and Secretary to confer and correspond with signers of the petition of Applied Spectroscopy concerning the scope and name of the proposed division."

The Society has lost through death the following Members and Fellow: F. L. Cooper (Yale University), W. S. Day (formerly of Columbia University), and John L. Rose (F., New York University).

Elected to Fellowship: Allen, J. S.; Burt, R. C.; Salisbury, W. W.; Staub, Hans.

Elected to Membership: Alzofon, Frederick E.; Anway, H. Wilbur; Bader, Frank; Beer, Albert Carl; Berenda, Carlton W.; Berry, Chester Ridlon; Beth, Erich W.; Birzis, Lucy; Blum, Victor J., S.J.; Bobrowsky, Alfred R.; Boor, Ladislav; Bowman, John Charles; Braendle, H. A.; Byerly, Paul R., Jr.; Burbank, Burr G.; Carlson, F. D.; Cocke, Albert Kirven; Cohen, Robert Sonne; Conner, Willard P., Jr.; Cooper, Marcella; Cosler, Arthur Stackdale, Jr.; Cox, David C.; Davis, Francis J.; Deutsch, Robert A.; Dietz, Frank Tobias; Di Toro, Michael J.; Dwight, Barbara; Eastmond, E. John; Eggen, Donald T.; Eisner, Elmer; Elder, Fred Kingsley, Jr.; Feitelberg, Sergei; Ferrell, O. Perry; Frazier, Thomas Vernon; Gans, David M.; Gettner, Mark Earl; Gibson, Robert John, Jr.; Gross, Milton H.; Hall, James W.; Halpern, Isaac; Hart, Stephen D.; Havas, Peter; Hemenway, Curtis L.; Hickman, R. E.; Holton, Gerald James; Jeffries, Jasper Brown; Jones, V. L.; Jordan; A. Raymond; Ke, T'ing-sui; Kleckner, U. Frederick, Knight, Walter David, Jr.; Kuhlthau, Alden Robert; Laing, Kenneth M.; Landers, Harry M., Jr.; Lapsley, Alwyn C.; Lee, Donald E.; Lefler, Ralph W.; Lepore, Joseph V.; Lock, Charles; Loeb, Arthur L.; Lofgren E. J.; Lovins Gerald H.; Loughman, James C.; MacLean, William R.; MacRae, Duncan, Jr.; Mann, Alfred K.; Marcus, Jules Alexander; McDonald, Robert S.; Merritt, Thomas P.; Mills, Peter J.; Moeckel, Wolfgang E.; Moore, Donald Clark; Moore, John Wilson; Needels, Theodore S.; Nicoll, Frederick H.; Oetjen, Robert A.; Ohlheiser, Carlton E.; Osborne, M. F. M.; Owens, Ralph G.; Peacock, Wendell; Pederzani, Gregory; Peterson, Rolf E.; Pomerantz, Jacob; Pratt, Orison S.; Proskauer, Richard; Ream, Donald F.; Reichenbach, Hans; Richards, Albert Gustav; Rose, Albert; Rossi, Harold H.; Roth, Raymond E.; Rothstein, Jerome; Rovner, Leopold; Sable, Morris; Sachs, Donald Charles; Saunders, Bernard G.; Schuman, Robert Paul; Sedwitz, Ira M.; Smith, Paul Kenneth; Sondheimer, Ernst Helmut; Stafford, Jerome W.; Stanton, Henry E.; Stock, Charles R.; Stowens, Bernard H.; Sutro, Peter John; Swearingen, Thomas; Taxwood, Vincent C.; Taylor, James E.; Taylor, William J.; Tuerck, William, Jr.; Turkevich, John; Vargus, Joseph Anthony, Jr.; Vine, Benjamin H.; Wack, Paul E.; White, A. H.; Whitehead, Walter Dexter; Wightman, Arthur Strong; Wikstrand, Wm. Carl; Williams, Neal T.; Williams, S. E.; Wilson, William Solomon; Withrow, Robert B.; Witte, Robert S.; Wolfe, Ralph A.; Wylde, Ronald James; Zihlman, Charlotte.

KARL K. DARROW
Secretary

Contributed Papers

A1. The Small Gulf Gravimeter. ANTHONY CARNVALE, *Gulf Research & Development Company.*—For greater portability under difficult field conditions, a small and light modification of the Gulf Torsion Spring Gravimeter[1] has been constructed. The instrument consists essentially of a helical ribbon with a mass hanging freely at the lower end. Around the moving system are built the elaborate details needed to insure the necessary precision. These include the proper choice of spring material, temperature control, optical system, damping, magnetic shielding, and the elimination of air buoyancy errors. The salient features of the instrument and the extreme stability requirements of the moving system are discussed. In geophysical prospecting with a gravimeter, it is desirable to measure gravity differences from point to point to a precision of 10^{-7} g. The probable error of a single observation with the Gulf Gravimeter in routine field use is about 4×10^{-8} g. For stationary set-up (e.g., for measuring variations in tidal forces) the probable error is 1×10^{-8} g or better.

[1] R. D. Wyckoff, Geophys. 6, 13–33 (1941).

A2. A Thermopile for Micro-Calorimetry. L. S. MASON, *University of Pittsburgh.* (Introduced by A. G. Worthing.)—In the study of the thermodynamics of solutions it is desirable to measure heat effects (of the order of 0.001 cal.) which occur during the dilution of dilute solutions. In the Lange-type calorimeter[1] a thermopile of approximately 1000 junctions is used differentially. For this purpose a thermopile has been constructed using constantan-chromel-P couples[2] mounted in a sheet of Micarta, $5''\times10''\times\frac{5}{16}''$, and electrically insulated with a Vinylite resin which has an insulation resistance greater than 25 megohms. This instrument appears to offer somewhat better behavior than previously used units with respect to stability, sensitivity, and rapidity of response to temperature changes. The thermopile consists of two sections of equal numbers of junctions which are connected in parallel to a Leeds and Northrup HS galvanometer in series. At a scale distance of nine meters the sensitivity of the system is 0.25 microdegree per mm. Since one liter of diluent (water of dilute solution) is contained in each half of the

calorimeter, this corresponds to a mean sensitivity of 2.5×10^{-4} cal./mm, with a probable error of the mean of ±0.03. The heat conductivity constant of the calorimeter is 0.004 min.$^{-1}$ and that of the thermopile is 0.03 min.$^{-1}$ Measurements with the present thermopile of the heats of dilution of sodium chloride solutions agree satisfactorily with well-established values.

[1] E. Lange and A. L. Robinson, Chem. Rev. **9**, 89 (1931).
[2] H. F. Launer, Rev. Sci. Inst. **11**, 98 (1940).

A3. Amplifier with Logarithmic Response. J. A. HIPPLE AND D. J. GROVE, *Westinghouse Research Laboratories.*—An amplifier with d.c. output voltage logarithmically proportional to the input signal over a range of three decades has been developed. This response characteristic is based on the charging and discharging of a condenser through a resistance and is thus independent of the characteristics of the individual tubes in the circuit. At any fixed setting the d.c. output is constant to better than 0.2 percent. The condenser discharge is initiated periodically by means of a trigger circuit which also synchronizes a saw-tooth oscillator with the exponential circuit. The d.c. level of this saw-tooth is varied by means of the input signal so that a thyratron can be made to fire at any time from the beginning to the end of the interval. The impulse developed by the firing thyratron drives the grid of a hard vacuum tube from very negative to positive for an instant. The plate supply for this tube is the exponential voltage from the condenser-charging series resistance so that for the instant the grid is driven positive a signal appears across the load resistance equal to the voltage of the exponential at that instant. The output thus consists of a series of pulses of magnitude logarithmically proportional to the input voltage. These pulses are then averaged and filtered to d.c.

A4. Deflection of a Beam of Cesium Atoms by Gravity. I. ESTERMANN, O. C. SIMPSON, AND O. STERN, *Carnegie Institute of Technology.*—In the course of experiments for the exact measurement of the Bohr magneton[1] it was found necessary to determine the actual velocity distribution in a beam of cesium atoms 2 meters long with a cross section of 2 mm by 0.02 mm. In the apparatus used, this velocity distribution was measured by gravity deflection. The results showed that deviations from the Maxwell distribution in the range of low velocities occur at much lower oven pressures than expected.[2] The slow atoms remain longer in the neighborhood of the oven slit and have therefore a higher probability to be deflected from the beam by collisions. The results agree with an approximate calculation of this effect.

[1] O. Stern, Phys. Rev. **51**, 852 (1937).
[2] Compare V. W. Cohen and A. Ellett, Phys. Rev. **52**, 502 (1937).

A5. Performance Tests on the Penn State Type of G-M Circuits. HAROLD E. WALCHLI, *The Pennsylvania State College.*—Descriptions of the Penn State type of Geiger-Mueller circuits for the measurements of x-ray intensities were published in February, 1944 in *The Review of Scientific Instruments.* It is the purpose of the present paper to give the results of performance tests on such circuits. These tests are: 1. G-M high voltage supply, temperature effects, effects of changes in input voltage, effects of rheostat settings, improvements in circuits resulting from above tests. 2. Power and stabilized-bias supply, temperature effects, effect of load, voltage regulation, time constants. 3. Main amplifier, changes from original circuit, temperature effect, time constants. 4. Preamplifier, time constant, impedance, change in fixed bias *vs.* plate current. 5. Auxilliary amplifier, temperature effects and improvements in the circuit intended to reduce heating effects. 6. Complete circuit, voltage recovery of G-M supply, oscillograph records of pulses through G-M counter.

A6. The Influence of Statistical Fluctuations on the Observed Size-Frequency Distribution of Bursts in a Single Ionization Chamber. L. G. LEWIS AND R. HAYDEN, *The University of Chicago.*—A particular burst of ionization occurring in an ionization chamber will be recorded as a burst larger or smaller than its true size by an amount equal to the statistical fluctuation in the non-burst particles occurring within the collecting time of the ions generated by that burst. This phenomenon causes the shape and absolute values of the observed size-frequency distribution curve to differ from the true curve by an amount given by:

$$f(a)=\int_0^\infty F(x)\exp\left[-b(x-a)^2\right]dx.$$

$f(a)$ is the observed differential size-frequency distribution function and $F(x)$ is the true function. The constant b is obtained from the conditions of observation in the ionization chamber. The true distribution $F(x)$ corresponding to the observed size-frequency distribution curve for a single chamber given by Lewis and Lewis[1] has been determined.

[1] L. G. Lewis and E. W. Lewis, Phys. Rev. **65**, 63A (1944).

A7. The Ratio of the Average Current Generated by Cosmic-Ray Air Showers to the Total Current Observed in the Ionization Chamber. E. W. LEWIS AND L. G. LEWIS, *The University of Chicago.*—The average ionization current generated in a single unshielded ionization chamber by air showers producing bursts of more than 50 particles has been computed from the size-frequency distribution curve given by Lewis and Lewis[1] for an elevation of 10,650 ft. The average shower current was found to be 1.8×10^{-15} ampere. The current produced by all ionizing radiation in the chamber was 2×10^{-13} ampere. This value was obtained by measuring the voltage drop produced by the ionization current flowing through a 10^{12}-ohm resistor. The ratio of these currents is then 0.9 percent.

[1] L. G. Lewis and E. W. Lewis, Phys. Rev. **65**, 63A (1944).

A8. Calculations on Extensive Cosmic-Ray Showers in Air. LINCOLN WOLFENSTEIN, *University of Chicago.* (Introduced by M. Schein.)—Large cosmic-ray showers in air, investigated with ionization chambers and coincidence counters, have been explained hitherto as originating from primary electrons of very high energy. The recent measurements by Lewis[1] of the frequency of coincident bursts in

two unshielded ionization chambers provide a more complete picture of these showers. The theoretical coincidence frequency as a function of the particle density and the separation of the chambers has been calculated using the cascade theory of showers and the theory of the lateral spread of showers.[2] The calculations give much smaller values than the experiments for (1) the absolute value of all the frequencies observed, (2) the drop in frequency as the chambers are separated, and (3) the increase in frequency with elevation of bursts in a single chamber. These discrepancies strongly indicate that the bursts observed in the experiments are not due to showers from primary electrons. It is considered possible that the bursts may be explained by showers originating not at the top of the atmosphere, but relatively close to the chamber.

[1] L. Lewis, Phys. Rev. 65, 63A (1944).
[2] J. Roberg, Phys. Rev. 61, 735A (1942); 62, 304A (1942).

A9. Theory of Counter Experiments on Collision Electrons Ejected in Air by Mesotrons. ANATOLE ROGOZINSKI, *University of Chicago.*—It was found in recent counter-tube experiments[1] that mesotrons are associated with particles present at several meters distance from the mesotron trajectories. These particles together with the mesotron possibly belong to an Auger-shower, but at least part of them are collision electrons (CE) ejected by the mesotron along its path in the air. The results of a theoretical calculation show that: (a) Only mesotrons of momenta $p > p_0 \sim 5\times10^8$ ev/c can eject in air CE sufficiently energetic to reach and to traverse a counter (C) placed at a distance D (a few meters) from the mesotron trajectory. (b) The number ν of CE, which arise from a single mesotron and which are able to discharge (C), is practically independent of the mesotron momentum p, if the spin dependent term is neglected, and is given, in first approximation, by $\nu_0 = (BS/\pi D)\times\Theta_{max}(D, E_1)$, where: $B = 10^{-2}$ for standard air, S = effective area of (C) in m², D is expressed in meters, and E_1 = minimum energy necessary for an electron to traverse the counter wall; for $E_1 = 2$ Mev, e.g., the function Θ_{max} decreases from 0.50 for $D = 2$ m, to 0.30 for $D = 10$ m. (c) When the mesotron spin (0 or ½) is taken into account, $\nu \leq \frac{1}{2}\nu_0$ for the lowest mesotron momenta, but approaches asymptotically ν_0 as p increases. (d) Shower production in air of the CE adds a very small contribution to the counting rate in (C).

[1] P. Auger and An. Rogozinski, Phys. Rev. 65, 64 (1944); An. Rogozinski, Phys. Rev., in print.

A10. Measurement of High Energy Electrons in *A* Showers. R. E. LAPP, *Ryerson Physical Laboratory, University of Chicago.*—A discussion is given of the energies associated with high energy particles (electrons and photons) present in the cores of A showers at sea level. The approximate values of these energie are obtained from an analysis of the number of cosmic-ray bursts found to be coincident with A showers as a function of the iron shielding the ionization chamber in which the bursts occur. The A showers are detected by lateral arrangements of G-M counter coincidence sets.

B1. The Mechanics of the Metal Cutting Process. I. Simple Straight-Edged Tool and Continuous Chip. M. EUGENE MERCHANT, *Cincinnati Milling Machine Company.*—The analysis of the mechanics of a simple straight-edged cutting tool removing a continuous chip in the absence of a built-up edge, and traveling in a direction perpendicular to the cutting edge, as introduced by Ernst and Merchant,[1] has been expanded and correlated with experiment. In this special case, the chip is formed by a process of shear in a direction perpendicular to the cutting edge, in a plane extending from the cutting edge to the work surface, and the resultant force on the tool or on the work is coplanar with all its significant components and with the direction of relative motion of tool and work. Relationships pertinent to the geometry of chip formation are derived. Significant relationships are derived between the various force components and such quantities as the shear strength of the metal, the coefficient of friction between chip and cutting tool, and the work done in shearing the metal and in overcoming friction on the tool face. Relationships are presented showing how the direction of shear of the metal ahead of the cutting edge is determined by the geometry of the force system, for certain special cases.

[1] H. Ernst and M. E. Merchant, *Surface Treatment of Metals* (American Society for Metals, 1941), pp. 299–378.

B2. Anomalous Behavior of the Electrical Resistivity of Some Iron-Cobalt Alloys. SIDNEY SIEGEL AND ROBERT MCGREARY, *Westinghouse Research Laboratories.*—In the course of the development of iron-cobalt alloys for magnetic purposes, erratic variations in the resistivity of alloys of presumably similar composition and thermal history had been observed. Systematic attempts to determine the cause of these variations were made. The possibility of these being due to an order-disorder transition was investigated. The equilibrium electrical resistivity of alloys containing 42 percent Co, and 30 or 42 percent Co plus 2 percent V, was measured over the range 20°C to 1100°C. The resistance rises monotonically up to about 950°C, the phase change temperature, where a discontinuous increase occurs. Above this temperature, the resistivity again increases, with a smaller constant, temperature coefficient. No evidence for an ordered structure was found from these measurements. A series of experiments attempting to relate the room temperature resistivity of these alloys to thermal history showed that the cold-rolled alloy has a lower resistivity than the presumably equilibrium value of the alloy slowly cooled from high temperatures; the alloy quenched from above the point has higher resistivity than the cold-worked alloy, but still is lower than the annealed material. Cold work following quenching reduces the resistivity again; repeated quenching and annealing result in cyclic decrease and increase in resistivity. These effects are only present in alloys containing V, and are absent in the 30 percent Co alloys. They are difficult to account for with any of the usual hypotheses concerning the resistivity of alloys.

B3. Magnetic Permeability at Very Rapid Rates of Change of Induction. H. L. GLICK AND SIDNEY SIEGEL, *Westinghouse Research Laboratories.*—The permeability of several magnetic materials in the form of strip 0.003 inch thick or less was measured at rates of change of induction as high as 10^{10} gauss/sec. The measurements were made from cathode-ray oscilloscope observations of B and H, a square pulse of voltage about one microsecond in duration being applied to coils surrounding the sample. During this pulse, the induction rises linearly. The eddy current effects present in such a situation have been calculated by T. D. Holstein and the B-H loops observed are in qualitative agreement with those predicted with these calculations from the d.c. magnetic properties, the electrical resistivity, and the thickness of the strip material. Quantitatively, however, the observed loops indicate a permeability, during the rise of induction, about 30 to 50 percent lower than the d.c. permeability. This indicates that the mechanism of the magnetization process, at rates of change of induction so great that the average velocity of domain boundary movement must be of the order of 10^5 cm/sec., is appreciably different from that obtaining in slow field changes.

B4. Curie Transition in Ferromagnetic Alloys and Glass Containing Nickel. W. R. HAM AND HOWARD S. COLEMAN, *The Pennsylvania State College.*—The experimental results obtained by Bennett and Ham in their studies of hydrogen diffusion through ferromagnetic binary alloys showed breaks not only associated with a Curie transition for a particular alloy, but also Curie transitions corresponding to the metals from which the alloy was made. It has been suggested that such Curie transitions corresponding to the components of the alloy were caused by segregation. Magnetic experiments have been performed on the same alloys used by Bennett and Ham and the positions of the Curie transitions reported by them have been confirmed; however, it was found that the intensity of the Curie transitions corresponding to the components of the alloy were several orders of magnitude less than the Curie of the alloy itself. Further experimental work involving magnetic torsional measurements of glasses containing various amounts of nickel-oxide show a persistence of Curie transition at 360°C, even though the nickel-oxide content was less than one percent. This latter fact again suggests that the Curie transition in some cases is not altered by a chemical combination of ferromagnetic elements with certain other elements, since it is rather unlikely that there would be any appreciable segregation of nickel in a glass having a low nickel content. Although the experimental work to date does not justify saying there could be no segregation in the cases cited, it is felt that the evidence is against segregation as an explanation of the results.

B5. Crystal Structure of Tellurium. JOHN D. ORNDOFF, *Purdue University.*—Results of Hall effect, thermoelectric power, and resistivity measurements on tellurium have been interpreted as evidence[1-3] that tellurium exists in two crystalline modifications, present in various proportions depending on the temperature and the heat treatment of the sample. To decide whether these anomalies in electrical behavior as a function of temperature are really due to the development of various modifications, the crystal structure of tellurium as a function of temperature has been investigated. X-ray diffraction pictures taken with Seeman-Bohlin[4] and Debye-Scherrer cameras at temperatures from −192°C to 160°C fail to show any evidence of two modifications, nor do they show any peculiar change in lattice parameters with temperature. Tellurium evaporated in vacuum upon a glass plate produces two types of deposits: in contact with the glass a thin homogeneous metallic layer of tellurium, on the outside a second film finely dispersed, black and sooty. X-ray investigations of both layers give the ordinary tellurium pattern. Electron diffraction patterns[5] show complete but diffuse electron diffraction rings for the metallic film, while the tellurium black[4] yields a very sharp orientation pattern. This orientation and the non-symmetry of the pattern can be explained as due to the fact that the crystals did not have random distribution about the orientation axis but tended toward an alignment in a preferred direction.

[1] Haken, Ann. d. Physik **32**, 291 (1910).
[2] Smith, Phys. Rev. **1**, 352 (1913).
[3] Wold, Phys. Rev. **7**, 169 (1916).
[4] Lark-Horovitz, Science **64**, 303 (1926).
[5] We are indebted to Mr. T. S. Renzema for taking the electron diffraction pictures.

B6. Spontaneous Time-Dependent Changes in Crystalline Material. D. D'EUSTACHIO AND SELMA BLAZER BRODY, *Brooklyn Polytechnic Institute.*—Freshly broken crystalline material undergoes a change during the first few hours after being prepared. The phenomenon may be described tentatively as a further breaking up of freshly broken material. In one experiment particles of adularia (orthoclase) between 200 and 300 mesh in size were photographed a few minutes after preparation with a focusing camera using unfiltered copper radiation. After an interval of several hours, during which the sample was not disturbed, another photograph was taken. A marked increase in the number of spots was observed. The original spots were still present. The experiment has been tried with other materials. There is good reason to believe that the change is associated with the surface rather than the interior of the material.

B7. Operating Characteristics of Ceramic Dielectrics with Dielectric Constants in Excess of 1000. R. B. GRAY, *Erie Resistor Corporation.*—Within the past several years there have been introduced ceramic condensers which have extremely high dielectric constants. These materials are somewhat similar in their properties to Rochelle salt. However, their high dielectric constant obtains over much wider temperature and frequency ranges. There are quite a great many possible combinations, and curves showing some of the temperature and frequency variations are presented. Materials are subject to certain aging and voltage effects which produce deviations from the nominal capacity. The temperature variation of capacity usually

exhibits a peak which may be explained by referring to the thermal expansion curve of the material. More exact explanation in terms of composition and crystal structure must be deferred until a later date when conditions will permit such discussion. Materials are somewhat affected by humidity and at least a certain fraction of them is water soluble so that the production of commercial condensers requires fairly stringent waterproofing methods. Probably the greatest difficulty with these materials is the fact that they are subject to ionic conduction if certain trace impurities are present. This results in failure on life test, particularly at slightly elevated temperatures. Data showing the effects of several impurities will be presented.

B8. A Resonant Cavity Method for Measuring Dielectric Properties at Ultra-High Frequencies (50–1000 Megacycles). C. N. WORKS, T. W. DAKIN, AND F. W. BOGGS, *Westinghouse Research Laboratories.*—A re-entrant cylindrical cavity has been adapted to measure the dielectric constant and power factor of small disk samples of insulating materials. The disk of dielectric is placed between the flat ends of the cylindrical posts which form the re-entrant part of the cavity. The circuit is analogous to a less than $\frac{1}{4}$-wave-length section of air-filled coaxial transmission line shorted at one end and ending in a capacitor with dielectric at the other end. This cavity with the dielectric inserted is brought to resonance by tuning the frequency of a loosely coupled oscillator. The power factor of the dielectric is determined from the breadth of the resonance curve and the dielectric constant is obtained by removing the disk of dielectric and decreasing by a measured amount the separation of the flat ends of the re-entrant posts until resonance is again obtained at the same frequency as previously. The precision differential screw for varying the extension of the re-entrant post and other mechanical details are described. Electrical coupling and detecting methods are also discussed as well as the theory of the measurements. Each individual cavity can be utilized only over a frequency range of about 1.5 ratio from lowest to highest frequency. Therefore, several different sized cavities would be required to cover a range of frequency from 50 to 1000 megacycles. An accuracy of ± 0.00005 in tan δ and ± 1 percent in dielectric constant may be obtained in routine measurements. Because the cavity has a very high Q (>2000), it is much more sensitive to low power factor dielectric samples than any conventional coil and capacitor resonant circuit. Operation of the apparatus is simple and rapid and very similar to the susceptance variation technique now used at lower radio frequencies.

B9. Decomposition of Water with the Permanent Magnet. F. EHRENHAFT, *New York City*—Permanent Alnico magnets, "Blue Streak," are used. They are semicircular rings with outer radius of 5.1 cm and inner radius of 1.58 cm, 1.75 cm thick. These were fitted with pole pieces of pure soft Swedish iron having circular cylindrical extensions 1 cm in diameter, 12.5 mm long, terminating in a truncated cone, the end 6 mm in diameter. The extensions passed through rubber gaskets into a glass cell divided by a partition so that the gas evolved from either pole could be collected separately. This partition had four holes 1 mm in diameter plugged with asbestos. The pole faces were about 3 mm apart. The field strength was much less than that in the earlier described experiments with the electromagnet.* Using 4 percent H_2SO_4 in the cell, oxygen was found to be coming from both poles together with the hydrogen formed by chemical action. More oxygen was found to be coming from the north pole than from the south. For instance, 1.43 percent and 1.12 percent in one experiment, 0.87 percent and 0.57 percent in another. Using the pole pieces alone without applying the magnet, 0.00 percent oxygen was found. Measuring the pole strength of one magnet by means of a search coil and ballistic galvanometer before and after one magnetolysis, the decrease in strength was from 16,980 to 15,380 maxwells. The flux value of this magnet was at a steady state before and after this test. The evidence here given shows that water can be decomposed by a permanent magnet as well as by the electromagnet, that magnetism is polar, and that the energy for this process is supplied by the magnet as shown by its loss in pole strength.

* Felix Ehrenhaft, Phys. Rev. **60**, 169 (1941); **61**, 733 (1942); **63**, 216, 461 (1943); **64**, 43 (1943), etc.

C1. Magnetic Potential Energy and the Zeeman Effect. F. W. WARBURTON, *University of Kentucky.*—The quantization of orbital angular momentum in units of $h/2\pi$ remains unchanged in obtaining the Schroedinger equation from the Hamiltonian function which includes magnetic potential energy. When intrinsic electron spin is omitted and the magnetic potential energy of an orbit used instead, the vector model description of the Zeeman effect needs revision. Bohr's original assumption that the magnetic field affects the mechanism of transitions between energy levels, together with the mutual electrostatic oscillating dipole force of neighboring atoms during a transition, provides a qualitative explanation of certain anomalous Zeeman patterns, and it avoids the incongruity of including classical magnetic force in setting up the energy states then suspending this force during a transition between states.

C2. Sensitized Fluorescence of Copper and Test of Selection Rule for Collisions of the Second Kind. F. K. MCGOWAN AND J. G. WINANS, *University of Wisconsin.*—Sensitized fluorescence and Tesla discharge spectra of copper vapor were obtained with the simplified procedure used for other elements.[1] Particles of copper were heated to 1377° without collapsing the fused quartz tube. The Tesla discharge spectrum showed 28 copper lines and the sensitized fluorescence showed four. These were the resonance doublet 3273 and 3247 and lines at 2492 and 2441. Microphotometer comparison of intensities of lines in sensitized fluorescence and arc showed 2492 greatly enhanced in fluorescence. The selection rule[2] found for collisions of the second kind for Sn and Pb was found to apply to copper excited by collision with Hg $^3P_0$. The rule states that for atoms A and B colliding $J=J_A+J_B$ remains

constant during collisions of the second kind. This rule requires Cu 3273 to be stronger than 3247 for excitation by Hg $^3P_0$. 3247 is stronger than 3273 in the arc spectrum. Fluorescence excitation by Hg $6\,^3P_0$ alone was produced by introducing a time lag of about 10^{-4} sec. between excitation and emission.

[1] J. G. Winans and R. M. Williams, Phys. Rev. **52**, 930 (1937).
[2] J. G. Winans, Phys. Rev. **60**, 169A (1941).

C3. Raman Spectra of Normal-heptane and Normal-hexane. FORREST F. CLEVELAND AND DONALD E. LEE, *Illinois Institute of Technology.*—Continuing work on hydrocarbons, Raman frequencies, relative intensities, and depolarization factors have been obtained for *n*-heptane and *n*-hexane. The relative intensities and depolarization factors were obtained by use of a Gaertner microdensitometer. The Raman frequencies will be compared with the previous results of Kohlrausch and Köppl and of Rosenbaum, Grosse, and Jacobson. No previous polarization data seem to exist and the previous relative intensities are only visual estimates. The results will be discussed in the light of the selection rules for various possible equilibrium configurations. For example, if *n*-hexane has a symmetry corresponding to the point group C_i, 27 of the 54 fundamentals are forbidden in the Raman spectrum and all of the allowed Raman fundamentals should be polarized. Furthermore, for this symmetry, combination frequencies of two A_g or two A_u frequencies, overtones of A_g frequencies, and first, third, fifth, etc. overtones of A_u frequencies, are all allowed in the Raman spectrum and could bring about Fermi resonance interactions if they should fall sufficiently close to one of the type A_g Raman lines.

C4. Some Double-Bond Absorptions in the Vacuum Ultraviolet. JOHN R. PLATT, *Northwestern University.*—Recent measurements in heptane solution[1] are compared with the theoretical predictions of Mulliken[2] and McMurry[3] on the absorption below 2000A of conjugated and unconjugated C=C and C=O groups, with very satisfactory agreement. The data shed light on the theory of −COOR: the first true maximum above $N\rightarrow Q$ (54,000 cm^{-1}) must be above 66,000 cm^{-1} (by extrapolation) with $f>0.1$, and so is probably the $N\rightarrow V$ transition. The splitting and red shift of the 1850A ethylenic peak with increasing number of double bonds (unconjugated) may be attributable to hyperconjugation (f values increasing almost linearly, as predicted), but the reason for the red shift (about 1000 cm^{-1} of the *trans*-ethylenes from the *cis*-ethylenes is not clear. Secondary maxima near 55,000 cm^{-1} in the conjugated acids and dienes may be the $N\rightarrow V_{2,3}$ transition.

[1] Platt, Rusoff, and Klevens, J. Chem. Phys. **12**, 535 (1943); Rusoff, Platt, Klevens and Burr, in preparation.
[2] Mulliken, Reports on Progress in Physics (Physical Society of London, 1941), Vol. VIII, p. 231.
[3] H. L. McMurry, J. Chem. Phys. **10**, 655 (1942).

C5. Apparatus for the Determination of Dispersion at Supersonic Frequencies. L. N. LIEBERMANN, *University of Kansas.*—Variation of the velocity of sound with frequency yields useful information on the rate of transfer of translational energy to molecular vibrational energy. Variations have been measured by a method which allows the direct observation of small velocity changes. The apparatus permits comparison of the phases at various frequencies in two gases, one being a non-dispersive gas. If the phases are measured in the two gases at positions which correspond to equal numbers of wave-lengths from the source, then $\Delta\phi/\phi=\Delta V/V$ where $\Delta\phi$ is the phase difference in the two gases and V is the velocity in the dispersive gas. A 90-kilocycle quartz bar is excited at its fundamental and upper harmonics to produce the various frequencies. The sound is received by an L-cut Rochelle salt microphone and the phase determined by a 360° electrostatic phase shifter accurate to ±3°. ϕ was 3600° (10 wave-lengths) at the fundamental. V is taken from the literature. Five frequencies between 90 and 450 kilocycles were used; these differed by approximately 90 kilocycles. Insufficient amplifier gain at higher frequencies prevented extension of this range. Measurements on the dispersion of CO_2 at atmospheric pressure are in agreement with previous values.

C6. Precision Measurement of the Velocity of Sound at Supersonic Frequencies Using a Microphone. E. J. GROTH AND L. N. LIEBERMANN, *University of Kansas.*—The most precise measurements on the velocity of sound at supersonic frequencies have been made with the Pierce interferometer. The present method which is adapted from audible frequency technique offers greater precision together with certain advantages. The horizontal plates of a cathode-ray tube are connected to a radiofrequency oscillator which excites a quartz bar; the vertical plates are connected through a video amplifier to a microphone. The ellipse formed indicates wave-length as the microphone position is changed. The microphone is an L-cut Rochelle salt crystal. The microphone screw, 8 cm long, is calibrated to 0.001 mm. Frequencies are measured to 1 part in 10^5 using standard equipment. Measurements made on the velocity of sound in air (uncorrected for CO_2 and H_2O content) at 0°C indicate a value of 332.99±0.01 m/sec. at a frequency of 477.72 kilocycles/sec. Values at other frequencies are obtained by exciting the quartz at various harmonics. The apparatus can readily be adapted to measure sound absorption.

C7. The Kinetics of the Thin Oxide Film Formation of Iron and Copper. EARL A. GULBRANSEN, *Westinghouse Research Laboratories.* (Introduced by S. Siegel.)—The oxidation measurements are obtained by means of a sensitive vacuum microbalance. The temperature regions of 100 to 200°C for copper and 200 to 450°C for iron are covered. The pressure is varied from 0.2 to 0.0002 atmosphere of oxygen. Several types of empirical equations are shown to fit the data. The parabolic equation is found to fit after a certain initial period of the reaction. The form of the equation can be correlated with diffusion phenomenon. The influence of temperature pressure and surface effects are discussed.

C8. Mechanism of Electrolytic Oxidation of Aluminum. SCOTT ANDERSON, *Carleton College.*—When an aluminum sheet is made the anode in certain electrolytes, a layer of oxide forms on its surface and constitutes a barrier between the metal and the electrolyte. Further oxidation can occur only as a result of (1) the aluminum or (2) oxygen ions penetrating this film. A reaction mechanism is proposed in which one of three aluminum ions diffuses from the metal to the electrolyte and the other two occupy aluminum sites in an extension of the oxide lattice. The oxygen sites so created are filled by ions from the oxide and the oxygen ion vacancies diffuse to the oxide-electrolyte interface. The mechanism is successful in explaining the strong adherence of the films, and in predicting the experimental ratio of the weight of oxide formed to the weight of metal removed, as well as other properties.

C9. A New Research Tool—Irreversible Solution Potential Measurements. R. H. BROWN AND R. B. MEARS, *Aluminum Research Laboratories.*—Reversible solution potential measurements are contrasted with irreversible solution potential measurements. The advantages and limitations of each are discussed. The importance of selecting suitable conditions, especially methods of surface preparation and composition of the solution used for making the measurements, is emphasized. It is pointed out that the limitations of the method are largely dependent on the type of solution used. The interpretation of results obtained using solutions producing relatively high anodic polarization is presented and compared to results from solutions causing relatively high cathodic polarization. Methods are given for applying irreversible solution potential measurements to studies of: (a) solid phase diffusion of metals, (b) solid phase metallurgical transformations, (c) distribution and mechanism of corrosion, (d) cathodic protection and galvanic action, (e) metallic and nonmetallic coatings. Each of the above is illustrated by specific examples. In most cases the results of solution potential measurements are correlated with results obtained by other methods.

[1] Chemical Metallurgy Division, Aluminum Research Laboratories.
[2] Chief, Chemical Metallurgy Division, Aluminum Research Laboratories.

D1. Deviations in the Classification of Stable Nuclei. J. D. KURBATOV, *The Ohio State University.*—One case of deviation from the rule imposed in the classification is in even nuclei of period four, $I=20$. The mass number of the last nucleus of the group is higher than that of the first of the following group, $I=28$. This is due to ${}_{62}Sm^{144}$. The isobaric nucleus ${}_{60}Nd^{144}$ and the next in the sequence ${}_{62}Sm^{148}$ of P_8 are said to be radioactive. Other gaps in groups of even nuclei are found mainly in periods 6 and 8. The deviations in odd nuclei are in groups of $I=1$, 11, 23, and 25 and are due to the following shifts:

Non-existent stable nuclei expected by the classification		Actually existing stable nuclei	
Species	I	Species	I
${}_{18}A^{39}$	3	${}_{19}K^{39}$	1
${}_{43}Ma^{97}$	11	${}_{42}Mo^{97}$	13
${}_{58}Ce^{139}$	23	${}_{57}La^{139}$	25
${}_{57}La^{137}$	23	${}_{56}Ba^{137}$	25
${}_{61}Il^{146}$	23	${}_{60}Nd^{146}$	25

The position of ${}_{57}La^{139}$ remains unique in the classification. This odd-even nucleus is located in the midst of a group of the even-odd series. Three of four odd isobars could not be placed in the classification.

D2. Classification of Stable Nuclei by Means of Particles of Mass Numbers Three and Four. M. H. KURBATOV AND J. D. KURBATOV, *The Ohio State University.*—The requirements imposed in the classification are: (1) that the difference between isotopic numbers of groups of nuclei having common characteristics remain constant and (2) that the mass number of the last nucleus in a group be no higher than that of the first of the following group. The odd-even and even-odd series of nuclei form 22 groups which satisfy these requirements. With the even-even unequal series the conditions are fulfilled by the division of its 22 groups into four periods: P_2, $I=8a+2$, $A=4b+18$: P_6, $I=8a'+6$, $A=4b'+46$: P_4, $I=8a+4$, $A=4b''+36$: P_8, $I=8a'+8$, $A=4b'''+48$: where $a=0, 1\cdots 5$; $a'=0, 1\cdots 4$; $b=0, 1\cdots 47$; $b'=0, 1\cdots 38$; $b''=0, 1\cdots 43$; $b'''=0, 1\cdots 39$. $\Delta I=8$ is constant and the periods 2 and 6 and 4 and 8, respectively are isobaric. The nuclei of a given sequence are built up by the addition of the group $(2p2n)$. The use of the particles $(p2n)$ and $(n2p)$ results in the continuity of groups of even-odd and odd-even nuclei. A group of even-odd nuclei always precedes one of odd-even nuclei having the same number of particles of mass-number three. The isotopic number of even-odd nuclei, therefore, is two units lower than that of odd-even nuclei in the same sequence. A periodicity of nuclei with common characteristics is observed in the appearance of odd sequences alternating with consecutive periods of even nuclei.

D3. Radioactive Silver. L. K. HURST AND M. L. POOL, *The Ohio State University.*—In the continuance of the study of the radioactive isotopes of silver, variations from former results* were observed. Bombardments of silver with high energy deuterons have given an extremely long silver period of the order of 225 days. Results have been obtained to support the postulation of K-electron capture. X-rays of 0.6A which are close to the K-α x-rays of Pd and a gamma-ray of 1.0 Mev which could be expected from the excited Pd have been observed. Low intensity electrons of 0.5 Mev were also obtained. During this study neutrons which are produced from deuteron bombardment of silver were observed to be energetic enough to produce the n, $2n$ reaction leading to the 24.5-minute Ag^{106} isotope. In consequence of this observation the production of the Ag^{106} isotope by the d, H^3 or d, $p2n$ reaction* must be seriously questioned.

* R. S. Krishnan, Proc. Camb. Phil. Soc. **36**, 500 (1940).

D4. Transmutation of Titanium. CARL T. HIBDON, M. L. POOL, AND J. D. KURBATOV, *The Ohio State University.*—A study of the 16-day period of V^{48} produced by activation of titanium with deuterons has led to a re-evaluation of the energies of the positrons and gamma-rays. The positron upper limit has been found to be 0.58 Mev. Lead absorption measurements indicate a gamma-ray of 1.50 Mev. The probability of V^{48} decaying by K-electron

capture to that of positron emission is approximately 18 to 1. The scandium fraction from titanium bombarded with deuterons indicates that the (d, α) reaction is unusually strong. The isomers of Sc^{44} and the isotopes Sc^{46}, Sc^{47}, and Sc^{48} were produced. It has been found that the yield of the 85-day period of Sc^{46} from the Ti^{49} (d, α) reaction is greater than from the Sc^{45} (d, p) reaction. Two new reactions, Ti^{49} (d, α) and Ti^{51} (d, α) are established. The previously reported 72-day period of Ti^{51} was looked for but has not been produced in observable quantities. Alpha-particle bombardments of titanium free of calcium have failed to produce the 3.7-hour period of V^{50}.

D5. The Regularities in Energy Levels of Light Nuclei. W. Y. CHANG, *Princeton University.*—It is found, from the energy levels of about fifty nuclei, that in each of the four series, $4n$, $4n+2$, $4n\pm1$, the nuclei with the same value of the isotopic number $N-Z$ have similar level systems, and that the general distribution of the levels reveals a strong dependence of the level density on the values of $N-Z$. These two points have also been discussed from the standpoint of the "alpha-particle model." In each series the levels of the nuclei having the same value of $N-Z$ can be well expressed by the following formula: $E=as-b/s$, where s is an integer, and a and b are two constants different for different series and $N-Z$. It is found possible to interpret the first term as the contribution of the nuclear particles as if they were not interacting with one another, and the second term as the correction for the interactions. The results stated above are for the levels below dissociation energy. The data for those above dissociation energy is insufficient to make any correlation. However, one point is noted: In a given group of nuclei (i.e., of the same $N-Z$) the energies of the level systems seem to decrease with increasing mass number as would be expected generally from theoretical consideration.

D6. Excitation Functions Obtained by Bombardment of Sodium Bromide with 14-Mev Deuterons. E. T. CLARKE AND J. W. IRVINE, JR., *Massachusetts Institute of Technology.*—Excitation functions for production of the radioactive isotopes Na^{24} (14.8 h), Br^{82} (34 h), and Kr (34 h) were obtained by bombardment of NaBr films obtained by evaporation in high vacuum onto aluminum foil. Deuteron energy determinations were made by measurement of range in aluminum, using the relationship given by Livingston and Bethe.[1] The three activities were separated by solution of each foil in water to liberate the krypton, and precipitation of the bromine as AgBr, leaving the radiosodium in solution. The activities of each fraction were measured on a calibrated gamma-ray counter, which yielded three excitation curves and the absolute disintegration rates for the Na^{24} and the Br^{82} whose disintegration schemes are known. The reaction $Br^{81}(d, p)Br^{82}$ exhibits an excitation function which begins at about 3 Mev, rises to a maximum absolute cross section of 3.8×10^{-25} cm^2 at 8.5 Mev, and decreases with further increase in energy. The excitation of the reaction $Na^{23}(d, p)Na^{24}$ shows the same shape but begins at about 1 Mev and reaches its maximum value of 4.7×10^{-25} cm^2 at 6 Mev. The reaction $Br(d, 2n)Kr$ shows a definite threshold at 5.3 Mev and rises almost linearly with increase in deuteron energy.

[1] M. S. Livingston and H. A. Bethe, Rev. Mod. Phys. **9**, 261 (1937).

D7. The Variation of the γ-Ray Activity of Radioactive Minerals with Particle Size. F. MORGAN, *Gulf Research and Development Company.*—In oil well logging, carnotite or other radioactive material is frequently added to cement or mud in order to determine subsequently the location of the mixture by γ-ray counters or equivalent devices. To permit a quantitative interpretation of the resulting γ-ray logs, it is necessary to know the strength of the γ-ray source. This information also permits a choice of the optimum quantity of the radioactive tracer to be added to the cement or mud. The strengths of a variety of radioactive minerals, including a number of carnotites, were accordingly measured. As was expected from previous field observations, the results show large differences in activity. For example, one carnotite sample was found to have at least six times the strength of another of approximately the same cost. For the carnotites tested, the activity was found to be a function of particle size of the mineral. In most cases the activity was a minimum at an intermediate particle size, but for all the samples the finest particles showed by far the greatest activity. Samples of gummite and uraninite gave a more uniform distribution of activity with particle size. These differences can be correlated with the geological origin of the minerals involved.

D8. Charge Distribution around Protons. J. M. BLATT, *Cornell University.*—The calculations of Fröhlich, Heitler, and Kahn[1] for the deviation from the Coulomb law for a proton due to mesons are reexamined and extended to the scalar and pseudoscalar meson theory. It is sufficient to calculate the charge density around the nucleon. The potential energy $U(r)$ for a test particle is then obtained as the solution of Laplace's equation, $\Delta V=4\pi\epsilon\rho$. A perturbation calculation is used and only the terms proportional to the square of the coupling constant are considered It is found that in all standard theories (scalar, pseudoscalar, vector) the total charge diverges with some negative power of r. Some physical meaning may be attributed to the charge density in a distance larger than the Compton wave-length of the proton. The same problem was investigated using the recent theory of Dirac[2] which involves negative energy states of the mesons. It turns out that the total charge is exactly zero for all types of meson theories if the recoil of the nucleon is neglected. It has a finite value when the recoil is taken into account.

[1] Fröhlich, Heitler, and Kahn, Proc. Roy. Soc. **A171**, 269 (1939).
[2] P. A. M. Dirac, Proc. Roy. Soc. **A180**, 1 (1942); W. Pauli, Rev. Mod. Phys. **15**, 175 (1943).

E1. Paths of Electrons and Ions in Non-Uniform Magnetic Fields. N. D. COGGESHALL AND M. MUSKAT, *Gulf Research and Development Company.*—The integration of the Lorentz force equations to give electron or ion paths has been reduced to simple quadratures for systems in which the electric field is zero and the magnetic field is a function of one Cartesian or cylindrical coordinate.

For several interesting types of magnetic field variation the quadrature can be carried through analytically, and even for complicated magnetic fields, or such as are known only empirically, the numerical integration can be effected without difficulty. From general considerations of the functions involved, it is possible to determine the extension and periodicity of the orbits for any set of initial conditions. The representation used is also convenient for obtaining information regarding the dispersion and focusing characteristics of the trajectories, such as may be used for instrument design. Illustrations of such results will be presented, including the manner in which the nature of the orbits varies with changing initial conditions.

E2. Energy Distribution of Electrons Within Dense Electron Beams. C. J. CALBICK, *Bell Telephone Laboratories.*—An electron beam injected into an enclosure having equipotential walls sets up a non-uniform potential distribution within the enclosure because of space charge.[1] The non-uniformity increases with beam current until an unstable condition is reached when current falls rapidly and a virtual cathode forms. Calculations are presented for beams and enclosures of two- and three-dimensional symmetry. In the first case, the maximum possible beam current is $i=9.4\times10^{-6}y\Phi^{3/2}$ when the beam, of half-width y, completely fills the enclosed space whose walls are at potential Φ relative to the electron source. When the virtual cathode forms, the maximum current drops to $i=4.65\times10^{-6}y\Phi^{3/2}$. In the second case, the corresponding values are $i=3.8\times10^{-5}\Phi^{3/2}$ and $i=3\times10^{-5}\Phi^{3/2}$ and do not depend on beam radius. If the beam does not fill the enclosure, the maximum currents are reduced, especially in the second case. With dense beams, deflection of an electron by electric or magnetic fields depends on its trajectory within the beam, and thus deflection distortion of an electron "spot" may become serious.

[1] A. V. Haeff, Proc. I.R.E. **27**, 5 (1939).

E3. Limiting Stable Current in Electron Beams in the Presence of Ions. J. R. PIERCE, *Bell Telephone Laboratories.*—If an electron current at a given voltage is injected into the space between two grids, there is a limiting stable value of electron current beyond which a virtual cathode will form. There is a similar limiting current for electrons restrained by an infinite magnetic field to axial motion through a conducting tube. There are similar limiting stable currents even if the electronic space charge is neutralized by positive ions of infinite mass. Such a limiting current is a constant times the limiting current in the absence of ions. For parallel grids the limiting current density is

$$i_m=2^{7/2}\pi^2(e/m)^{1/2}\epsilon V_0^{3/2}/x^2.$$

For a conducting tube of infinite length capped by grids the limiting current is

$$I_m=2^{3/2}(2.4)^2\pi(e/m)^{1/2}\epsilon V_0^{3/2}.$$

E4. Mass Spectrometer with a Small Magnet. R. E. FOX, J. A. HIPPLE, AND T. W. WILLIAMS, *Westinghouse Research Laboratories.*—A five-inch radius, 60° type mass spectrometer with a unique magnet design has been constructed. The magnet pole faces are sealed into the analyzer tube by means of a Kovar cylinder to which the glass is sealed, thus establishing the vacuum seals. The magnetic flux is transmitted to the pole faces through the Kovar cylinder from an external source which is either a permanent or an electromagnet. Uniform magnetic fields of about 1500 gauss in a quarter-inch gap have been obtained with an instrument in which the complete analyzer tube plus the magnet weighed less than twenty-five pounds. The design and construction of the magnet allows the pole faces to be accurately aligned to less than 0.001 inch. With a larger external magnet it is possible to obtain stronger fields, since the size of the magnet is not fundamentally limited. Two metal cylinders bolted to the 60° magnet faces act as shields for the ion beam and also serve to mount the ion source and collector. These metal cylinders are so constructed that when bolted to the magnet the ion source and collector slits are automatically aligned with the magnet gap.

E5. The Reversed Cyclotron. LAURENCE ELLSWORTH DODD, *University of California at Los Angeles.*—A procedure based on theory and practicable experimentally would be to operate the cyclotron backward. Such reversal would permit the slowing down to some desired speed, perhaps zero, of an ionic particle having initially a high velocity. The principle is applicable theoretically for the stopping in this manner of a high speed cosmic-ray ion. Whether this is practicable for example in the case of a six-billion-volt cosmic-ray electron appears to be a question of attaining experimentally the ultra-high frequency of reversal of potential that would be necessary.

E6. Portable Demonstration Electron Microscope. IGOR BENSEN, *General Electric Company.*—A discussion of the design features making possible a compact light-weight instrument completely contained in two suitcase units.

E7. Potential Nuclear Monochromatic Electron Sources. M. L. POOL, *Ohio State University.*—Among the some 300 synthesized radioactive nuclei now available a few have been found which emit electrons in a narrow energy range. Most nuclei, however, emit the well-known continuous beta-ray spectrum. The above-mentioned few special nuclei are identified with internally converted nuclear gamma-rays. It is desirable that the internal conversion coefficient be close to 100 percent. Monochromatic electron energy bands between 50 and 300 Kev may be had originating from certain nuclei with half-lives up to several months. Detail data for the isotopes Pb^{203}, Tl^{202}, Ba^{133}, and Ba^{135} will be presented as well as a summary of the field. Eventual applications of nuclear sources seem probable for certain uses in electron microscopes, electron diffraction, and special radio tubes. (*Invited Paper*—20 minutes.)

E8. Electron Microscope Study of Ferromagnetic Domains. L. MARTON, *Stanford University.*—Ferromagnetic domains can be investigated by means of the electron microscope by using a replica technique. Such replicas

can be prepared by suspending a ferromagnetic colloid in the solution of a plastic to be cast on the polished surface of a ferromagnetic material. After solidifying the plastic on the surface of the magnetized sample it can be stripped in the same way as any other metallographic replica. Preliminary experiments show that gelatine is a good suspending medium; however, it offers difficulties in stripping. The preparation of similar colloids in the usual plastics of replica technique offer some difficulties also. A variant of the method consists in placing a very thin collodion film in contact with the sample and placing a droplet of the ferromagnetic colloid on the film. After evaporation of the solvent the film is lifted and placed in the microscope. Patterns obtained on different materials and at different degrees of magnetization are shown.

E9. Studies of Purified Preparations of the MV Strain of Poliomyelitis Virus by Means of the Electron Microscope. H. S. LORING, C. E. SCHWERDT, AND L. MARTON, *Stanford University.*—Several highly purified preparations of the MV strain of poliomyelitis virus have been examined in the Stanford electron microscope. The samples were prepared by the procedures previously described[1] with the exception that in some cases the extracts were allowed to stand in the refrigerator for several weeks before the solution was ultracentrifuged. In biological tests for activity with some preparations 100 percent of the animals developed poliomyelitis when injected at concentrations of 5×10^{-10} g of nitrogen. The micrographs show the presence of a relatively homogeneous material. The majority of the particles appear spherical or nearly spherical in shape. They are also considerably less well-defined than the reference particles on the same micrographs. Estimations of the diameters of the presumed virus particles range from 15 to 20 mμ. There is, however, a definite indication of asymmetry ranging from 1 : 2 to 1 : 5 in some of the micrographs. The possible explanation of this asymmetry, as being due to a chain-like aggregation of the smaller particles, must be left open at present. No evidence has been obtained in any of the preparations for the highly asymmetric or thread-like particles reported for the murine strain by Gard and Pedersen.

[1] H. S. Loring and C. E. Schwerdt, J. Exper. Med. **75**, 395 (1942).

T1. Note on the Inductive Measurement of Magnetic Field Strength* F. T. ROGERS, JR.,† *The University of Houston.* To be read by title.—Two of the minor corrections[1] to which the standard expression[1] $MI/2AN$ for magnetic field strengths is subject, are listed here in a convenient approximate form. For small effects of twisted leads to the rotating coil, multiply $MI/2AN$ by

$$F_1=1-a/2AN, \tag{1}$$

where a is the small "projected area" of the (equal) "loops" in the leads. For small effects of incorrect orientations of the coil, multiply $MI/2AN$ by

$$F_2=2\sec\phi/[\cos(\theta-\epsilon)+\cos\theta], \tag{2}$$

where ϵ is the small defect of the rotation angle from 180°, ϕ is the small angle between the axis of rotation and the plane (P) perpendicular to the field, and θ is the small angle between the plane of the coil in its initial prerotational position and P.

* Contribution No. 90 from The Division of Sciences of The University of Houston.
† Now with The Lukas-Harold Corporation, Indianapolis.
[1] See F. T. Rogers, Jr., Phys. Rev. **52**, 381 (1937) for the definitions of symbols.

Proceedings of the American Physical Society

MEETING OF THE NEW ENGLAND SECTION HELD AT BOSTON, MASSACHUSETTS ON APRIL 15, 1944

THE twenty-third regular meeting of the New England Section of the American Physical Society was held at Simmons College, Boston, Massachusetts, on Saturday, April 15, 1944. Forty-four members were in attendance. The invited papers were as follows:

The Review of the Papers Given at the January 14–15 Meeting of the American Association of Physics Teachers at Columbia University. Given by LOUISA BILLINGS AND LILLY LORENTZ, *Smith College*, AND MILDRED ALLEN, *Mount Holyoke College*.

Physics at Simmons College. JAMES M. HYATT, *Simmons College*.

Echo-Sounding by Flying Bats. DONALD R. GRIFFIN, *Fatigue Laboratory, Harvard University*.

Opportunities in and Training for Industrial Optics. ALLAN E. PARKER, *Worcester Polytechnic Institute*.

Some Reflections on the Relation of Mathematics and Physics. R. B. LINDSAY, *Brown University*.

In addition the following short research paper was presented.

MILDRED ALLEN
Secretary-Treasurer

Magneto-Current Phenomena in Nickel. HENRY A. PERKINS, *Trinity College*.—Two experiments on related magneto-current effects in a nickel bar may be outlined as follows. In one of these a bored-out bar was used and the effect on residual magnetism, caused by a current sent through the metal during the process of demagnetization, was compared with that caused by a current flowing through a wire run through the hollow center of the cylindrical bar. When the current in the nickel was stopped after the magnetizing field had been reduced to zero, there was an abrupt decrease in the residual flux, but this decrease was much larger when the sense of the current was in opposition to that of the flux than when with it. This suggests that in one direction the current favors the magnetic state more than it does when in the opposite direction. When the same current flows along the axis and not through the metal, there is about the same change of flux caused by breaking it, but a much smaller alteration in this change when the current's direction is reversed.

To see if any difference due to reversing the current exists in the often observed magneto-resistance phenomenon, a slender nickel bar, donated (like the one above) by the International Nickel Company, was tested in a Kelvin double bridge. Its resistance was measured when unmagnetized, and then when magnetized to a strength of 1900 gauss. The proportional increase $\Delta R/R$ due to magnetization was about 0.6 percent, but no difference could be detected when either the field or the current was reversed. However, an alternating 60-cycle field, of about the same intensity as before, produced a *decrease* in $\Delta R/R$ of an even greater magnitude. This was so marked that it easily overcame the increase of resistance due to heating when the field was applied, although this increase was fairly large. When iron was substituted for nickel, neither of the above effects could be observed with any certainty.

Proceedings of the American Physical Society

MEETING OF THE SOUTHEASTERN SECTION HELD AT ATLANTA, GEORGIA ON MAY 5 AND 6, 1944

THE tenth annual meeting of the Southeastern Section of the American Physical Society was held in the Atlanta Biltmore Hotel and at the Georgia School of Technology, Atlanta, Georgia, on Friday and Saturday, May 5–6, 1944. Approximately sixty-five members and guests attended the meeting. Local arrangements were made by a committee headed by J. H. Howey.

The regular program consisted of eight papers, abstracts for five of which are appended hereto. Abstracts of the other papers will be found in the August, 1944 issue of the *American Journal of Physics*.

Additional features of the program were a talk by H. T. Briscoe of the Manpower Commission's Professional and Technical Division of the Bureau of Training, on "Manpower problems in

the sciences;" an address at the annual dinner by Homer L. Dodge, Director of the Office of Scientific Personnel; and a review by F. L. Brown of some of the papers presented at the recent New York meeting of the American Association of Physics Teachers.

At the business meeting the election of the following officers for the Section was announced: Chairman, O. T. Koppius; Vice Chairman, F. L. Brown; Secretary, E. Scott Barr; Treasurer, C. B. Crawley; and Member of the Executive Committee, Eric Rodgers.

The time and place for the 1945 meeting is to be announced later.

E. SCOTT BARR
Secretary

1. Transient Arc Discharge Between a Stationary and a Rotating Electrode. JAMES C. BARNES, *University of Virginia.**—This paper reports a study of the transient arc discharge in air and in hydrogen between a stationary and a rotating electrode. A highly damped series circuit consisting of a condenser, spark gap, and resistance was used to form the electrical discharge between the fixed electrode and the cylindrical surface of a rotor. It has been previously found[1] that the luminous column of the discharge is carried around on the rotor surface. The distance this column is carried is as long as 12 cm for an applied voltage of 16 kv. This distance has been studied in the present work as a function of the rotor speed, the rotor material, and the gas pressure. Rotational speeds ranged from 7 to 900 r.p.s. (peripheral speeds of 0.17×10^3 to 28×10^3 cm/sec.); rotor materials included copper, bronze, duraluminum, and steel; gas pressures ranged from one centimeter to atmospheric pressure. It was found that the arc column elongates in a different manner depending on whether the rotor is anode or cathode. Arc current was investigated and found to be a function of luminous column length. Some calculations of the potential gradient in the arc column and the current density at the electrode have been made.

* Present address Kendall Mills, Paw Creek, North Carolina.
[1] J. W. Beams and L. B. Snoddy, Phys. Rev. **55**, 504 (1939); **55**, 1145 (1939).

2. Simple Relaxation Models to Explain the Dependence of Fracture Type of Deformation-Speed and Temperature. ARTHUR E. RUARK, *University of North Carolina.*—There are materials (such as tars and asphalts) which break with a so-called brittle fracture when suddenly deformed, while they exhibit considerable plastic deformation when they are slowly loaded. Such effects depend also on the experimentation-temperature. Since the actual mechanisms of flow and fracture may be very complex and may differ considerably from one material to another, it is advantageous to have a simple mechanical model which exhibits the essential features of such behavior. We shall discuss a suitable model, the essential feature being that in the model two or more deformation processes leading to final fracture proceed at different rates which depend on the temperature. [The temperature dependence is assumed to be on the form $\exp(-E/KT)$, although the exact nature of this dependence is not essential.]

3. The Biological Action of X-Rays as a Function of Intensity. A. A. BLESS, *University of Florida.*—It is a well-known fact that for the same amount of energy absorbed the biological action of alpha- and neutron rays is several times as great as the action of x-rays. This difference in action was attributed by Zircle and by Failla to be due to the higher ionization density produced by alpha-particles and by neutron ejected protons compared to the density of ionization produced by x-rays. Zircle estimates the density of ionization produced by alpha-particles to be 100 times as great as that produced by x-rays. The object of this work was to investigate whether or not x-rays for a given dose administered at high intensity produce effects different from those administered at low intensity. Wheat seedlings were subjected to given doses of x-rays at intensities varying from 25 to 5000 r.p.m. No intensity effects were observed; the effects are a function of the energy absorbed and not of the rate at which the energy is administered. It is possible that the action of alpha- and neutron rays is different from that of x-rays in character as well as in ionization density.

4. Dynamics of Rise of Water in a Capillary Tube. WM. A. RENSE, *Louisiana State University.*—Water was caused to rise in a tube 0.0632 cm in diameter. The rise was photographed in stroboscopic light of interval 1/20 sec. The data obtained were found to fit the curve: $z=4.65+1.042\log_e t$, z being the height and t the time. The nature of the rise can be predicted by assuming that the rise is turbulent (resistance proportional to the velocity squared). If v is the speed: $dv/dt=-k^2v^2$, k^2 being a constant. A simple integration yields the form of the equation which explained the observed points. An abrupt deviation near the end of the rise indicates a change from turbulent to streamline flow and suggests a dynamic method of finding Reynolds number.

5. Statistical Variations in the Maximum Load and Elongation of Copper Wire and Their Relation to Size Effect. RODNEY M. SQUIRES AND ARTHUR E. RUARK, *University of North Carolina.*—The distribution of maximum loads and the distribution of elongations are obtained for 200 15-cm samples from a single continuous length of No. 24 copper wire. The average deviation of the breaking loads is only 0.37 percent and for shorter lengths, properly chosen, it is only 0.16 percent. These deviations are much smaller than those recorded for larger and presumably less homogeneous bodies of copper. The deviations are not due to diameter variations, but to variations in the structure or composition of the metal. The smallness of the deviations implies a corresponding smallness of size effect. It is shown how the test data can be used directly to determine the size effect associated with change of specimen length. Larger bodies of commercial copper show an average deviation of the tensile strength amounting to about 1.3 percent. The usual value encountered in tests of glass is 12 to 18 percent.

Proceedings of the American Physical Society

Meeting of the Ohio Section Held at Columbus, Ohio on May 6, 1944

THE 1944 spring meeting of the Ohio Section of the American Physical Society was held at Ohio State University, Columbus, on May 6. About fifty were present. At the business session J. M. Davies, W. E. Singer, and Leon E. Smith were elected as Chairman, Vice Chairman, and Secretary-Treasurer, respectively, for the ensuing year; and plans were initiated for a meeting of the Section in conjunction with the meeting of the A.A.A.S. scheduled for September 11–16 at Cleveland. The programme of the scientific sessions follows.

Contributed Papers

The Application of Radioactive Tracers to the Chemistry of Minute Concentrations. J. D. Kurbatov and M. H. Kurbatov, *Ohio State University.*

Spontaneous Neutron Emission. M. L. Pool, *Ohio State University.*

Radioactive Isotopes of Tantalum. R. V. Zumstein, *Ohio State University.*

A Comparison of Donders' and Duane's Tables of the Amplitude of Ocular Accommodation. Henry William Hofstetter, *Ohio State University.*

An Animated Diagram of the Oscillating L-C Circuit. J. H. Rush, *Denison University.*

A New Double Monochromator for the Infra-Red Region. R. H. Noble, *Ohio State University.*

Rotation Vibration Energies of the Non-Linear XYZ Molecular Model. Robert P. Schuman and W. H. Shaffer, *Ohio State University.*

Infra-Red Spectrum of Methyl Fluoride. K. P. Yates, *Ohio State University.*

Invited Paper

The Use of the Netatron in Nuclear Physics. T. J. Wang, *Ohio State University.*

Leon E. Smith
Secretary

Author Index to Volume 65

References with (A) are to abstracts of papers presented at meetings of the American Physical Society. References with (L) are to Letters to the Editor, and those with (T) designate title only.

Alexander, J. H. (see Lapp, R. E.)—253(A)
Allen, Mildred (see Billings, Louisa)—355(T)
Allison, H. W. (see Moore, George E.)—254(A)
Anderson, R. T. (see Kruger, P. Gerald)—62(A)
Anderson, Scott. Mechanism of electrolytic oxidation of aluminum—351(A)
Antonoff, George. On some physical properties in the problem of rubber—64(A)
Aston, J. G. Potential barriers to internal rotation in organic compounds—344(T)
Auger, P. and A. Rogozinski. Non-shower producing particles in *A* showers—64(A)

Baker, W. O. X-ray diffraction in high polymers—257(T)
Barnes, James C. Transient arc discharge between a stationary and a rotating electrode—356(A)
Barnes, R. B. Physical methods of analysis of synthetic and natural rubber—60(T)
Barrett, C. S. Electron microscope in metallurgical research—344(T)
—— X-ray diffraction as a tool in metallurgy—257(T)
Beeck, Otto. Physical methods in hydrocarbon research—151(T)
Benedict, D. L. (see Hanson, A. O.)—33
Bensen, Igor. Portable demonstration electron microscope—353(A)
Bethe, H. A. and F. C. Von der Lage. Method of determining the energies and wave functions in solids—255(A)
Billings, Louisa, Lilly Lorentz, and Mildred Allen. Review of the papers given at the January 14–15 meeting of the American Association of Physics Teachers at Columbia University—355(T)
Blatt, J. M. Charge distribution around protons—352(A)
Bless, A. A. Biological action of x-rays as a function of intensity—356(A)
Bloomenthal, S. Proposed substitute for instrument oil—64(A)
Boggs, F. W. (see Works, C. N.)—349(A)
Bose, D. M., Bibha Choudhuri, and M. Sinha. Cosmic-ray meson spectra—341
Boyer, R. F. (see Spencer, R. S.)—60(T)
Braendle, H. A. and W. B. Wiegand. GR-S an elastically inverted polymer—60(T)
Brentano, J. C. M. and H. Froula. Evaluation of the intensities of line patterns recorded on a moving film in its application to the measurement of x-ray intensities—254(A)
Broadwell, S. J. (see Goetz, Alexander)—151(T)
Brody, Selma Blazer (see D'Eustachio, D.)—348(A)
Brown, R. H. and R. B. Mears. New research tool-irreversible solution potential measurements—351(A)
Brown, S. Leroy. Frequency-band character of shock vibrations—153(A)
Bryant, R. C. (see Kelsey, R. H.)—60(T)
Buerger, M. J. X-ray diffraction in the study of soap—257(T)
Bunge, Mario. New representation of types of nuclear forces—249(L)

Calbick, C. J. Energy distribution of electrons within dense electron beams—353(A)
—— Historical background of electron optics—344(T)
Carnvale, Anthony. Small gulf gravimeter—345(A)
Chakrabarty, S. K. and R. C. Majumdar. On the spin of the meson—206(L)
Chang, W. Y. Regularities in energy levels of light nuclei—352(A)
Ch'en, Shang-Yi. New absorption band of alkalis in the presence of foreign gases—338
Chertock, George. Hydrogen content of white dwarf stars—51
Choudhuri, Bibha (see Bose, D. M.)—341
Clarke, E. T. and J. W. Irvine, Jr. Excitation functions obtained by bombardment of sodium bromide with 14-Mev deuterons—352(A)
Cleveland, Forrest F. Raman spectra of 2,5-dimethyl-1,5-hexadiene and 2,5-dimethyl-2,4-hexadiene—65(A)
—— **and Donald E. Lee.** Raman spectra of normal-heptane and normal-hexane—350(A)
Cobas, A. and W. E. Lamb, Jr. On the extraction of electrons from a metal surface by ions and metastable atoms—327
Coggeshall N. D. and M. Muskat. Paths of electrons, and ions in non-uniform magnetic fields—352(A)
Colbey, N. C. (see Kruger, P. Gerald)—62(A)
Coleman, Howard S. (see Ham, W. R.)—348(A)
—— **and H. L. Yeagley.** Comments on the anisotropy of metals—56
Coolidge, Albert Sprague. Experimental verification of the theory of the continuous spectra of H_2 and D_2—236
Cooper, John N. Auger transitions and widths of x-ray energy levels—155
Copeland, Paul L. and Carroll Lufcy. Stability of a mercury arc as a function of cathode pool area—66(A)

Dakin, T. W. (see Works, C. N.)—349(A)
Davey, Wheeler P. Mechanism of crystal growth and its consequences—344(T)
Debye, P. Light scattering in solutions—60(T)
Deisenrod, M. Y. (see Zhdanov, A. P.)—202(L)
D'Eustachio, D. and Selma Blazer Brody. Spontaneous time-dependent changes in crystalline material—348(A)
Deutsch, Martin and Lloyd G. Elliott. Disintegration schemes of radioactive substances. VIII. Mn^{54} and Co^{58}—211
Dillon, J. H. (see Kelsey, R. H.)—60(T)
—— (see Tobolsky, A. V.)—60(T)
——, **I. B. Prettyman, and G. L. Hall.** Hysteretic and

elastic properties of rubberlike materials under dynamic shear stresses—60(T)
Dodd, Laurence Ellsworth. Reversed cyclotron—353(A)
Donnay, J. D. H. Diffraction methods in organic chemistry —257(T)

Edlén, Bengt. Magnetic-dipole transitions in the configurations $5p^5$, $5p^4$, and $6p^5$ of xenon and radon—248(L)
Ehrenhaft, Felix. Continuation of experiments with the magnetic current—256(A)
—— Decomposition of water by the so-called permanent magnet and the measurement of the intensity of the magnetic current—287(L)
—— Decomposition of water with the permanent magnetic —349(A)
—— New experiments about the magnetic current—62(A)
Eisenschitz, R. Configurations of a binary mixed crystal—204(L)
Eisner, E. Interpretation of the angular distribution of alphas from $Li^7(P;\alpha)\alpha$—85
Ekstein, H. Free vibrations of aeolotropic bodies—254(A)
Elliott, Lloyd G. (see Deutsch, Martin)—211
Emmett, P. H. Measurement of the surface area of carbon black by low temperature absorption—60(T)
Epstein, Paul S. On the elastic vibrations of cylindric shells —152(A)
Estermann, I., O. C. Simpson, and O. Stern. Deflection of a beam of cesium atoms by gravity—346(A)
Evans, Robley D. and Clark Goodman. Alpha-helium method for determining geological ages—216

Fankuchen, I. and H. Mark. Crystallization of long-chain compounds—60(T)
Feshbach, Herman. On the perturbation of boundary conditions—307
Fett, G. H. Series generator as a negative resistance—62(A)
Field, J. E. (see Gehman, S. D.)—60(T)
Fisher, Leon H. Sparking potentials in air in a plane parallel gap at and below atmospheric pressure—153(A)
Fox, R. E., J. A. Hipple, and T. W. Williams. Mass spectrometer with a small magnet—353(A)
Frevel, L. K. Diffraction methods in analytical chemistry—257(T)
Froula, H. (see Brentano, J. C. M.)—254(A)

Gallagher, Charles J. Adsorption of thorium on tantalum —46
Gamow, G. Evolution of contracting stars—20
Gehman, S. D. and J. E. Field. X-ray observations on the structure of rubber and the size and shape of rubber crystallites—60(T)
Geisler, A. H. (see Keller, F.)—344(T)
Glick, H. L. and Sidney Siegel. Magnetic permeability at very rapid rates of change of induction—348(A)
Goetz, Alexander, S. J. Broadwell, and D. C. Warner. Problem of rendering sea water potable—151(T)
Goldhaber, M. Nuclear disintegrations produced by cosmic radiation—344(T)
——, **G. S. Klaiber, and G. Scharff-Goldhaber.** Investigation of high energy gamma-ray of Na^{24} by the photoneutron method—61(A)
Goodman, Clark (see Evans, Robley D.)—216
Gray, R. B. Operating characteristics of ceramic dielectrics with dielectric constants in excess of 1000—348(A)
Greene, J. B. (see Kruger, P. Gerald)—62(A)
Griffin, Donald R. Echo-sounding by flying bats—355(T)
Groetzinger, G. K. (see Kruger, P. Gerald)—62(A)
Groth, E. J. and L. N. Liebermann. Precision measurement of the velocity of sound at supersonic frequencies using a microphone—350(A)
Grove, D. J. (see Hipple, J. A.)—346(A)
Gulbransen, Earl A. Kinetics of the thin oxide film formation of iron and copper—350(A)

Hall, G. L. (see Dillon, J. H.)—60(T)
Ham, W. R. and Howard S. Coleman. Curie transition in ferromagnetic alloys and glass containing nickel—348(A)
Hammer, Sigmund. Address of welcome—344(T)
Hanson, A. O. and D. L. Benedict. Independent determination of fixed points on the high voltage scale—33
Harkins, William D. (see Jura, George)—66(A)
—— **and George Jura.** New adsorption isotherm and polymolecular films on solids—66(A)
Harrison, A. E. Kinematics of reflection oscillators—344(T)
Hasler, M. F. Present status of spectroscopic methods of analysis—152(A)
Hayden, R. (see Lewis, L. G.)—346(A)
Hazen, Wayne E. Average ionization and energy loss of cosmic-ray mesotrons in air—259
—— Average specific ionization of the mesotrons 100 ft. underground—152(A)
—— Cascade showers and nuclear disintegrations at 10,000 feet—67
—— Note concerning the multiple production of penetrating secondary cosmic rays in lead—249(L)
Heitz, M. P. (see Winans, J. G.)—65(A)
Hibdon, Carl T., M. L. Pool, and J. D. Kurbatov. Transmutation of titanium—351(A)
Hipple, J. A. (see Fox, R. E.)—353(A)
—— **and D. J. Grove.** Amplifier with logarithmic response —346(A)
Hofstetter, Henry William. Comparison of Donders' and Duane's tables of the amplitude of ocular accommodation—357(T)
Hsueh, Chao-Wang. Light source for the primary standard of wave-length—151(A)
Hu, Ning (see Jauch, J. M.)—289(L)
Hu, Tsi-Ming. On the term values of x-ray spectra—76
Hudson, Douglas Rennie. Thixotropy in silver amalgams—247(L)
Hurst, L. K. and M. L. Pool. *K*-electron capture in radioactive silver—60(A)
—— **and M. L. Pool.** Radioactive silver—351(A)
Hutter, R. G. E. (see Marton, L.)—161
Hyatt, James M. Physics at Simmons College—355(T)

Inglis, D. R. (see Swartz, C. D.)—80
Iona, Mario, Jr., Marcel Schein, and Julius Tabin. Secondary radiation produced by cosmic-ray primaries in paraffin—64(A)
Irvine, J. W., Jr. (see Clarke, E. T.)—352(A)

Iwanenko, D. and I. Pomeranchuk. On the maximal energy attainable in a betatron—343(L)

Jaffé, George. On the currents carried by electrons of uniform initial velocity—91
James, H. M. Present status of theory of elasticity of rubber—60(T)
Jauch, J. M. (see Pauli, W.)—255(A)
—— **and Ning Hu.** On the mixed theory of nuclear forces —289(L)
Jennings, B. (see Swartz, C. D.)—80
Jura, George (see Harkins, William D.)—66(A)
—— **and William D. Harkins.** Adsorption method for the determination of the area of a solid—66(A)

Keller, F. and A. H. Geisler. Extending microscopic examination of metals—344(T)
Kelsey, R. H., J. H. Dillon, H. A. Schultz, and R. C. Bryant. New extrusion plastometer—60(T)
Kikuchi, Chihiro (see Podolsky, Boris)—228
King, Allen. Tensile strength of water—256(A)
Klaiber, G. S. (see Goldhaber, M.)—61(A)
Kohman, Truman P. Counter corrections at high counting rates—63(A)
Korff, S. A. Production of neutrons by cosmic radiation—344(T)
—— (see Kupferberg, Max)—253(A)
—— **and R. D. Present.** On the role of polyatomic gases in fast counters—274
—— **and R. D. Present.** Quenching mechanism in "self-quenching" counters—253(A)
Krasnooshkin, P. E. On supersonic waves in cylindrical tubes and the theory of the acoustic interferometer—190
Kruger, P. Gerald (see Ogle, W. E.)—61(A)
——, **J. R. Richardson, G. K. Groetzinger, E. M. Lyman, W. E. Ogle, M. E. Nelson, G. Schwarz, J. B. Greene, R. T. Anderson, N. C. Colbey, R. W. Lee, C. E. McClellan, D. Scag, Lloyd Smith, and F. K. Tallmadge.** Cyclotron which allows the accelerated particles to emerge in a direction parallel to the dee interface—62(A)
Kupferberg, K. and F. Reines. Determination of mesotron mass-lifetime ratio by correlation with meteorological data—253(A)
Kupferberg, Max and S. A. Korff. Determination of the rate of production in paraffin of neutrons by the cosmic radiation at sea level—253(A)
Kurbatov, J. D. Deviations in the classification of stable nuclei—351(A)
—— (see Hibdon, Carl T.)—351(A)
—— (see Kurbatov, M. H.)—351(A)
—— (see Lutz, Arthur L.)—61(A)
—— **and M. H. Kurbatov.** Application of radioactive tracers to the chemistry of minute concentrations—357(T)
—— **and M. L. Pool.** Isolation of pure radioactive cerium—61(A)
Kurbatov, M. H. (see Kurbatov, J. D.)—357(T)
—— **and J. D. Kurbatov.** Classification of stable nuclei by means of particles of mass numbers three and four—351(A)
Kyropoulos, S. Friction of binary alloys with thin film lubrication—152(A)

Lamb, W. E. (see Cobas, A.)—327
Landé, Alfred and Llewellyn H. Thomas. Finite self-energies in radiation theory. Part III—175
Lapp, R. E. Measurement of high energy electrons in *A* showers—347(A)
—— Origin of large cosmic-ray bursts—63(A)
—— (see Schein, Marcel)—63(A)
—— **and J. H. Alexander.** Experiments on large cosmic-ray bursts in relation to *A* showers—253(A)
Lee, Donald E. (see Cleveland, Forrest F.)—350(A)
Lee, R. W. (see Kruger, P. Gerald)—62(A)
Levy, Saul. Simplified method of plate calibration for analytical spectroscopy—256(A)
Lewis, E. W. (see Lewis, L. G.)—63(A)
—— **and L. G. Lewis.** Radio of the average current generated by cosmic-ray air showers to the total current observed in the ionization chamber—346(A)
Lewis, L. G. (see Lewis, E. W.)—346(A)
—— **and R. Hayden.** Influence of statistical fluctuations on the observed size-frequency distribution of bursts in a single ionization chamber—346(A)
—— **and E. W. Lewis.** Study of cosmic-ray air showers using the method of coincident bursts in two unshielded ionization chambers—63(A)
Liebermann, L. N. Apparatus for the determination of dispersion at supersonic frequencies—350(A)
—— (see Groth, E. J.)—350(A)
Liebowitz, Benjamin. Kinematical probability—255(A)
Lindsay, R. B. Some reflections on the relation of mathematics and physics—355(T)
Lockenvitz, A. E. High sensitivity string galvanometer—153(A)
Lorentz, Lilly (see Billings, Louisa)—355(T)
Loring, H. S., C. E. Schwerdt, and L. Marton. Studies of purified preparations of the MV strain of poliomyelitis virus by means of the electron microscope—354(A)
Lufcy, Carroll (see Copeland, Paul L.)—66(A)
Lutz, Arthur L., M. L. Pool, and J. D. Kurbatov. Beta-ray spectra of the artificially radioactive isotopes, Pb^{205} and Bi^{207}—61(A)
Lyman, E. M. (see Kruger, P. Gerald)—62(A)

Majumdar, R. C. (see Chakrabarty, S. K.)—206(L)
Margenau, Henry. Physics and phenomenology—344(T)
—— (see Meyerott, Roland)—255(A)
Mark, H. (see Fankuchen, I.)—60(T)
Marton, L. Electron microscope study of ferromagnetic domains—353(A)
—— (see Loring, H. S.)—354(A)
—— **and R. G. E. Hutter.** On apertures of transmission type electron microscopes using magnetic lenses—161
Mason, L. S. Thermopile for micro-calorimetry—345(A)
Mattoon, Richard W. Polymer spectra of a cyanine dye—65(A)
McClellan, C. E. (see Kruger, P. Gerald)—62(A)
McCue, J. J. G. Ionization cross section of the silver L_{III} state—168

McGowan, F. K. and J. G. Winans. Sensitized fluorescence of copper and test of selection rule for collisions of the second kind—349(A)
McGreary, Robert (see Siegel, Sidney)—347(A)
McMaster, R. C. X-ray inspection of spotwelds in aluminum alloys—153(A)
Mears, R. B. (see Brown, R. H.)—351(A)
Meissner, K. W. (see Mundie, L. G.)—65(A), 265
Merchant, M. Eugene. Mechanics of the metal cutting process. I. Simple straight-edged tool and continuous chip—347(A)
Merrill, Paul W. Forbidden lines of Ca II in a stellar spectrum—152(A)
Meyerott, Roland and Henry Margenau. Exchange forces between Li^+ and He, and the mobility of Li^+ in He—255(A)
Miles, John. Excitation of electromagnetic waves in waveguides and cavities—153(A)
Miller, Franklin, Jr. Auger electrons resulting from K capture—254(A)
Millikan, R. A., H. V. Neher, and W. H. Pickering. Further studies on the least penetrating component of the incoming cosmic rays—152(A)
Mooney, M., W. C. Wolstenholme, and D. S. Villars. Drift and relaxation of rubber—60(T)
Moore, George E. and H. W. Allison. Thermionic effects of thin films of alkaline earth oxides on metals—254(A)
Moquin, William N. and M. L. Pool. Artificial radioactivity of columbium and zirconium—60(A)
Morgan, F. Variation of the γ-ray activity of radioactive minerals with particle size—352(A)
—— **and M. Muskat.** Effect of rate of shear on the viscosity of oils—255(A)
Mrozowski, S. Forbidden lines of bismuth Bi I—65(A)
Mundie, L. G. and K. W. Meissner. Isotope shift in magnetism—65(A), 265
Murray, R. T. K. Recording negative ions and electrons in a gas with a Geiger-Müller counter—63(A)
Muskat, M. (see Coggeshall, N. D.)—352(A)
—— (see Morgan, F.)—255(A)

Neher, H. V. (see Millikan, R. A.)—152(A)
Nelson, M. E. (see Kruger, P. Gerald)—62(A)
Noble, R. H. New double monochromator for the infra-red region—357(T)
Nordheim, L. W. On the lateral spread of cosmic-ray showers—344(T)

Ogle, W. E. (see Kruger, P. Gerald)—62(A)
—— **and P. Gerald Kruger.** Energy of gamma-rays from $Na^{24}Mg^{24}$—61(A)
Onsager, Lars. Crystal statistics. I. A two-dimensional model with an order-disorder transition—117
Opatowski, I. Refractive index in electron optics—54, 62(A)
Orndoff, John D. Crystal structure of tellurium—348(A)

Page, Leigh. Electrical oscillations of a prolate spheroid. Paper II. Prolate spheroidal wave functions—98
—— Electrical oscillations of a prolate spheroid. Paper III. The antenna problem—111
Parker, Allan E. Opportunities in and training for industrial optics—355(T)
Patterson, A. L. Ambiguities in the x-ray analysis of crystal structures—195
—— Ideas behind x-ray diffraction—257(T)
Pauli, W. and J. M. Jauch. On the application of Dirac's method of field-quantization to the problem of emission of low frequency photons—255(A)
Pauling, Linus. Specificity of intermolecular interaction—151(T)
Payne, Mary Hewlett. Interpretation of the spinning electron with bipolar coordinates—39
Perfilov, N. A. (see Zhdanov, A. P.)—202(L)
Perkins, Henry A. Magneto-current phenomena in nickel—355(A)
Pickering, W. H. (see Millikan, R. A.)—152(A)
—— **and S. C. Snowden.** Voltage regulator for high voltages—151(A)
Pierce, J. R. Limiting stable current in electron beams in the presence of ions—353(A)
Platt, John R. Some double-bond absorptions in the vacuum ultraviolet—350(A)
Podolsky, Boris and Chihiro Kikuchi. Generalized electrodynamics. Part II—Quantum—228
Pomeranchuk, I. (see Iwanenko, D.)—343(L)
Pool, M. L. Potential nuclear monochromatic electron sources—353(A)
—— Spontaneous neutron emission—357(T)
—— (see Hibdon, Carl T.)—351(A)
—— (see Hurst, L. K.)—60(A), 351(A)
—— (see Kurbatov, J. D.)—61(A)
—— (see Lutz, Arthur L.)—61(A)
—— (see Moquin, William N.)—60(A)
Present, R. D. (see Korff, S. A.)—253(A), 274
Prettyman, I. B. (see Dillon, J. H.)—60(T)
—— (see Tobolsky, A. V.)—60(T)

Radavich, F. J. and R. Smoluchowski. Influence of pressure on intermetallic diffusion—62(A); Erratum—248(L)
Rank, D. H. Photoelectric measurement of weak emission spectra—344(T)
Reichenbach, Hans. Philosophical foundations of quantum mechanics—344(T)
Reines, F. (see Kupferberg, K.)—253(A)
Rense, Wm. A. Dynamics of rise of water in a capillary tube—356(A)
Richardson, J. R. (see Kruger, P. Gerald)—62(A)
Robinson, H. A. Some physical properties of commercial polymerized methyl methacrylate—60(T)
Rogers, F. T., Jr. Note on the inductive measurement of magnetic field strength—354(A)
Rogozinski, Anatole. High energy particles in Auger showers—207
—— On the problem of the existence of mesotrons in Auger showers—291
—— Theory of counter experiments on collision electrons ejected in air by mesotrons—300, 347(A)
—— (see Auger, P.)—64(A)
Rolf, Pauline. Accommodation coefficient of helium on platinum—185

Rossi, H. E. (see Swartz, C. D.)—80
—— **and C. D. Swartz.** Angular distribution of alphas from $F^{19}(P, \alpha)O^{16}$—83
Roth, F. L. (see Wood, L. A.)—60(T)
Ruark, Arthur E. Differential equations for the probability distribution of events—88
—— Note on events distributed according to chance—287(L)
—— Simple relaxation models to explain the dependence of fracture type of deformation-speed and temperature—356(A)
—— (see Squires, Rodney M.)—356(A)
Rush, J. H. Animated diagram of the oscillating L-C circuit—357(T)

Sack, H. S. Hysteresis losses in high polymers—60(T)
Sakmann, B. W. Electric birefringence of colloidal solutions—254(A)
Sarabhai, Vikram. Method of shower anticoincidences for measuring the meson component of cosmic radiation—203(L), 250(L)
Scag, D. (see Kruger, P. Gerald)—62(A)
Scharff-Goldhaber, G. (see Goldhaber, M.)—61(A)
Schein, Marcel. Nature of cosmic-ray phenomena—344(T)
—— (see Iona, Mario, Jr.)—64(A)
—— **and R. E. Lapp.** Analysis of large cosmic-ray bursts—63(A)
Schultz, H. A. (see Kelsey, R. H.)—60(T)
Schuman, Robert P. and W. H. Shaffer. Rotation vibration energies of the non-linear XYZ molecular model—357(T)
Schwarz, G. (see Kruger, P. Gerald)—62(A)
Schwerdt, C. E. (see Loring, H. S.)—354(A)
Seitz, Frederick. Modern theories of plasticity in solids—344(T)
Shaffer, W. H. (see Schuman, Robert P.)—357(T)
Siegel, Sidney (see Glick, H. L.)—348(A)
—— **and Robert McGreary.** Anomalous behavior of the electrical resistivity of some iron-cobalt alloys—347(A)
Simpson, O. C. (see Estermann, I.)—346(A)
Sinha, M. (see Bose, D. M.)—341
Skellett, A. M. Magnetically focused radial beam vacuum tube—344(T)
Smith, Lloyd (see Kruger, P. Gerald)—62(A)
Smoluchowski, R. (see Radavich, F. J.)—62(A), 248(L)
Snowden, S. C. Analysis of a multivibrator—151(A)
—— (see Pickering, W. H.)—151(A)
Spencer, R. S. and R. F. Boyer. Second-order transition in high polymers—60(T)
Squires, Rodney M. and Arthur E. Ruark. Statistical variations in the maximum load and elongation of copper wire and their relation to size effect—356(A)
Stambaugh, R. B. Retraction of stretched rubber—250(L)
Stanton, H. E. Electrons in equilibrium with mesotrons—64(A)
Stern, O. (see Estermann, I.)—346(A)
Strobel, Charles Kennedy. Effect of intense electrostatic fields on the reflectivity of tungsten—283
Swann, W. F. G. Role of the primary cosmic radiation—344(T)
Swartz, C. D. (see Rossi, H. H.)—83
——, **H. H. Rossi, B. Jennings, and D. R. Inglis.** Angular distribution of alphas from $Li^7(P, \alpha)\alpha$—80

Tabin, Julius. Production of mesotrons by non-ionizing radiation at altitudes of 10,618 ft. and 14,230 ft.—64(A)
—— (see Iona, Mario, Jr.)—64(A)
Tallmadge, F. K. (see Kruger, P. Gerald)—62(A)
Thomas, Llewellyn H. (see Landé, Alfred)—175
Tobolsky, A. V., I. B. Prettyman, and J. H. Dillon. Stress relaxation of natural and synthetic rubber stocks—60(T)
Townes, Charles Hard. Theory of cathode sputtering in low voltage gaseous discharges—319

Villars, D. S. (see Mooney, M.)—60(T)
Von der Lage, F. C. (see Bethe, H. A.)—255(A)

Walchli, Harold E. Performance tests on the Penn State type of G-M circuits—346(A)
Wang, T. J. Use of the netatron in nuclear physics—357(T)
Warburton, F. W. Magnetic potential energy and the Zeeman effect—349(A)
Warner, D. C. (see Goetz, Alexander)—161(T)
Wataghin, G. Relativity and supplementary indeterminacy—205(L)
Weinstock, Robert. Continuous x-ray spectrum: note to experimenters—150(L)
—— Inelastic scattering of slow neutrons—1
Wiegand, W. B. (see Braendle, H. A.)—60(T)
Wiens, Jacob H. Structure of λ5461 of mercury (198)—58(L)
Williams, Robley C. and Ralph W. G. Wyckoff. Thickness of electron microscopic objects—344(T)
Williams, T. W. (see Fox, R. E.)—353(A)
Winans, J. G. (see McGowan, F. K.)—349(A)
—— **and M. P. Heitz.** Energy of dissociation of Hg_2—65(A)
Wolfenstein, Lincoln. Calculations on extensive cosmic-ray showers in air—346(A)
Wolstenholme, W. C. (see Mooney, M.)—60(T)
Wood, L. A. and F. L. Roth. Stress-temperature relations in natural rubber—60(T)
Works, C. N., T. W. Dakin, and F. W. Boggs. Resonant cavity method for measuring dielectric properties at ultra-high frequencies (50–1000 megacycles)—349(A)
Worley, R. E. Note on the spectrum of N_2—249(L)
Wyckoff, W. G. (see Williams, Robley C.)—344(T)

Yates, K. P. Infra-red spectrum of methyl fluoride—357(T)
Yeagley, H. L. (see Coleman, H. S.)—56
Yensen, T. D. Hipersil, the new transformer iron—344(T)

Zarem, A. M. Explosion of ether-air mixtures by electrical sparks—153(A)
Zhdanov, A. P., N. A. Perfilov, and M. Y. Deisenrod. Anomalous rate of nuclear disintegration effected by cosmic rays—202(L)
Zumstein, R. V. Radioactive isotopes of tantalum—357(T)
Zwicky, Fritz. Morphology of nebulae and clusters of nebulae—151(T)

Analytic Subject Index to Volume 65

References with (A) are to abstracts of papers presented at meetings of the American Physical Society. References with (L) are to Letters to the Editor.

Accommodation coefficient
Of He on Pt, P. Rolf—185
Acoustics
Dispersion at supersonic frequencies, L. N. Liebermann—350(A)
Perturbation of boundary conditions, H. Feshbach—307
Precision measurement of velocity of sound, supersonic frequencies, E. J. Groth and L. N. Liebermann—350(A)
Supersonic waves in cylindrical tubes, P. E. Krasnooshkin—190
Adsorption (see **Thermionic emission; Emitting surfaces**)
Arcs (see **Discharge of electricity in gases**)
Astrophysics
Evolution of contracting stars, G. Gamow—20
Forbidden lines of Ca II, stellar spectrum, P. W. Merrill—152(A)
Hydrogen content of white dwarf stars, G. Chertock—51
Atomic and molecular beams
Deflection of beam of Cs atoms by gravity, I. Estermann, O. C. Simpson, and O. Stern—346(A)

Biophysics
Poliomyelitis virus electron microscope studies, H. S. Loring, C. E. Schwerdt, and L. Marton—354(A)
Biological action of x-rays, A. A. Bless—356(A)

Capillary action (see **Surface tension**)
Colloids
Electric birefringence, B. W. Sakmann—254(A)
Constants, physical
Fixed points on high voltage scale, A. O. Hanson and D. L. Benedict—33
Standard of wave-length, light source, C. W. Hsueh—151(A)
Cosmic radiation
Cascade showers, nuclear disintegrations, W. E. Hazen—67
Coincident bursts in two chambers; Energy spectrum, L. G. Lewis and E. W. Lewis—63(A)
Collision electrons ejected by mesotrons, A. Rogozinski—347(A); 300
Current generated by showers to total current, E. W. Lewis and L. G. Lewis—346(A)
Electrons in equilibrium with mesotrons, H. E. Stanton—64(A)
Extensive showers in air, L. Wolfenstein—346(A)
He annihilation rays, R. A. Millikan, H. V. Neher, and W. H. Pickering—152(A)
High energy particles in *A* showers, A. Rogozinski—207; R. E. Lapp—347(A)
Ionization and energy loss of mesotrons, W. E. Hazen—259
Large bursts, analysis, M. Schein and R. E. Lapp—63(A)
Large bursts in relation to *A* showers, R. E. Lapp and J. H. Alexander—253(A)
Large bursts, origin, R. E. Lapp—63(A)
Meson spectra, D. M. Bose, B. Choudhuri, and M. Sinha—341
Mesotron mass-lifetime ratio, K. Kupferberg and F. Reines—253(A)
Mesotrons in *A* showers, A. Rogozinski—291
Mesotrons 100 ft. underground, W. E. Hazen—152(A)
Multiple production of penetrating secondary rays, W. E. Hazen—249(L)
Non-shower producing particles in *A* showers, P. Auger and A. Rogozinski—64(A)
Nuclear disintegration, anomalous rate, A. P. Zhdanov, N. A. Perfilov, and M. Y. Deisenrod—202(L)
Nuclear forces, J. M. Jauch and N. Hu—289(L)
Production of mesotrons at high altitudes, J. Tabin—64(A)
Production of neutrons in paraffin, M. Kupferberg and S. A. Korff—253(A)
Secondary radiation in paraffin, M. Iona, Jr., M. Schein, and J. Tabin—64(A)
Shower anticoincidences, meson component, V. Sarabhai—203(L); 250(L)
Size-frequency distribution of bursts, statistical fluctuations, L. G. Lewis and R. Hayden—346(A)
Spin of meson, S. K. Chakrabarty and R. C. Majumdar—206(L)
Crystal structure
Ambiguities in x-ray analysis, A. L. Patterson—195
Configurations of a binary mixed crystal, R. Eisenschitz—204(L)
Of Te, J. D. Orndoff—348(A)
Spontaneous time-dependent changes, D. D'Eustachio and S. B. Brody—348(A)
Crystalline state
Anisotropy of metals, H. S. Coleman and H. L. Yeagley—56
Determination of area of crystalline solid, G. Jura and W. D. Harkins—66(A)
Electrical resistivity of some Fe-Co alloys, S. Siegel and R. McGreary—347(A)
Energies and wave functions in solids, H. A. Bethe and F. C. Von der Lage—255(A)
Intermetallic diffusion, influence of pressure, F. J. Radavich and R. Smoluchowski—62(A); 248(L)
Thixotropy in silver amalgams, D. R. Hudson—247(L)
Two-dimensional model, L. Onsager—117

Dielectric constants (see **Dielectrics and dielectric properties**)
Dielectrics and dielectric properties
Ceramic dielectrics, R. B. Gray—348(A)
Resonant cavity method for measuring dielectric prop-

erties, C. N. Works, T. W. Dakin, and F. W. Boggs—349(A)

Discharge of electricity in gases
Arc between stationary and rotating electrode, J. C. Barnes—356(A)
Cathode sputtering, theory of, C. H. Townes—319
Electrical sparks in ether-air mixtures, A. M. Zarem—153(A)
Electron beams in presence of ions, J. R. Pierce—(353A)
Polyatomic gases in fast counters, S. A. Korff and R. D. Present—274
Recording negative ions with a G-M counter, R. T. K. Murray—63(A)
Sparking potentials, L. H. Fisher—153(A)
Stability of Hg arc, P. L. Copeland and C. Lufcy—66(A)

Discharge of electricity in high vacua (see also **Vacuum tubes**)
Currents carried by electrons, G. Jaffé—91
Energy distribution of electrons in beams, C. J. Calbick—353(A)

Disintegration and excitation of nucleus (see also **Radioactivity**)
Angular distribution of α's from $F^{19}(p, \alpha)O^{16}$, H. H. Rossi and C. D. Swartz—83
Angular distribution of α's from $Li^7(p, \alpha)\alpha$, C. D. Swartz, H. H. Rossi, B. Jennings, and D. R. Inglis—80
Angular distribution of α's, interpretation, E. Eisner—85
Anomalous rate by cosmic rays, A. P. Zhdanov, N. A. Perfilov, and M. Y. Deisenrod—202(L)
Fixed points on high voltage scale, A. O. Hanson and D. L. Benedict—33

Dissociation, heat of
Of Hg_2, J. G. Winans and M. P. Heitz—65(A)

Dynamics
Perturbation of boundary conditions, H. Feshbach—307

Elasticity
Free vibrations of aeolotropic bodies, H. Ekstein—254(A)
Physical properties of rubber, G. Antonoff—64(A)
Rate of retraction of stretched rubber, R. B. Stambaugh—250(L)
Relaxation of models, A. E. Ruark—356(A)
Shock vibrations, frequency character, S. L. Brown—153(A)
Statistical variation; maximum load and elongation, R. M. Squires and A. E. Ruark—356(A)
Tensile strength of water, A. King—256(A)
Vibrations of cylindric shells, P. S. Epstein—152(A)

Electrical circuits (see **Methods and instruments**)

Electrical conductivity and resistance
Of Fe-Co alloys, S. Siegel and R. McGreary—347(A)

Electrolysis
Mechanism of oxidation of Al, S. Anderson—351(A)

Electromagnetic theory
Finite self-energies in radiation theory, A. Landé and L. H. Thomas—175
Generalized electrodynamics, B. Podolsky and C. Kikuchi—228
Oscillations of prolate spheroid, wave functions, L. Page—98; the antenna problem, L. Page—111
Waves in wave-guides and cavities, J. Miles—153(A)

Electron optics
Electron microscopes, apertures, L. Marton and R. G. E. Hutter—161
Refractive index, I. Opatowski—54; 62(A)

Electrons
Spinning electron, bipolar coordinates, M. H. Payne—39
Betatron, maximal energy obtainable in, D. Iwanenko and I. Pomeranchuk—343

Electrons, secondary
By impact of ions and metastable atoms, A. Cobas and W. E. Lamb, Jr.—327

Electro-optical effects
Birefringence of colloidal solutions, B. W. Sakmann—254(A)

E/m
Paths of ions in non-uniform magnetic fields, N. D. Coggeshall and M. Muskat—352(A)

Equations of state
Adsorption isotherm for films, W. D. Harkins and G. Jura—66(A)

Errata
Influence of pressure on intermetallic diffusion, F. J. Radavich and R. Smoluchowski—248(L)
Ultraviolet absorption spectrum of N_2 in extreme ultraviolet, R. E. Worley—249(L)

Films, properties of
Adsorption isotherm; polymolecular films on solids, W. D. Harkins and G. Jura—66(A)
Kinetics of oxide film formation, E. A. Gulbransen—350(A)

Fluorescence
Of Cu, selection rule, F. K. McGowan and J. G. Winans—349(A)

Friction
Of binary alloys, thin film lubrication, S. Kyropoulos—152(A)

Geophysics
Alpha-helium method, geological ages, R. D. Evans and C. Goodman—216
Small gravimeter, A. Carnvale—345(A)

Instruments (see **Methods and instruments**)

Ionization by collision
Ionization cross section of Ag L_{III} state, J. J. G. McCue—168

Ions, mobility
Exchange forces between Li^+ and He, R. Meyerott and H. Margenau—255(A)

Magnetic properties
Curie transition; alloy and glass containing Ni, W. R. Ham and H. S. Coleman—348(A)
Electron microscope study of domains, L. Marton—353(A)

Magnetic ions, F. Ehrenhaft—62(A); 256(A); 287(L); 349(A)
Magneto-current phenomena in Ni, H. A. Perkins—355(A)
Permeability at rapid rates of change of induction, H. L. Glick and S. Siegel—348(A)
Measurements (see **Methods and instruments**)
Mechanics (see **Dynamics**)
Mechanics, quantum-general
Field-quantization emission of low frequency photons, W. Pauli and J. M. Jauch—255(A)
Generalized electrodynamics, B. Podolsky and C. Kikuchi—228
Kinematical probability, B. Liebowitz—255(A)
Spinning electron, bipolar coordinates, M. H. Payne—39
Mesotrons
Mesotron mass-lifetime ratio, K. Kupferberg and F. Reines—253(A)
Spin of, S. K. Chakrabarty and R. C. Majumdar—206(L)
Methods and instruments
Alpha-helium method, geological ages, R. D. Evans and C. Goodman—216
Amplifier with logarithmic response, J. A. Hipple and D. J. Grove—346(A)
Analysis of a multivibrator, S. C. Snowden—151(A)
Cathode sputtering, theory of, C. H. Townes—319
Cyclotron, emergence of charged particles, P. G. Kruger, J. R. Richardson, G. K. Groetzinger, E. M. Lyman, W. E. Ogle, M. E. Nelson, G. Schwarz, J. B. Greene, R. T. Anderson, N. C. Colbey, R. W. Lee, C. E. McClellan, D. Scag, L. Smith, F. K. Tallmadge—62(A)
Determination of area of crystalline solid, G. Jura and W. D. Harkins—66(A)
Differential equations for probability distribution of events, A. E. Ruark—88; 287(L)
Dispersion at supersonic frequencies, L. N. Liebermann—350(A)
Electron microscopes, apertures, L. Marton and R. G. E. Hutter—161
Fixed points on high voltage scale, A. O. Hanson and D. L. Benedict—33
G-M circuits, performance tests, H. E. Walchli—346(A)
G-M counter corrections, T. P. Kohman—63(A)
Inductive measurement of magnetic field strength, F. T. Rogers, Jr.—354(A)
Instrument oil, S. Bloomenthal—64(A)
Ions, recorded with G-M counters, R. T. K. Murray—63(A)
Irreversible solution, potential measurements, R. H. Brown and R. B. Mears—351(A)
Mass spectrometer with small magnet, R. E. Fox, J. A. Hipple, and T. W. Williams—353(A)
Measurement of x-ray intensities, J. C. M. Brentano and H. Froula—254(A)
Metal cutting process, M. E. Merchant—347(A)
Monochromatic electron sources, radioactive nuclei, M. L. Pool—353(A)
Negative resistance, series generator, G. H. Fett—62(A)
Perturbation of boundary conditions, H. Feshbach—307
Plate calibration for analytical spectroscopy, S. Levy—256(A)
Polyatomic gases in fast counters, S. A. Korff and H. D. Present—274
Portable electron microscope, I. Bensen—353(A)
Precision measurement of velocity of sound, supersonic frequencies, E. J. Groth and L. N. Liebermann—350(A)
Radioactive pure Ce, isolation of, J. D. Kurbatov and M. L. Pool—61(A)
Regulator for high voltages, W. H. Pickering and S. C. Snowden—151(A)
Resonant cavity method for measuring dielectric properties, C. N. Works, T. W. Dakin, and F. W. Boggs—349(A)
Reversed cyclotron, L. E. Dodd—353(A)
"Self-quenching" counters, S. A. Korff and R. D. Present—253(A)
Shock vibrations, frequency character, S. L. Brown—153(A)
Small gravimeter, A. Carnvale—345(A)
Spectroscopic methods of analysis, M. F. Hasler—152(A)
String galvanometer, high sensitivity, A. E. Lockenvitz—153(A)
Thermopile for micro-calorimetry, L. S. Mason—345(A)
X-ray inspection of spotwelds, R. C. McMaster—153(A)
Mobility of ions (see **Ions, mobility**)

Neutrons
Inelastic scattering, R. Weinstock—1
Nuclear structure (see also **Disintegration of nucleus**)
Charge distribution around protons, J. M. Blatt—352(A)
Classification of stable nuclei, deviations, J. D. Kurbatov—351(A); mass numbers 3 and 4, M. H. Kurbatov and J. D. Kurbatov—351(A)
Energy levels of light nuclei, W. Y. Chang—352(A)
Nuclear forces, meson theory, J. M. Jauch and N. Hu—289(L)
New representation of nuclear forces, M. Bunge—249(L)

Optical constants and properties
Intense electrostatic fields, effect on reflectivity, C. K. Strobel—283

Radioactivity (see also **Disintegration of nucleus**)
Alpha-helium method, geological ages, R. D. Evans and C. Goodman—216
Auger electrons from K capture, F. Miller, Jr.—254(A)
β-ray spectra of Pb^{205} and Bi^{207}, A. L. Lutz, M. L. Pool, and J. D. Kurbatov—61(A)
Disintegration of Mn^{54} and Co^{58}, M. Deutsch and L. G. Elliott—211
Excitation functions, bombardment of NaBr, E. T. Clarke and J. W. Irvine, Jr.—352(A)
γ-rays energy of Na^{24}, pair production, W. E. Ogle and P. G. Kruger—61(A); photo-neutron method, M. Goldhaber, G. S. Klaiber, and G. Scharff-Goldhaber—61(A)
K-electron capture in Ag, L. K. Hurst and M. L. Pool—60(A)

Monochromatic electron sources, radioactive nuclei, M. L. Pool—353(A)
Of Cb and Zr, W. N. Moquin and M. L. Pool—60(A)
Of Ag, L. K. Hurst and M. L. Pool—351(A)
Of V^{48}, transmutation of Ti, C. T. Hibdon, M. L. Pool, and J. D. Kurbatov—351(A)
Radioactive pure Ce, isolation of, J. D. Kurbatov and M. L. Pool—61(A)
Variation with particle size, F. Morgan—352(A)

Raman spectra
Of normal-heptane and normal-hexane, F. F. Cleveland and D. E. Lee—350(A)
Of olefinic hydrocarbons, F. F. Cleveland—65(A)

Relativity
Supplementary indeterminacy, G. Wataghin—205(L)

Resistance, electrical (see **Electrical conductivity and resistance**)

Scattering of electrons, neutrons, and ions
Of slow neutrons, inelastic, R. Weinstock—1

Secondary electrons (see **Electrons, secondary**)

Solid state (see **Crystalline state**)

Spectra, absorption
Double-bond, in ultraviolet, J. R. Platt—350(A)
Of alkalis, bands near principal series, S. Y. Ch'en—338
Polymer spectra of a cyanine dye, R. W. Mattoon—65(A)

Spectra, atomic
Forbidden lines of Bi I, S. Mrozowski—65(A)
Forbidden lines of Ca II, P. W. Merrill—152(A)
Isotope shift in Mg, L. G. Mundie and K. W. Meissner—65(A); 265
Magnetic-dipole transitions in Xe and Rn, B. Edlén—248(L).
Structure of λ5461 of Hg^{198}, J. H. Wiens—58(L)

Spectra, continuous
Theory of spectra of H_2 and D_2, experimental verification, A. S. Coolidge—236

Spectra, general
Note on N_2, R. E. Worley—249(L)

Spectroscopy, technique
Plate calibration for analytical spectroscopy, S. Levy—256(A)
Standard of wave-length, light source, C. W. Hsueh—151(A)

Standards (see **Constants, physical**)

Surface tension
Dynamics of capillary action, W. A. Rense—356(A)

Thermionic emission; Emitting surfaces
Adsorption of Th on Ta, C. J. Gallagher—46
Thin films of alkaline earth oxides on metals, G. E. Moore and H. W. Allison—254(A)

Vacuum tubes
Currents carried by electrons, G. Jaffé—91

Viscosity
Effect of rate of shear in oils, F. Morgan and M. Muskat—255(A)

X-rays, absorption
Biological action in x-rays, A. A. Bless—356(A)

X-rays, emission
Auger transitions, widths of levels, J. N. Cooper—155
Continuous spectrum intensity measurements, R. Weinstock—150(L)
Ionization cross section of Ag L_{III} state, J. J. G. McCue—168
Measurement of x-ray intensities, J. C. M. Brentano and H. Froula—254(A)
Term values, x-ray spectra, T. M. Hu—76

Zeeman effect
And magnetic potential energy, F. W. Warburton—349(A)

JUL 13 1944

THE PHYSICAL REVIEW

VOLUME 65 *Second Series* NUMBERS 11 AND 12

JUNE 1 AND 15, 1944

Published for the

AMERICAN PHYSICAL SOCIETY

by the

AMERICAN INSTITUTE OF PHYSICS
Incorporated

LANCASTER, PA., AND NEW YORK, N. Y.

THE PHYSICAL REVIEW

A journal of experimental and theoretical physics established by E. L. Nichols in 1893

Published by the American Institute of Physics for the

AMERICAN PHYSICAL SOCIETY

Officers

President
A. J. DEMPSTER
University of Chicago
Chicago, Illinois

Vice President
HARVEY FLETCHER
Bell Telephone Laboratories
New York, New York

Secretary
K. K. DARROW
Bell Telephone Laboratories
Office:
Columbia University
New York, New York

Treasurer
G. B. PEGRAM
Columbia University
New York, New York

Local Secretary for the Pacific Coast
R. T. BIRGE
University of California
Berkeley, California

Editor
JOHN T. TATE*
University of Minnesota
Minneapolis, Minnesota

* On leave for 1946.

BOARD OF EDITORS

JOHN T. TATE, *Editor (on leave)* J. W. BUCHTA, *Acting Editor*

Associate Editors

W. H. FURRY	BRUNO ROSSI	J. W. BEAMS
LUIS ALVAREZ	MELBA PHILLIPS	V. ROJANSKY
E. M. MCMILLAN	W. H. ZACHARIASEN	F. SEITZ

Manuscripts for publication should be submitted to J. W. Buchta, University of Minnesota, Minneapolis, Minnesota.

Proof and all correspondence concerning papers in the process of publication should be addressed to the Publications Manager, American Institute of Physics, 57 East 55 Street, New York 22, New York.

Subscription Price

United States and Canada.....$15.00
Elsewhere.....$16.50

Back Numbers

Complete set: Series 2,[1] Vol. 1, 1913–Vol. 64, 1943—$465.00
Yearly rate: $16.50
Single copies: $1.50 each, prior to July, 1929;
$0.75 each, July, 1929–December, 1941.
Current issues: $1.50 each.

Subscriptions and orders for back numbers should be addressed to Prince and Lemon Streets, Lancaster, Pennsylvania, or to the American Institute of Physics, 57 East 55 Street, New York 22, New York.

Changes of address in the case of members of the American Physical Society should be addressed to the Treasurer; in the case of other subscribers to the Publications Manager.

[1] For Series 1 inquire of Physics Department, Cornell University, Ithaca, New York.

The Physical Review is published monthly at Prince and Lemon Streets, Lancaster, Pennsylvania.

Entered as second-class matter January 27, 1933, at the Post Office at Lancaster, Pennsylvania, under the Act of March 3, 1879.

Acceptance for mailing at special rate of postage provided for in paragraph 4, section 538, P. L. & R., authorized January 27, 1933.

THE AMERICAN INSTITUTE OF PHYSICS

INCORPORATED

ADMINISTRATIVE STAFF

HENRY A. BARTON, *Director*

MADELINE M. MITCHELL, *Publications Manager*

JOHN T. TATE, *Adviser on Publications*

Office: 57 East 55 Street, New York 22, New York

JOURNALS

THE PHYSICAL REVIEW
REVIEWS OF MODERN PHYSICS
JOHN T. TATE, *Editor (on leave)*
J. W. BUCHTA, *Acting Editor*

JOURNAL OF THE OPTICAL SOCIETY OF AMERICA
GEORGE R. HARRISON, *Editor*

THE JOURNAL OF THE ACOUSTICAL SOCIETY OF AMERICA
FLOYD A. FIRESTONE, *Editor*

AMERICAN JOURNAL OF PHYSICS
DUANE ROLLER, *Editor*
JOSEPH D. ELDER, *Assistant Editor*

THE REVIEW OF SCIENTIFIC INSTRUMENTS
GAYLORD P. HARNWELL, *Editor*

THE JOURNAL OF CHEMICAL PHYSICS
JOSEPH E. MAYER, *Editor*

JOURNAL OF APPLIED PHYSICS
ELMER HUTCHISSON, *Editor*

GOVERNING BOARD

PAUL E. KLOPSTEG, *Chairman*
Central Scientific Company

GEORGE B. PEGRAM, *Secretary*
Columbia University

For the American Physical Society:

L. A. DUBRIDGE
University of Rochester

GEORGE B. PEGRAM
Columbia University

JOHN T. TATE
University of Minnesota

For the Optical Society of America:

K. S. GIBSON
National Bureau of Standards

R. C. GIBBS
Cornell University

A. G. WORTHING
University of Pittsburgh

For the Acoustical Society of America:

FLOYD A. FIRESTONE
University of Michigan

WALLACE WATERFALL
The Celotex Corporation

HARVEY FLETCHER
Bell Telephone Laboratories

For the Society of Rheology:

R. B. DOW
Aberdeen Proving Ground

HERMANN MARK
Brooklyn Polytechnic Institute

N. W. TAYLOR
Minnesota Mining & Manufacturing Company

For the American Association of Physics Teachers:

PAUL E. KLOPSTEG
Central Scientific Company

T. D. COPE
University of Pennsylvania

L. W. TAYLOR
Oberlin College

The American Institute of Physics is a membership corporation of which five societies are the founding members. These five societies are the principal national societies devoted to pure and applied physics in America. Their names, and those of their representatives who form the Governing Board of the Institute, are given above. The principal work of the Institute is the publication of journals sponsored by the societies or by itself. The names and the editors of the journals are also listed above.

The broad purpose of the Institute is to represent, in all matters of wide or common interest, the five thousand or more members and subscribers associated with the Founder Societies and the journals. It aims to advance the science and profession of physics, and to promote cooperation between pure research, the applied sciences, and the industries. To achieve these aims, it is greatly in need of an endowment and is empowered by law to administer grants and funds of any kind.

CONTENTS

THE PHYSICAL REVIEW SECOND SERIES, VOL. 65, NOS. 11 AND 12 JUNE 1 AND 15, 1944

On the Problem of the Existence of Mesotrons in Auger Showers . . . ANATOLE ROGOZINSKI 291

Theory of Counter Experiments on Collision Electrons Ejected in Air by Mesotrons . . . . . ANATOLE ROGOZINSKI 300

On the Perturbation of Boundary Conditions . . . . . HERMAN FESHBACH 307

Theory of Cathode Sputtering in Low Voltage Gaseous Discharges . CHARLES HARD TOWNES 319

On the Extraction of Electrons from a Metal Surface by Ions and Metastable Atoms . . . . . A. COBAS AND W. E. LAMB, JR. 327

New Absorption Band of Alkalis in the Presence of Foreign Gases . . . . . CH'EN SHANG-YI 338

Cosmic-Ray Meson Spectra . . . . . D. M. BOSE, BIBHA CHOUDHURI, AND M. SINHA 341

Letter to the Editor:

On the Maximal Energy Attainable in a Betatron . . . : D. IWANENKO AND I. POMERANCHUK 343

Proceedings of the American Physical Society:

Meeting at Pittsburgh, Pennsylvania, April 28 and 29, 1944: Minutes and Abstracts 344
Meeting of the New England Section, April 15, 1944 353
Meeting of the Southeastern Section, May 5 and 6, 1944 355
Meeting of the Ohio Section, May 6, 1944 357

Author Index to Volume 65 358

Analytic Subject Index to Volume 65 363

Volume Table of Contents iii

LANCASTER PRESS, INC., LANCASTER, PA.